302

NATIONAL COOPERATIVE
HIGHWAY RESEARCH PROGRAM REPORT **302**

FATIGUE AND FRACTURE EVALUATION FOR RATING RIVETED BRIDGES

RECEIVED

SEP 16 1988

MAT. LAB.

MATERIALS	ACT	INF
Mtls Supv		
Research Supv		
QC Supv		
TESTS		
EIT		
File		

TRANSPORTATION RESEARCH BOARD
NATIONAL RESEARCH COUNCIL

NATIONAL COOPERATIVE HIGHWAY RESEARCH PROGRAM
REPORT **302**

FATIGUE AND FRACTURE EVALUATION
FOR RATING RIVETED BRIDGES

J. W. FISHER, B. T. YEN, D. WANG
Fritz Engineering Laboratory
Lehigh University
Bethlehem, Pennsylvania

J. E. MANN
Michael Baker Jr., Inc.
Beaver, Pennsylvania

AREAS OF INTEREST:

Structures Design and Performance
General Materials
Maintenance
(Highway Transportation, Rail Transportation)

TRANSPORTATION RESEARCH BOARD
NATIONAL RESEARCH COUNCIL
WASHINGTON, D.C.   DECEMBER 1987

NATIONAL COOPERATIVE HIGHWAY RESEARCH PROGRAM

Systematic, well-designed research provides the most effective approach to the solution of many problems facing highway administrators and engineers. Often, highway problems are of local interest and can best be studied by highway departments individually or in cooperation with their state universities and others. However, the accelerating growth of highway transportation develops increasingly complex problems of wide interest to highway authorities. These problems are best studied through a coordinated program of cooperative research.

In recognition of these needs, the highway administrators of the American Association of State Highway and Transportation Officials initiated in 1962 an objective national highway research program employing modern scientific techniques. This program is supported on a continuing basis by funds from participating member states of the Association and it receives the full cooperation and support of the Federal Highway Administration, United States Department of Transportation.

The Transportation Research Board of the National Research Council was requested by the Association to administer the research program because of the Board's recognized objectivity and understanding of modern research practices. The Board is uniquely suited for this purpose as: it maintains an extensive committee structure from which authorities on any highway transportation subject may be drawn; it possesses avenues of communications and cooperation with federal, state, and local governmental agencies, universities, and industry; its relationship to the National Research Council is an insurance of objectivity; it maintains a full-time research correlation staff of specialists in highway transportation matters to bring the findings of research directly to those who are in a position to use them.

The program is developed on the basis of research needs identified by chief administrators of the highway and transportation departments and by committees of AASHTO. Each year, specific areas of research needs to be included in the program are proposed to the National Research Council and the Board by the American Association of State Highway and Transportation Officials. Research projects to fulfill these needs are defined by the Board, and qualified research agencies are selected from those that have submitted proposals. Administration and surveillance of research contracts are the responsibilities of the National Research Council and the Transportation Research Board.

The needs for highway research are many, and the National Cooperative Highway Research Program can make significant contributions to the solution of highway transportation problems of mutual concern to many responsible groups. The program, however, is intended to complement rather than to substitute for or duplicate other highway research programs.

FOREWORD

By Staff
Transportation
Research Board

This report contains the findings of a study that was performed to evaluate the fatigue and fracture resistance of riveted steel bridge components and members. The report provides a detailed examination of all available fatigue and fracture test data on riveted components and members. It also includes recommended revisions to the evaluation requirements presently in the AASHTO *Manual for Maintenance Inspection of Bridges* for riveted steel bridges. The contents of this report will be of immediate interest and use to bridge engineers, researchers, specification writing bodies, and others concerned with the fatigue and fracture evaluation of existing riveted steel bridges.

Many transportation agencies have a significant number of older riveted steel bridges that must be inspected, evaluated, and rated on a periodic basis. The AASHTO *Manual for Maintenance Inspection of Bridges,* used for structural evaluation by most bridge engineers in the United States, does not provide an effective means of establishing the safe load capacity of these structures when fatigue and fracture toughness are of primary concern. Engineers are, therefore, obliged to evaluate the condition of such bridges with minimal information and guidance.

NCHRP Project 12-25, "Fatigue and Fracture Evaluation for Rating Riveted Steel Bridges," was initiated with the objective of developing a rational rating plan for riveted bridges based on available information on the fatigue and fracture resistance of such bridges and components. The research was performed at Lehigh University and included analytical studies of existing riveted steel fatigue data and laboratory tests on riveted girders and components.

This report summarizes the findings from that study. Numerous examples of fatigue and fracture initiating from rivet locations and details are provided through photographs and sketches.

The test data indicate that AASHTO Category D is a reasonable lower bound for fatigue crack development. However, because of the inherent internal redundancy of built-up sections, cracking in a component does not result in a complete loss of load carrying capacity in the member. The additional stress cycles needed to fail the section resulted in a fatigue strength that usually exceeded the Category C resistance curve.

The report includes recommendations for revisions to the fatigue and fracture provisions in the AASHTO *Manual for Maintenance Inspection of Bridges.* It also contains numerous examples demonstrating the use of the recommended provisions. It is expected that the AASHTO Subcommittee on Bridges and Structures will consider the recommendations in this report for possible adoption in the near future.

CONTENTS

FATIGUE AND FRACTURE EVALUATION FOR RATING RIVETED BRIDGES

SUMMARY   The research described in this report is the result of a review and study performed under NCHRP Project 12-25. It provides a detailed examination of fatigue test data that was reported in a DOT-sponsored research study (DTRS 5682-C-00013), entitled "Fatigue Strength of Weathered and Deteriorated Riveted Members," other data from studies elsewhere in the world, and the results of 14 fatigue and fracture tests on full-scale members removed from bridges.

The review and test data have indicated that the type of riveted connection does not significantly affect fatigue resistance. Simple shear splices, built-up sections in bending with or without coverplates, and truss-type connections and members provided similar results based on their net section stress range.

The available test data indicate that Category D is a reasonable lower bound for fatigue crack development. However, cracking a component of a built-up section did not result in a loss in load carrying capacity. Generally, the additional stress cycles needed to fail the section resulted in a fatigue strength that exceeded the Category C resistance curve.

Fracture toughness tests on materials removed from riveted bridge structures indicated that a significant percentage of riveted bridges can be expected to have materials that do not satisfy the AASHTO Zone 2 requirements. The lowest toughness material was found to provide a lower bound fracture resistance of 50 ksi$\sqrt{in.}$ (55 MP a$\sqrt{m}$) at minimum service temperatures as low as -40 F (-40 C). This results because of the low yield point and intermediate strain rate.

An examination of riveted highway bridge members and details indicated that seven groups of conditions had much in common. These included: (1) rivet patterns for built-up flexural members, (2) coverplate terminations, (3) stringer to floor-beam connections, (4) floor-beam end connections, (5) rivet patterns for truss members, (6) gusset plate connections, and (7) hanger connections. Rivets were generally $\frac{7}{8}$ in. (22 mm) or 1 in. (25 mm). The connected plates and components varied between $\frac{5}{16}$ in. (8 mm) and 1 in. (25 mm).

For riveted highway bridges, the current (1987) AASHTO rating provisions for fatigue and fracture are not very definitive and depend on the design criteria used for new structures. The general practice seems to ignore the possibility of fatigue damage as no significant adverse fatigue behavior has been observed in riveted highway bridges.

This study has confirmed that riveted highway bridges are not likely to develop fatigue cracks in the primary members because the cyclic loads do not result in stress range levels that exceed the estimated fatigue limit for riveted members (Category D).

Recommendations are provided in this report for rating riveted bridges for fatigue damage. These recommendations provide an easy format to establish whether or not a riveted bridge is susceptible to cracking from the cyclic stresses from truck loads.

The majority of cracking likely to develop in riveted highway bridges is from secondary distortion-induced stresses in connecting elements or small web gaps, from unanticipated restraint conditions such as "simple" end connections or pinned connections, and from welded repairs or tack welds. Examples of these types of cracking are shown and discussed in the report.

CHAPTER ONE

INTRODUCTION

BACKGROUND

Among the major concerns of bridge engineers today is the safety of old riveted structures and the potential fatigue damage that has accumulated. Many of these structures were fabricated and placed into service at the beginning of the century. The question of safety is of major importance because increasing traffic, deteriorating components and the accumulation of large numbers of cycles are a reality for highway, railroad, and mass transit bridges.

The criteria often adopted for control of fatigue and fracture in new bridge structures are based on studies of modern welded construction and ongoing laboratory research on welded members. Most older bridges are constructed of riveted built-up members. Better estimates of the fatigue resistance of riveted built-up sections are needed.

Most of the early laboratory work on riveted components has been carried out on simple butt splices. A further limitation is that few tests have been performed with stress ranges below 14 ksi (97 MPa). Both the American Association of State Highway and Transportation Officials (AASHTO) and American Railroad Engineering Association (AREA) specifications use a lower bound estimate, based on these limited data, to define the fatigue strength of riveted built-up members (1,2). This lower bound corresponds to Category D in the joint classification system. A brief description and summary of the early data base are given in the commentary to the AREA specifications (2).

OBJECTIVES AND SCOPE

The research to achieve the objective of the study was devoted

to reviewing existing test data and results of analysis; reviewing current practice of rating and retrofitting riveted bridge components; conducting full-scale, laboratory bridge member tests to observe the behavior of riveted members in fatigue and fracture; and correlating all information to develop the rating procedure.

RESEARCH APPROACH

The research to achieve the objective of the study was devoted to reviewing existing test data and results of analysis; reviewing current practice of rating and retrofitting riveted bridge components; conducting full-scale, laboratory bridge member tests to observe the behavior of riveted members in fatigue and fracture; and correlating all information to develop the rating procedure.

ORGANIZATION OF THE REPORT

The findings of the study are summarized in Chapter Two. Chapter Three presents the results of the data review and evaluation, including the review of existing rating provisions. Chapter Four describes the results of the full-scale laboratory testing conducted in this study. The recommendations for application of the results and the conclusions are presented in Chapters Five and Six, respectively. Further research needs are introduced in Chapter Seven. The data base format is presented in Appendix A. More detailed test results, not covered in Chapter Four, are documented in Appendix B. Examples of rating riveted bridges are given in Appendix C.

CHAPTER TWO

FINDINGS

The findings of the review and examination of all available test data on riveted steel and wrought iron joints and members are summarized in this chapter. The discussion also focuses on the review of details used in riveted steel bridges and the AASHTO criteria for rating riveted members. A more detailed evaluation of the experimental data is provided in Chapters Three and Four.

FATIGUE BEHAVIOR OF RIVETED STEEL COMPONENTS

The examination of test data on small double shear splices and more limited data on large-scale riveted members has demonstrated that Category D provides a reasonable lower bound to fatigue crack development. This was found in the sloping portion of the finite life stress range–cycle life relationship (S-N curve) as well as in the higher cycle region related to the fatigue limit (see Fig. 32).

The tests on riveted built-up sections also demonstrated that severing a component of the built-up section did not immediately impair the load-carrying capability of the member. At stress range levels exceeding 9 ksi (62 MPa), additional cycle life was available so that failure only occurred when the Category C resistance curve was exceeded. These results indicate that the "risk" of fatigue cracking is not as serious as in a welded built-up section. Should cracks develop in individual components they are likely to be detected before the section can no longer carry load.

The data review and beam tests also indicated that wide variations in detail type, rivet spacing, configuration, and the type of stress cycle had little effect on fatigue strength. Shear splices, truss connections, and flexural members with and without coverplates all exhibited the same fatigue resistance. The large scale truss connections did not exhibit the R-ratio effect of increased fatigue strength exhibited by small shear splices under partial reversal of the stress cycle.

FATIGUE BEHAVIOR OF RIVETED WROUGHT IRON

The available test data are not as extensive on riveted wrought iron connections and members as on steel components. Most of the tests are on plate-type specimens. In addition to tests on simple shear splices, a number of tests were conducted on wrought iron plates with open holes. The test results indicate that Category E provides a lower bound estimate of fatigue resistance. No test data are available in the high cycle region ($N > 10^7$ cycles).

FRACTURE RESISTANCE OF RIVETED DETAILS

Testing riveted members at reduced temperature has demonstrated that relatively large fatigue cracks can develop prior to crack instability of a component. These tests also indicated that failure of a single component did not result in a loss of load-carrying capability. Hence, both fatigue and fracture tests on built-up sections have demonstrated that they are inherently redundant and fully capable of redistributing the forces in a cracked component.

A review of available Charpy V-notch test data from about 90 riveted bridge structures indicated that a substantial number of bridges can be expected to have material with impact energy less than 15 ft-lb (20 J) at 40 F (5 C). Fracture toughness tests on these low-yield-point steels indicated that, for crack front conditions of plane strain, a lower bound fracture toughness of 50 ksi$\sqrt{\text{in.}}$ (55 MPa$\sqrt{\text{m}}$) could be expected at minimum service temperatures as low as -40 F.

The reduced temperature tests on fatigue cracked riveted beams reported in Ref. 30 as well as the results of this study demonstrated that static and intermediate strain rates were applicable. These tests were in agreement with observations on full-size welded details (36).

RIVETED AND BOLTED BEAM-END CONNECTIONS

Limited tests by Wilson (32) in the 1930's demonstrated that the distortion introduced into the outstanding legs of connection angles produced high flexural stresses and fatigue cracking. The flexural stress computed from a simple model which assumes the outstanding leg is fixed at the heel and centerline of the rivets was found to agree with the fatigue resistance provided by Category A.

This suggests that the predicted end rotation could be conservatively used to estimate the bending stress in the angle legs. An alternative check based on this model (see Wilson (33)) provided a relationship between the span length, angle thickness, and gage length of the rivets (or bolts) in the outstanding legs. When geometric conditions violate this relationship, stresses due to prying may cause cracking of overstressed angles or rivets (or bolts).

RIVETED BRIDGE DETAILS

A review of riveted bridge structures indicated that the members and details generally fell within seven classes or groups. Rivet size was $\frac{7}{8}$ or 1 in. (22 or 25 mm) diameter.

The classification groups were identified as follows:

Group I: Rivet patterns for built-up flexural members
Group II: Coverplate terminations
Group III: Stringer to floor-beam connections
Group IV: Floor-beam end connections
Group V: Rivet patterns for truss members
Group VI: Gusset plate connections
Group VII: Hanger connections

Plate and component thicknesses were found to vary from $\frac{5}{16}$ in. (8 mm) to 1 in. (25 mm). The end distance from the end of a plate or section to the first rivet generally varied from $1\frac{1}{2}$ in. (38 mm) to $2\frac{1}{2}$ in. (64 mm). Rivet spacing near the end of coverplates and the ends of members was often between $1\frac{1}{2}$ in. (38 mm) and 3 in. (76 mm). Near the center of members the spacing generally increased to between $3\frac{1}{2}$ in. (89 mm) and 6 in. (152 mm).

The gage length between rivets in the outstanding legs of connection angles was generally equal to or greater than the gage suggested by Wilson (g > $[Lt/8]^{\frac{1}{2}}$) for railroad bridges. Connection angle thickness seldom exceeded $\frac{5}{8}$ in. (16 mm).

No fatigue cracks were detected in the riveted bridge structures used for this evaluation. Furthermore, no fatigue cracks were detected in the riveted highway bridge structures unless distortion and restraint were involved, or the development of severe corrosion notching was observed, or weld repairs or tack welds were the cause.

DISTORTION AND RESTRAINT CRACKING

Distortion and unanticipated restraint are the primary causes of fatigue cracking in riveted bridges. Generally, distortion occurs in web gaps and in angles where out-of-plane movement causes high stresses because of large differences in stiffness. Numerous examples are discussed in Chapter Three. They range from small gaps where flange angles and web stiffeners intersect to corrosion restraint at pinned-end members.

Generally, the cracks developed under these conditions are not detrimental to the member's behavior and strength. They are often developed in low stress range areas and grow slowly once they propagate out of the restraint area. Often they can be arrested by simply drilling holes at the crack tips.

1987 AASHTO RATING PROVISIONS RELATED TO FATIGUE AND FRACTURE

Guidance for checking the capacities of existing steel bridges is provided in the *Manual for Maintenance Inspection of Bridges*

(37). A section on allowable fatigue stresses is provided in Article 5.5 on the Load Factor Method. Article 5.5.2.5 indicates that the AASHTO *Standard Specifications for Highway Bridges,* Article 1.7.2, shall serve as a guide to determining the allowable fatigue stress, F_r. It states that "Special structural or operational conditions, policies of the owner or rating agency, and the judgment of the engineer shall likewise influence the determination of fatigue strength."

No mention of fatigue is provided in the allowable stress method (Article 5.4).

The general practice seems to ignore the possibility of fatigue damage. This results from the positive experience with riveted structures with no significant cracking problems.

RECOMMENDATIONS FOR RATING RIVETED BRIDGES FOR FATIGUE AND FRACTURE

The results of this study have demonstrated that riveted members and connections have the ability to redistribute the load from a cracked element without adversely affecting their cyclic load carrying ability in the short term. Although cracking was often detected at cycle lives corresponding to Category D, the actual fatigue strength was consistent with Category C.

A procedure to evaluate the fatigue resistance of riveted highway bridges which considers both of the characteristics of crack development and fatigue strength is as follows. A simple check of the fatigue limit for Category D (7 ksi) is used to determine whether or not fatigue cracking will develop in a bridge member. For evaluating the remaining life of components found to be susceptible to fatigue cracking, Category C was found to be the appropriate resistance relationship for cumulative damage and fatigue life assessment.

CHAPTER THREE

DATA REVIEW AND EVALUATION

(It is noted that the numbering system used in the agency report has not been altered in the editing process of the published text (Chapters Three through Six) so that accuracy of cross references in the main text and, in particular, Appendix C can be retained.)

3.1 REVIEW OF TEST DATA ON RIVETED SHEAR SPLICES AND PLATE SPECIMENS

A detailed review of the available data on the fatigue behavior of riveted steel members or components is provided in this chapter. Data are included from studies performed in the United

States and Europe between 1934 and 1986 (3–9,11,13–18,20–23,27,28). Each test result provides data on the stress cycle versus number of cycles until failure (or observed cracking) or the test was discontinued with no reported cracks. In this investigation, primary focus is given to cyclic stress range as the main stress parameter influencing fatigue life. Other related stress variables, such as the stress ratio and the bearing ratio, are also examined.

The test data indicate that several variables have an influence on the cyclic stress-life relationship in addition to the stress range. The most important variables are: (1) stress ratio $R = S_{min}/S_{max}$, (2) yield stress, (3) rivet clamping force, (4) rivet bearing ratio, (5) method of hole preparation, (6) specimen state—manufactured from virgin material or cut out of existing structures, (7) specimen type—e.g., simple shear splice, coverplate end, or built-up girder in bending. Unfortunately, these conditions are not always clearly defined in the available literature.

In most of the studies the stress variables have been defined on the net section, and crack appearance defined the fatigue life. Very few crack size measurements have been reported except for the more recent studies.

All of the fatigue test data have been stored in a computer to form a data base, and a number of programs have been written to sort the data and help evaluate the major test variables. The primary means of assessing the significance of the variables was to construct S-N curves. Approximately 1,200 test results are included in the data base. The format of the data base is outlined in Appendix A.

In the following sections a number of S-N diagrams have been constructed for review. The lines are the fatigue design

lines C, D, E, and E', developed from tests on welded details, which serve as reference conditions. These lines were adopted in the 1986 Interim Specifications for Ref. 1. These lines all have a common slope of −3. They do not differ significantly from the curves used for earlier versions of the AASHTO and AREA specifications. Since most of the riveted structural component test data are not distributed over a wide range of cyclic stresses, their regression line was not included in the diagrams.

3.1.1 Factors Influencing Fatigue Resistance

Figure 1 summarizes all data points on simple riveted steel shear splice specimens, with no identification of the control variables. Most test results exceed design Category D, although a small number of data points fall below Categories D and E. Note that no tests on simple shear splices have been conducted at stress ranges below 14 ksi (97 MPa). Also, only a few specimens were subjected to more than two million cycles. The following sections examine the influence of the previously mentioned variables known to affect the fatigue strength of riveted structures.

a. Influence of the R-Ratio

In most of the fatigue tests, the R-ratio was used as a control variable. The R-ratio is defined as the algebraic ratio of minimum and maximum stress in a stress cycle, $R = S_{min}/S_{max}$. The published tests were divided into three categories: $-1 < R < 0$, $0 < R < 0.3$ and $R > 0.3$.
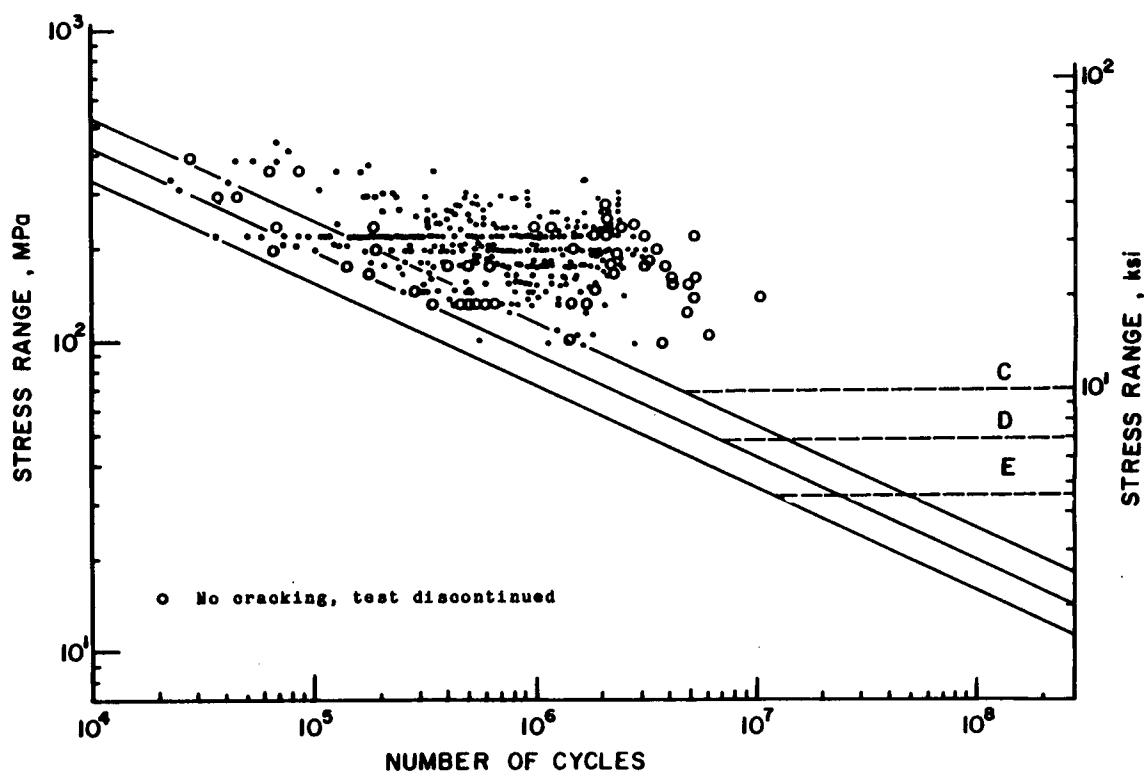
Figure 1. Summary of test data on riveted steel shear splices.

Figure 2 summarizes the test data for alternating loading, with $R < 0$. A large number of specimens did not exhibit cracking in the section and are identified by the symbol "o". The small specimen data indicate that the fatigue strength generally exceeds the Category C resistance line.

Figure 3 shows the test data with low R-ratios ($0 < R < 0.3$). It is apparent that most fatigue tests were conducted under this stress condition. A number of test results are seen to fall below the Category D resistance line. Many of these specimens were tested with reduced clamping force and high bearing ratios. Section 3.1c provides additional discussion on these factors.

Figure 4 summarizes the test data with high minimum stress levels ($R > 0.3$). High minimum stress resulted in net section yielding when the stress range is higher than 20 ksi (138 MPa). It seems likely that this is the primary reason for the reduction in fatigue resistance of most of these specimens. An examination of Figures 2, 3, and 4 indicates that the alternating stress condition is not as critical as a positive R-ratio for small-scale specimens. This was recognized in early European Convention for Constructional Steelwork (ECCS) Specification drafts which suggested a reduction in the stress range for connections without significant residual stresses (10). This was subsequently eliminated from the final specification. If the effective stress range is defined as $S_{reff} = S_{max} - 0.6 S_{min}$, where S_{max} is the tension component of the stress cycle and S_{min} is the compression component, the stress-reversal data plot closer to the higher R-ratio

tests. The adjusted stress cycle values for reversal loaded test specimens are given in Figure 5. The test data can be seen to be more compatible with the Category D resistance curve. A significant number of tests can still be seen to exceed the Category C resistance line, although not by the large margins apparent in Figure 2. However, it should be noted that the beneficial effect of a compressive minimum stress was not as significant with the large scale truss specimens (see Section 3.3.1).

b. Influence of Yield Stress

Figures 6, 7, and 8 summarize the fatigue resistance in terms of the material yield point. Little difference can be seen between Figures 6 and 7. The scatter in the test data is apparent by the number of data points below the Category D resistance curve. It is probable that yielding developed at the net section in the case of materials with a low yield strength, most likely in combination with a low clamping force and high bearing conditions.

The test data on higher yield strength material are seen to lie generally above the Category C resistance curve, as shown in Figure 8. Only the highest stress range tests can be seen to lie below Category C, again, because of net section yielding, which promotes low cycle fatigue.
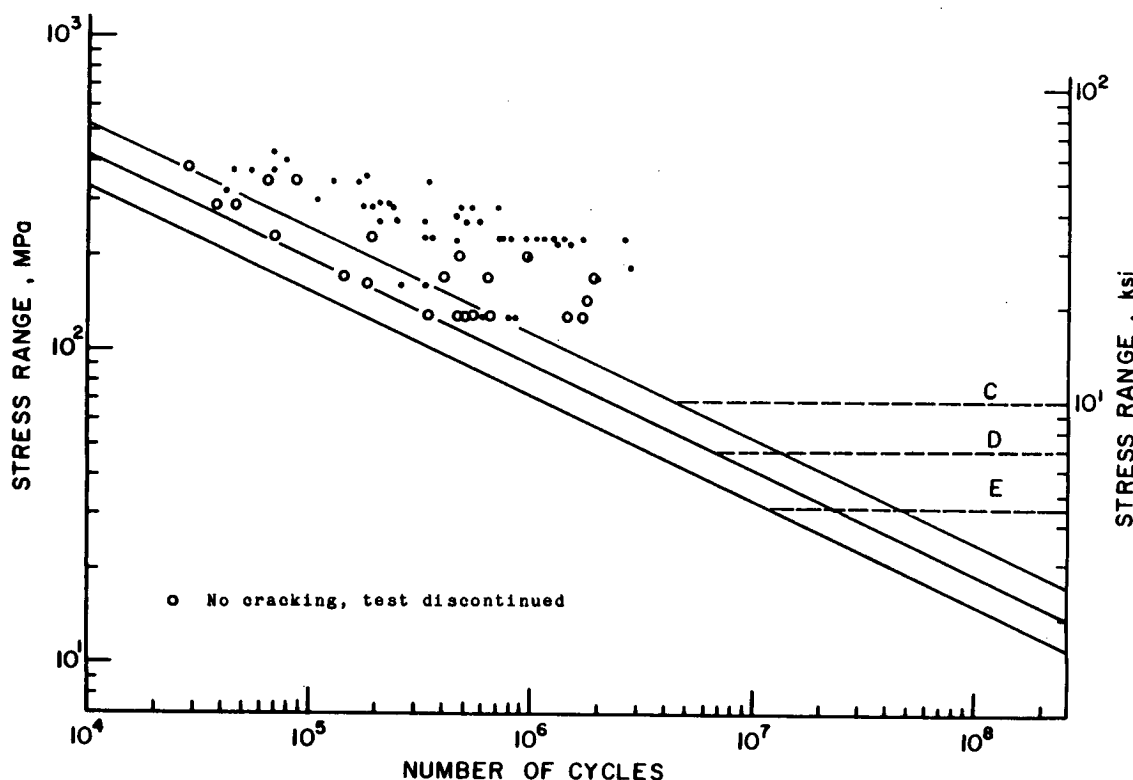
Figure 2. Fatigue resistance of riveted steel connections under reversal loading.

Figure 3. Fatigue resistance of riveted steel connections at low R ratios (0 ≤ R < 0.3).
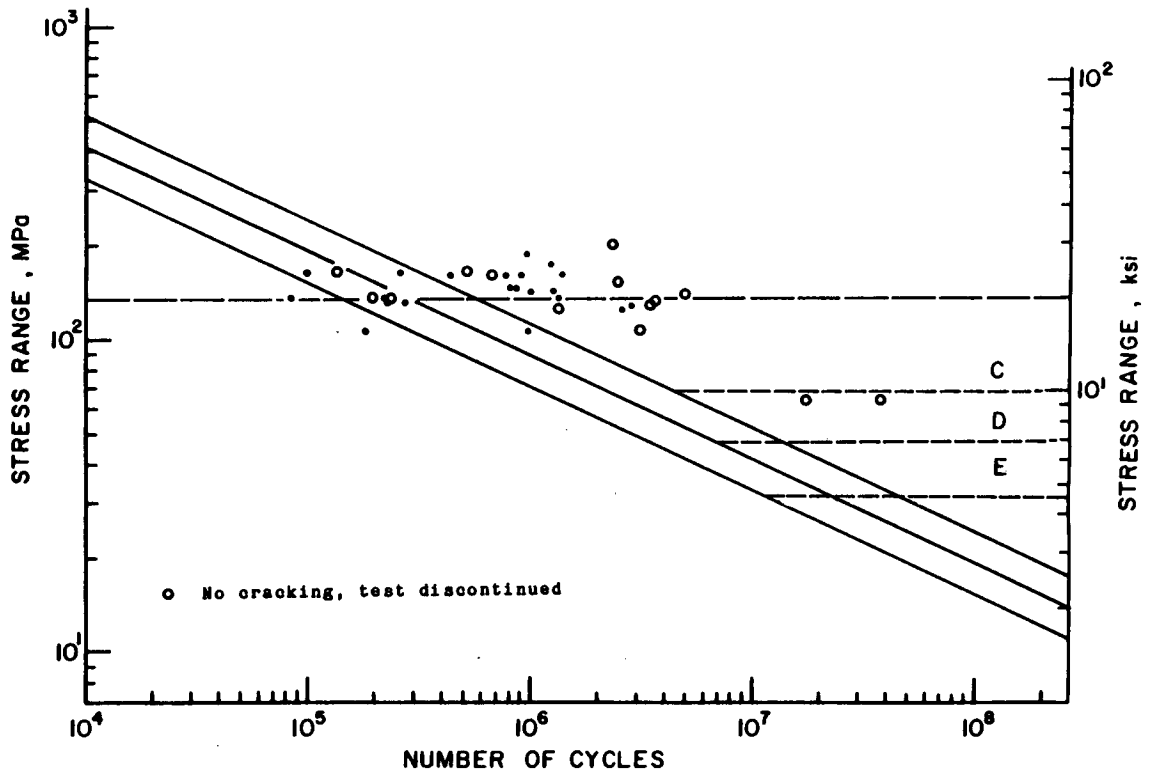
Figure 4. Fatigue resistance of riveted steel connections at high R ratios (R ≥ 0.3).

8
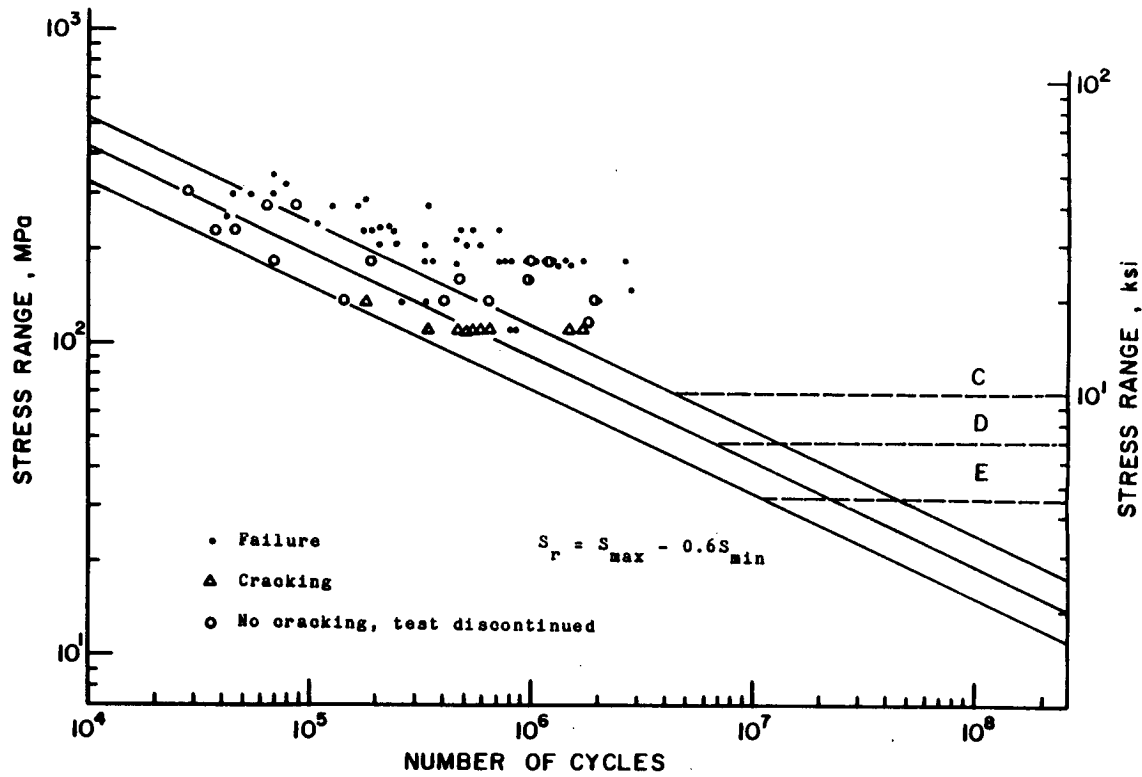
Figure 5. Adjusted fatigue resistance of small steel shear connections with stress reversal.

$$S_r = S_{max} - 0.6 S_{min}$$

- Failure
- Cracking
- No cracking, test discontinued

- No cracking, test discontinued
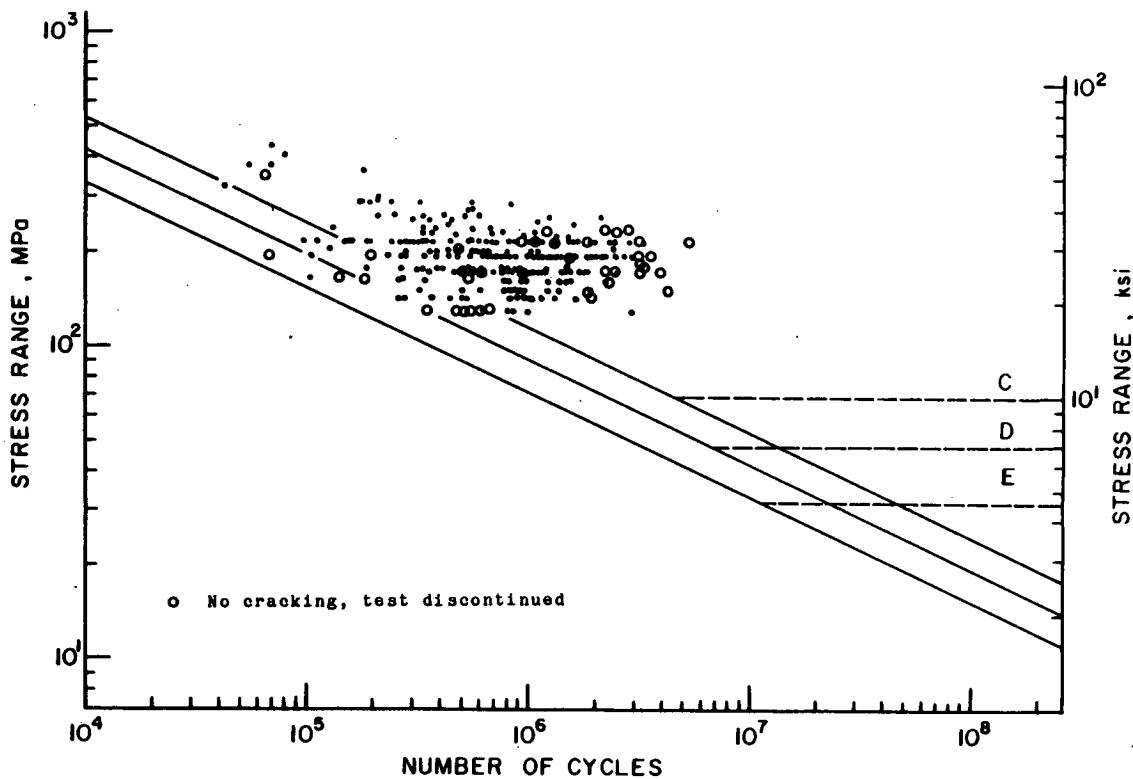
Figure 6. Fatigue resistance of riveted connections of plate materials with F_Y < 275 MPa (39.9 ksi).
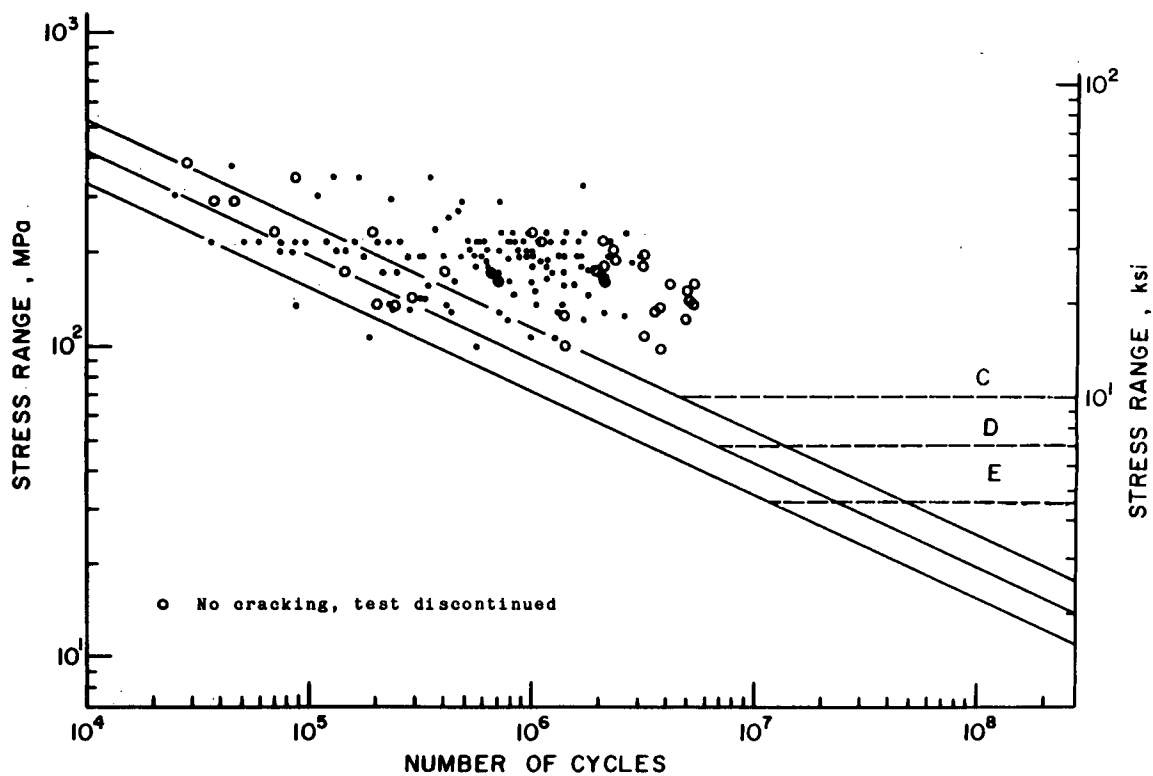
Figure 7. Fatigue resistance of riveted connections of plate materials with $275 \leq F_Y < 345$ MPa $(39.9 \leq F_Y \leq 50.04$ ksi).
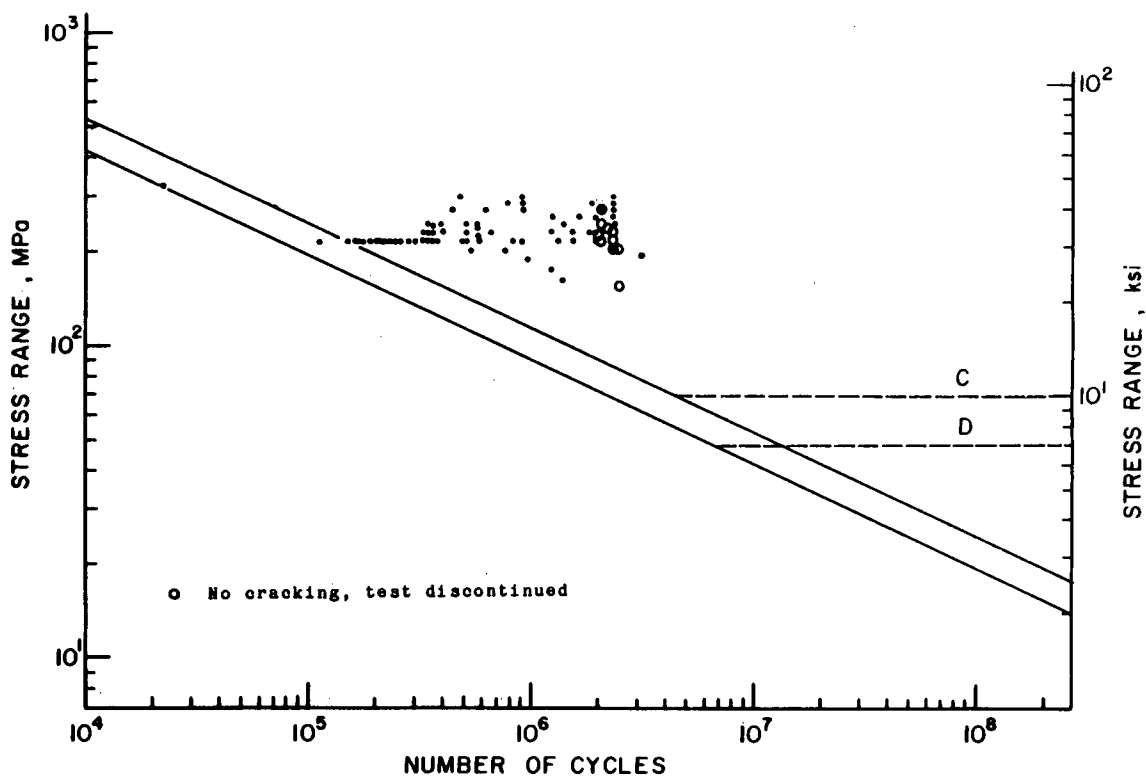
Figure 8. Fatigue resistance of riveted connections of plate materials with $F_Y \geq 345$ MPa $(50.04$ ksi).

c. Influence of Clamping Force and Bearing Ratio

The effects of rivet clamping force and rivet bearing ratio are illustrated in Figures 9 to 12. Test specimens with normal clamping force do not seem to be greatly affected by wide variations in the bearing ratio according to the data given in Figures 9 and 10. Category D can be seen to provide a lower bound resistance for both low and high bearing ratios with normal clamping force. Several tests can be seen to fall below Category D, when the bearing ratio exceeds 1.5. The clamping force was not measured. The differences correspond to "normal" conditions that result from driving the rivets and "reduced" when the rivet heads were machined away to relax the preload. The bearing ratio's are defined as the ratio of nominal stress of the rivet on the plate to the nominal tensile stress in the plate.

Figures 11 and 12 show the fatigue strength of specimens with reduced clamping force. This includes those specimens fabricated with cold-driven rivets. It is clear that a high bearing ratio decreases the fatigue strength of members with reduced clamping.

A comparison of Figures 9 and 11 shows that the effect of the reduction in clamping force does not greatly affect the fatigue resistance, when the bearing ratio is smaller than 1.5. Only one point is seen to fall below the Category D resistance line.

When the bearing ratio is larger than 1.5, the reduction in clamping force has a significant effect, as seen when comparing Figures 10 and 12. The fatigue resistance is less than Category E in two instances. Significant scatter in the test data is apparent in Figure 12.

The results summarized in Figures 9 and 11 suggest that Category D is a reasonable lower bound for riveted joints when the bearing ratio is compatible with the AASHTO and AREA specifications, i.e., smaller than or equal to 1.5.

d. Influence of Method of Hole Preparation

The common methods of producing rivet holes were drilling, punching, subdrilling and reaming, and subpunching and reaming. The effect of the method of hole preparation on the fatigue life of riveted steel specimens is shown in Figures 13 to 16.

Although punched holes were common in early steel structures, it can be seen that the majority of test data was acquired from specimens fabricated with drilled holes. A comparison of Figures 13 and 14 shows that the results for riveted joints with punched holes are well within the scatterband for the specimens with drilled holes. The size of the sample of punched hole specimens makes the reliability of any conclusion questionable. All respective data were developed from specimens fabricated for laboratory tests (with low bearing ratios) so that an unrealistically high quality of the punched holes might account for the small difference. In all cases the plate thickness was ½ in. (13 mm).
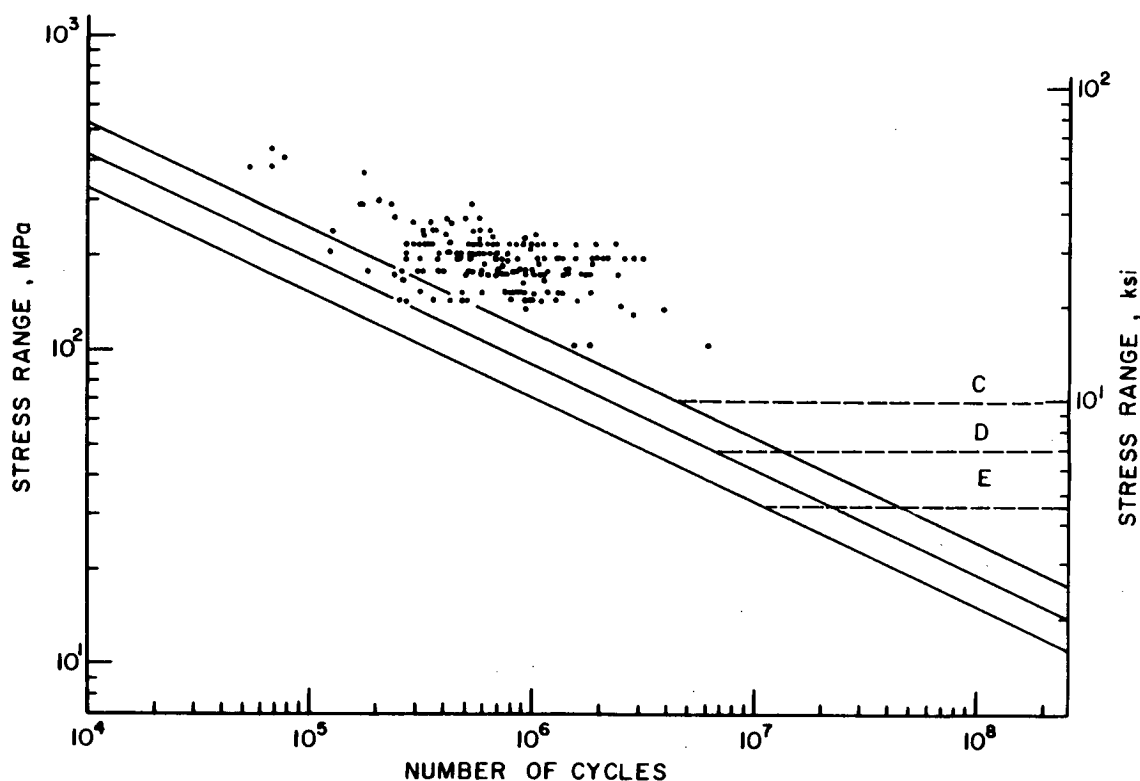
Figure 9. Fatigue resistance of riveted steel connections with normal clamping force and low bearing ratio (≤ 1.5).
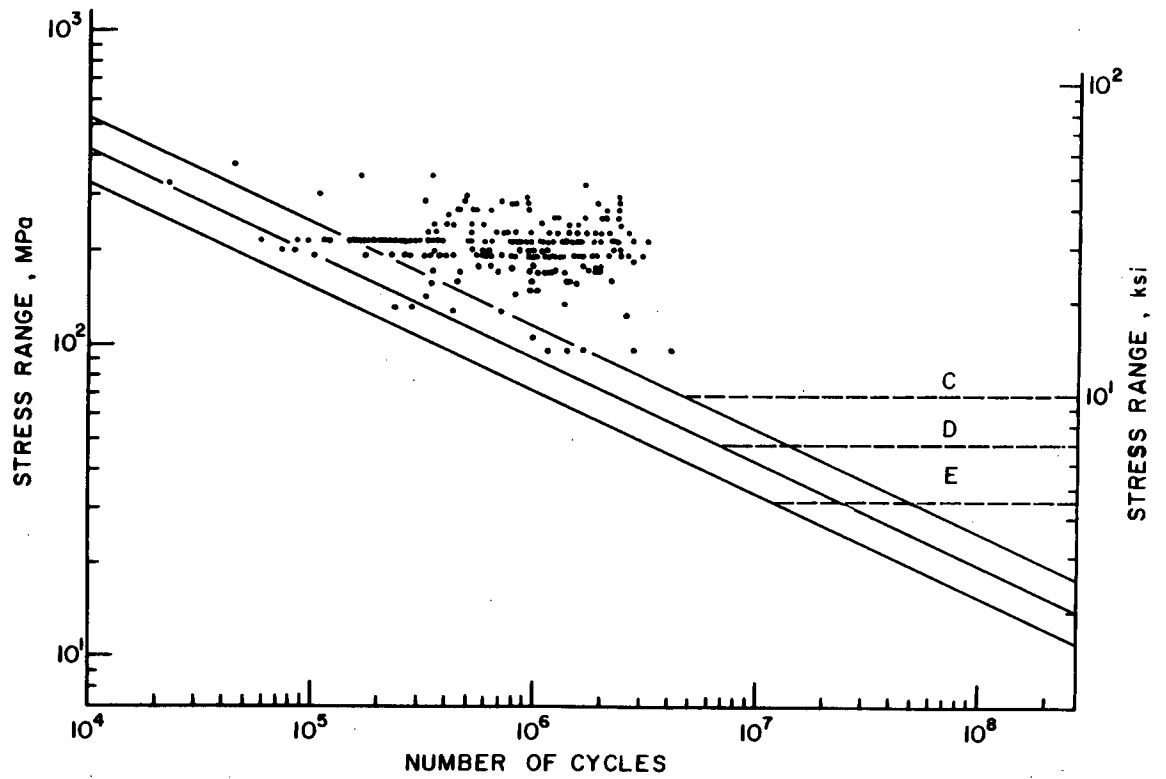
Figure 10. Fatigue resistance of riveted steel connections with normal clamping force and high bearing ratio
(> 1.5).
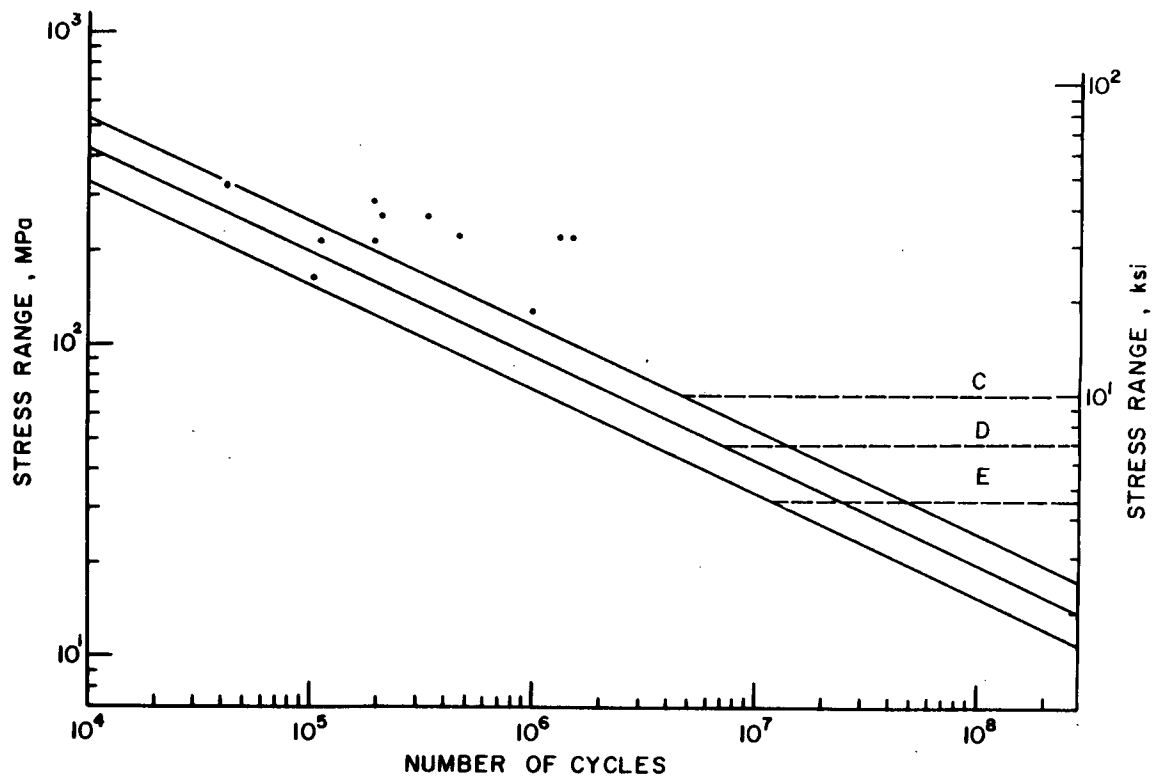
Figure 11. Fatigue resistance of riveted steel connections with reduced clamping force and low bearing ratio
(< 1.5).

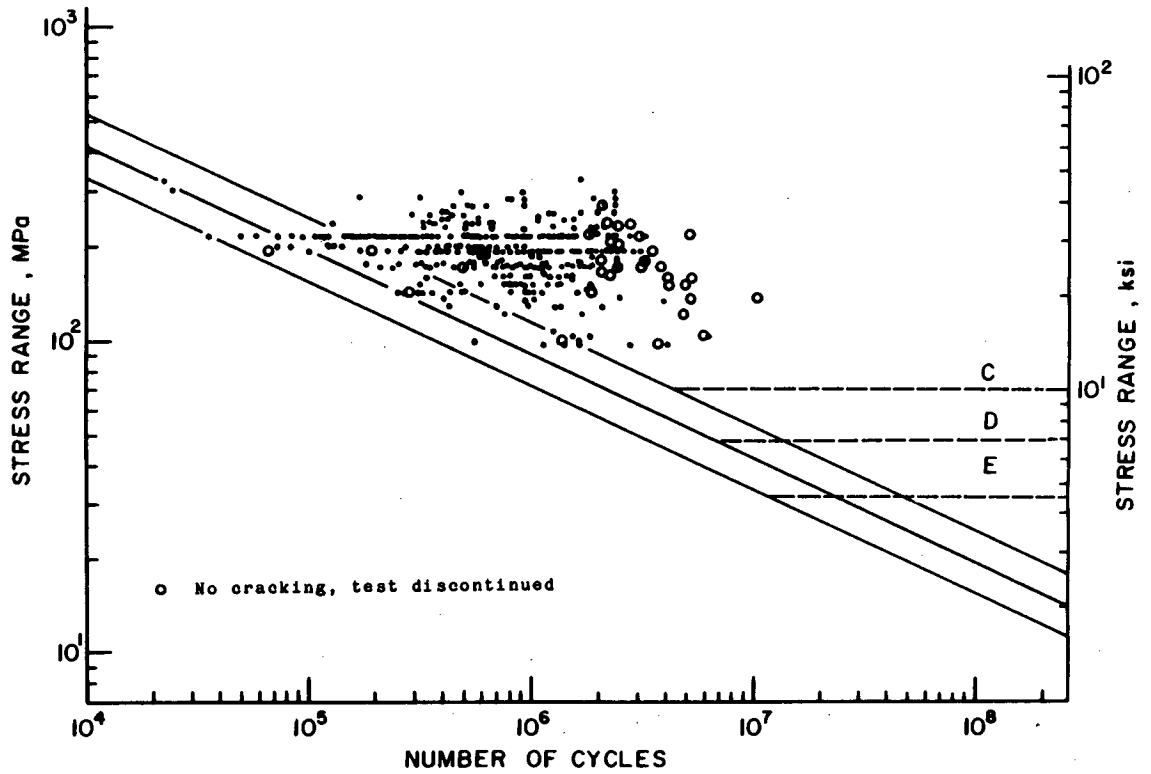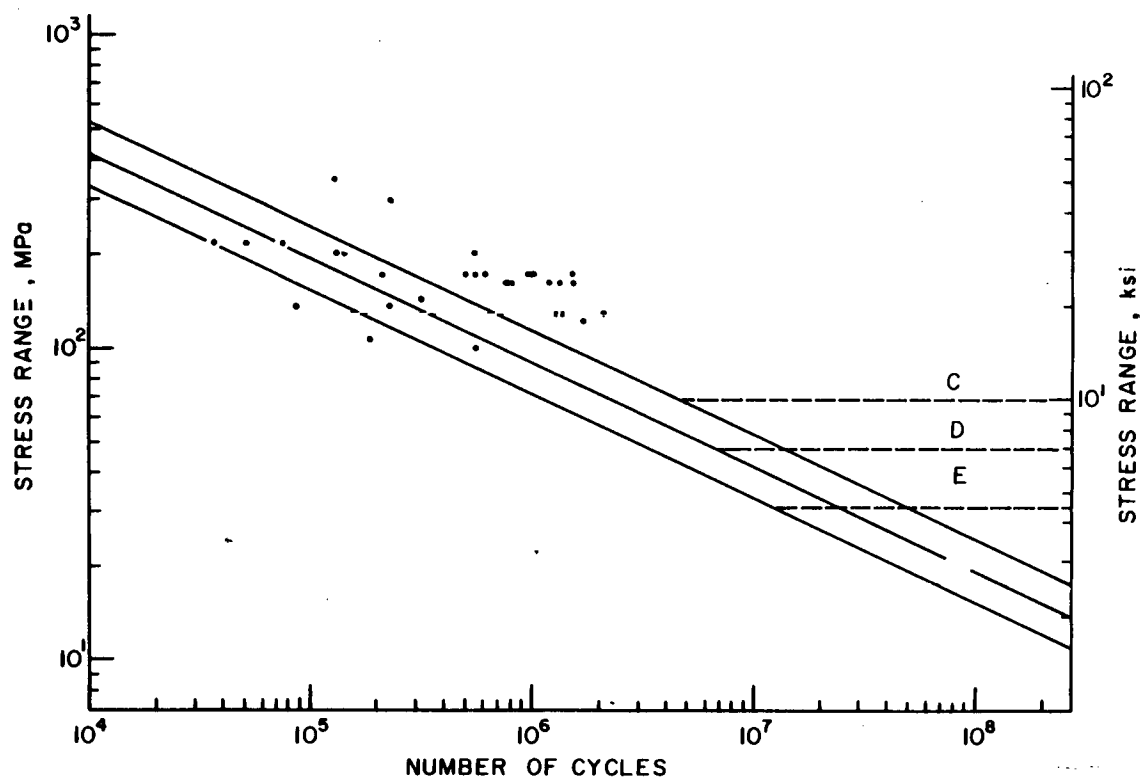Figure 12. Fatigue resistance of riveted steel connections with reduced clamping force and high bearing ratio (> 1.5).

Figure 13. Fatigue resistance of riveted steel connections with drilled holes.
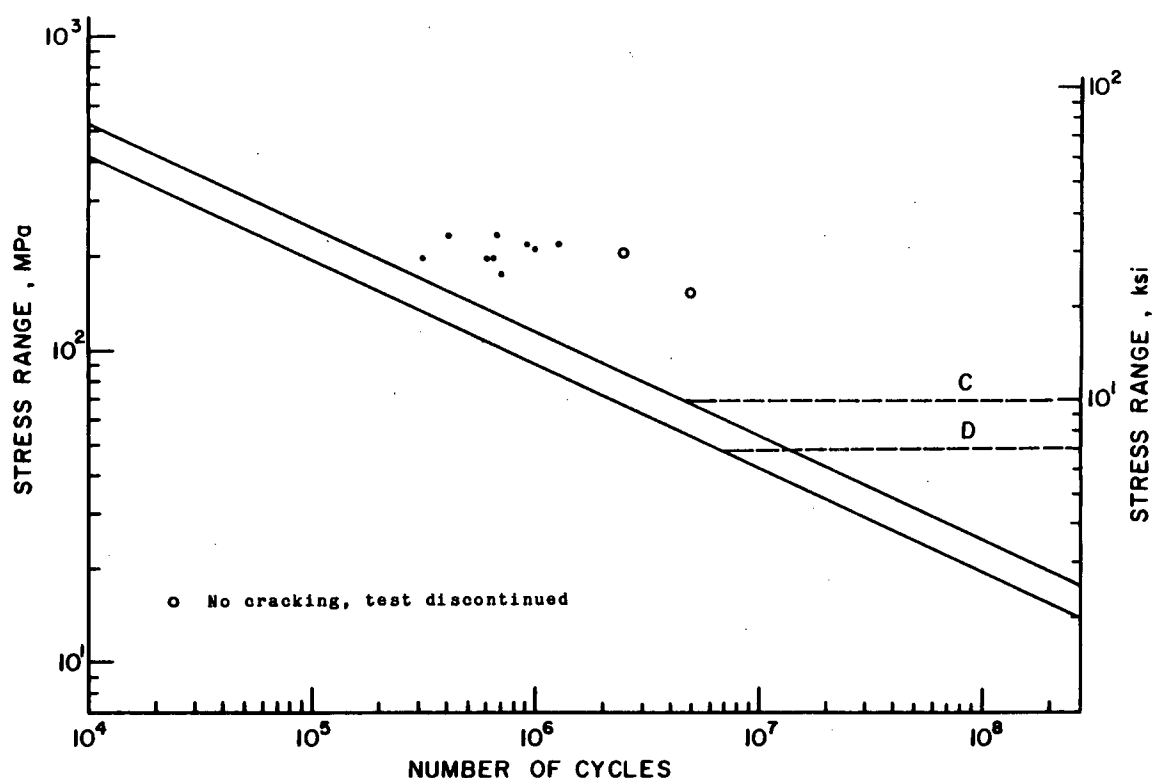
Figure 14. Fatigue resistance of riveted steel connections with punched holes.

Punch alignment and wear can result in minute cracks around the hole (*19,25*). Obviously, the orientation of such initial imperfections is critical. The reaming process seems to improve the fatigue strength, judging from the test data summarized in Figures 15 and 16. Both subdrilled and subpunched holes seem to be less susceptible to fatigue than the drilled holes. Nearly all the test data with subdrilled or subpunched holes can be seen to plot above the Category C resistance line.

On the whole it seems that the manner of hole preparation has minor influence on the fatigue resistance of riveted steel connections.

e. Influence of Specimen State

The specimens used in the previous studies can be divided into specimens specially fabricated for laboratory tests from as-rolled plate and specimens fabricated from members taken from existing structures. The former specimens have been fabricated and riveted under controlled conditions, whereas the latter contain the original rivets and have potential fatigue damage.

The test results associated with the newly fabricated specimens are summarized in Figure 17. Figure 18 shows the test results for the specimens taken from existing structures. It can be observed that the average fatigue strength of the "existing-structure" specimens is lower than that of the "new-material" specimens. The test data for the "existing-structure" specimens, however, fall within the scatterband of the data shown in Figure 17.

Therefore, it can be concluded that exposure to service conditions and differences in fabrication do not result in large differences in fatigue resistance. For both types of specimens, Category D appears to provide an appropriate lower bound.

3.1.2 The Fatigue Resistance of Steel Plate Specimens with Open Holes

a. General Remarks

A number of fatigue tests have been conducted on steel plate specimens with open holes. The results of these tests should provide a lower bound for the fatigue strength of riveted joints, since the clamping force of a plate specimen with open holes is zero. On the other hand, the bearing ratio of a plate with open holes is also zero, which suggests that the average fatigue strength would be higher. These variables are constant for this type of specimen, eliminating the two main variables that influence the fatigue resistance of riveted connections.

The plate specimens with open holes do provide a means of evaluating the method of hole preparation and the specimen state which is newly fabricated, used-material with new holes and used-material with original holes.

b. Influence of Method of Hole Preparation

The common ways to manufacture rivet holes in steel plates

14
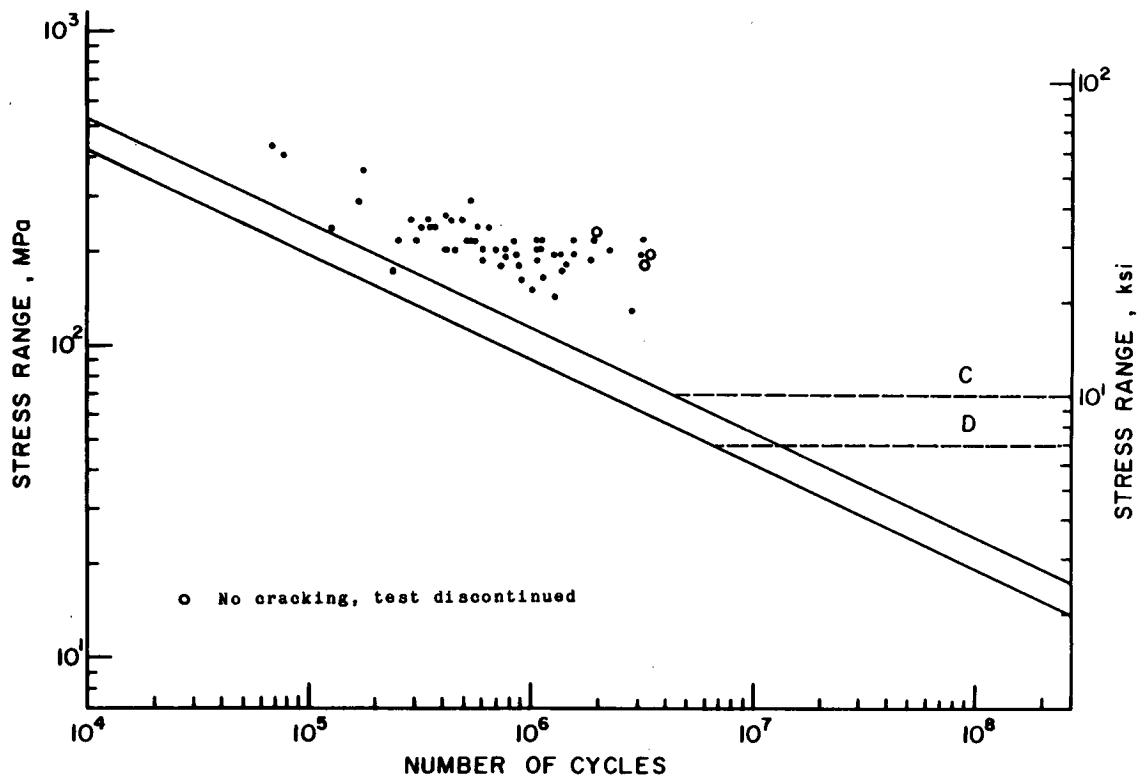
Figure 15. Fatigue resistance of riveted steel connections with subpunched and reamed holes.
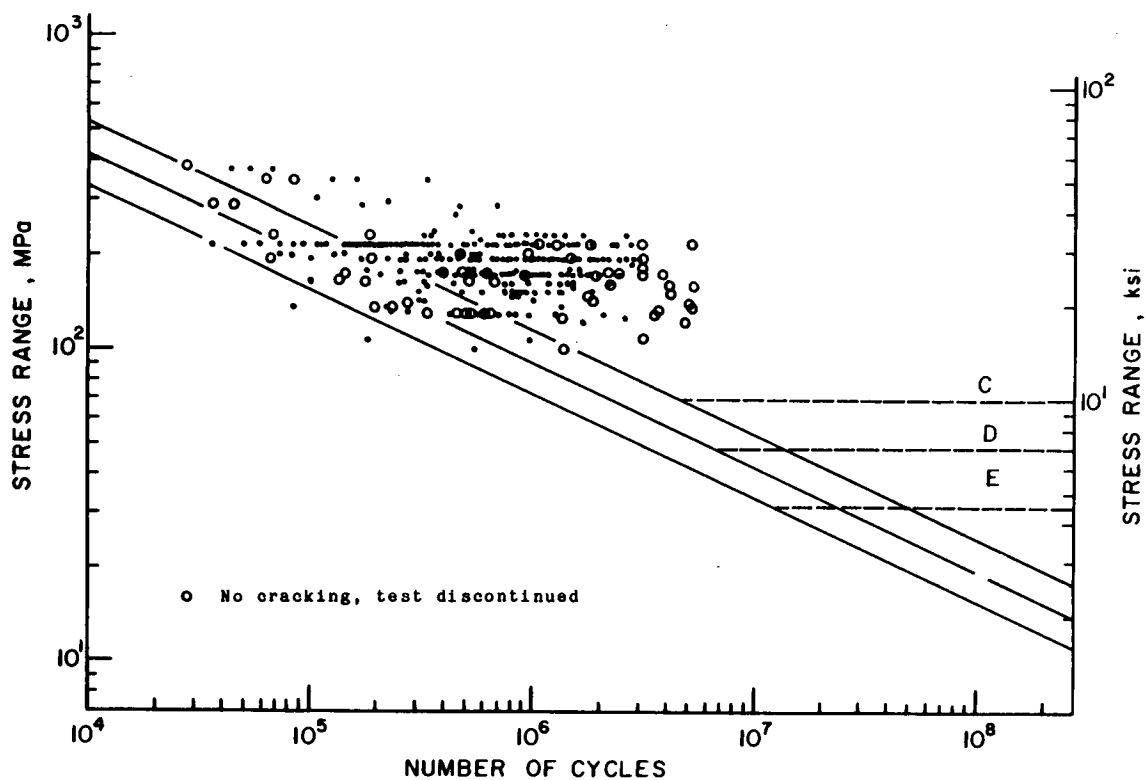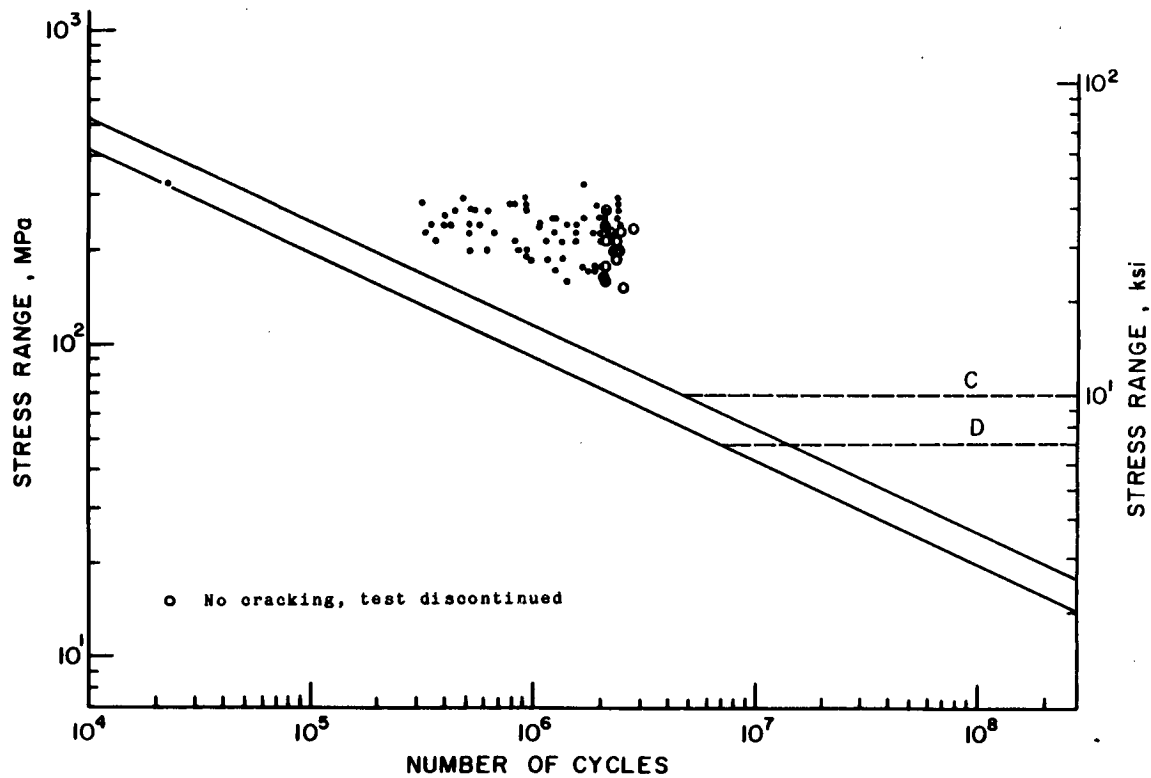

Figure 16. Fatigue resistance of riveted steel connections with subdrilled and reamed holes.
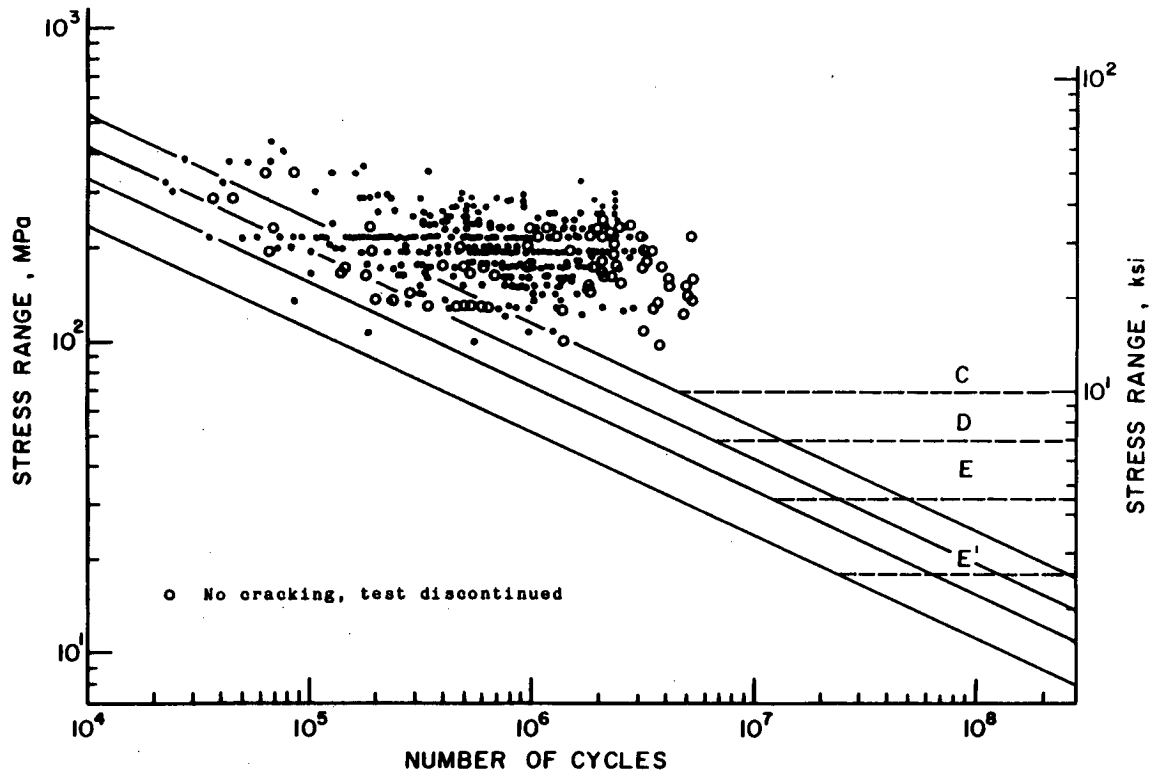
Figure 17. Fatigue resistance of riveted steel connections, specially fabricated for laboratory test.
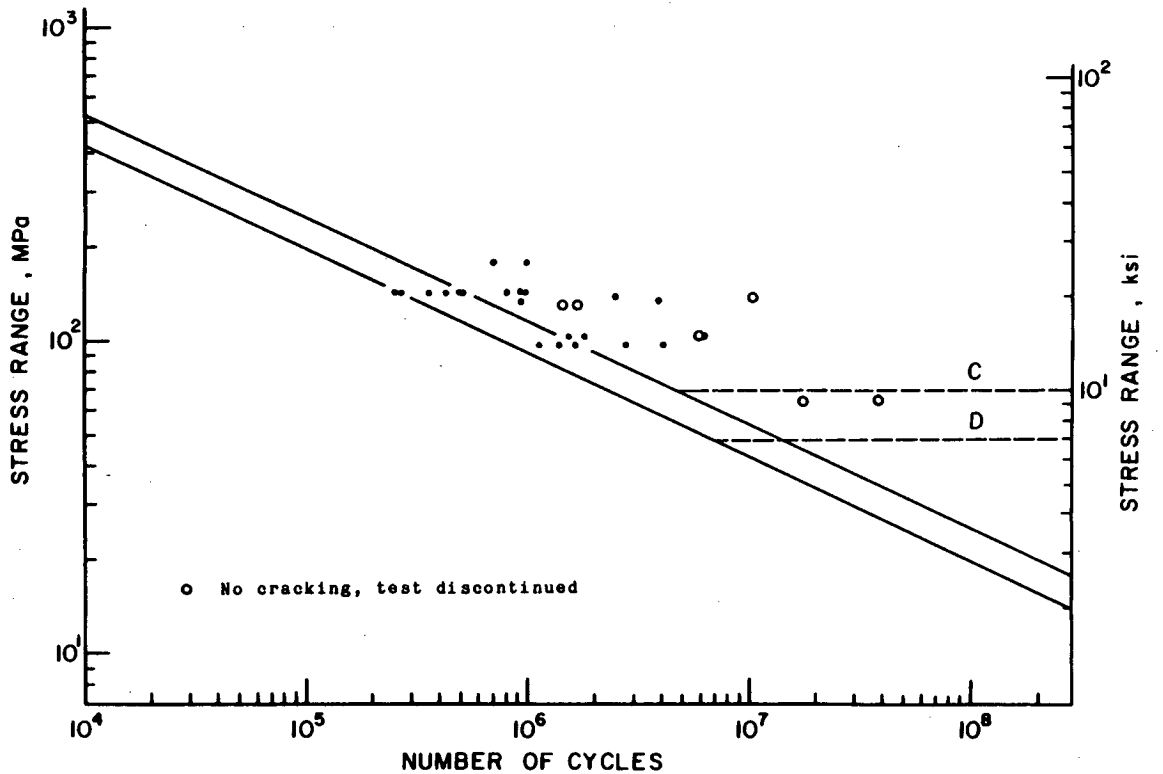
Figure 18. Fatigue resistance of riveted steel connections, fabricated from existing structures.

were drilling, punching, subdrilling and reaming, and subpunching and reaming. Figure 19 shows the test results for specimens with drilled and with punched holes, while Figures 20 and 21 show, respectively, the results for subpunched and reamed and subdrilled and reamed holes.

It is apparent that all plate tests with open holes exceed the Category C resistance curve, with the exception of the limited punched hole data shown in Figure 19. Both the subpunched and reamed, and the subdrilled and reamed, holes provide a fatigue resistance higher than the resistance of the drilled and punched holes. However, from Figure 19 it is clear that the amount of test data with the latter condition is too small to compare these respective conditions.

A comparison of the fatigue strength of plates with holes (Figs. 19 to 23) to the fatigue strength of riveted specimens (Figs. 13 to 16) shows the former is clearly higher than the latter. This indicates that bearing ratio has a detrimental effect which is larger than the beneficial effect of the clamping force on the fatigue resistance of riveted specimens.

c. Influence of Specimen State

The influence of the specimen state is shown in Figures 22 and 23. Figure 22 shows data points from specimens specially fabricated for laboratory tests from virgin material. Test results on specimens manufactured from old material, with either newly drilled or original holes, are shown in Figure 23.

It can be observed from these figures that specimens made from "new" material exhibit better fatigue resistance than specimens made from "old" material. Furthermore, newly drilled holes appear to produce longer fatigue lives than existing holes, as can be observed from Figure 23. It is likely that this difference can be explained by observing that the drilling of holes for laboratory tests would typically be done with more care than in outside practice, and by some accumulated fatigue damage from service in the case of existing holes. No existing cracks prior to testing were reported for any of these specimens.

Category C is applicable for specimens with newly produced open holes regardless of the age of the material, whereas Category D holds for old specimens with existing holes.

3.2 REVIEW OF TEST DATA ON WROUGHT IRON COMPONENTS

Wrought iron was the predecessor of mild steel as the principal construction material for riveted highway and railroad bridges. A number of these bridges survive and perform their function today. Little was known about the fatigue behavior of riveted wrought iron until in the recent past when national railroads started investigating this behavior (9,18,24).

Figures 24 and 25 summarize the available test data on riveted wrought iron specimens and wrought iron plate specimens with open holes. All of the specimens with open holes had original holes, although a few contained newly drilled holes. Addition-
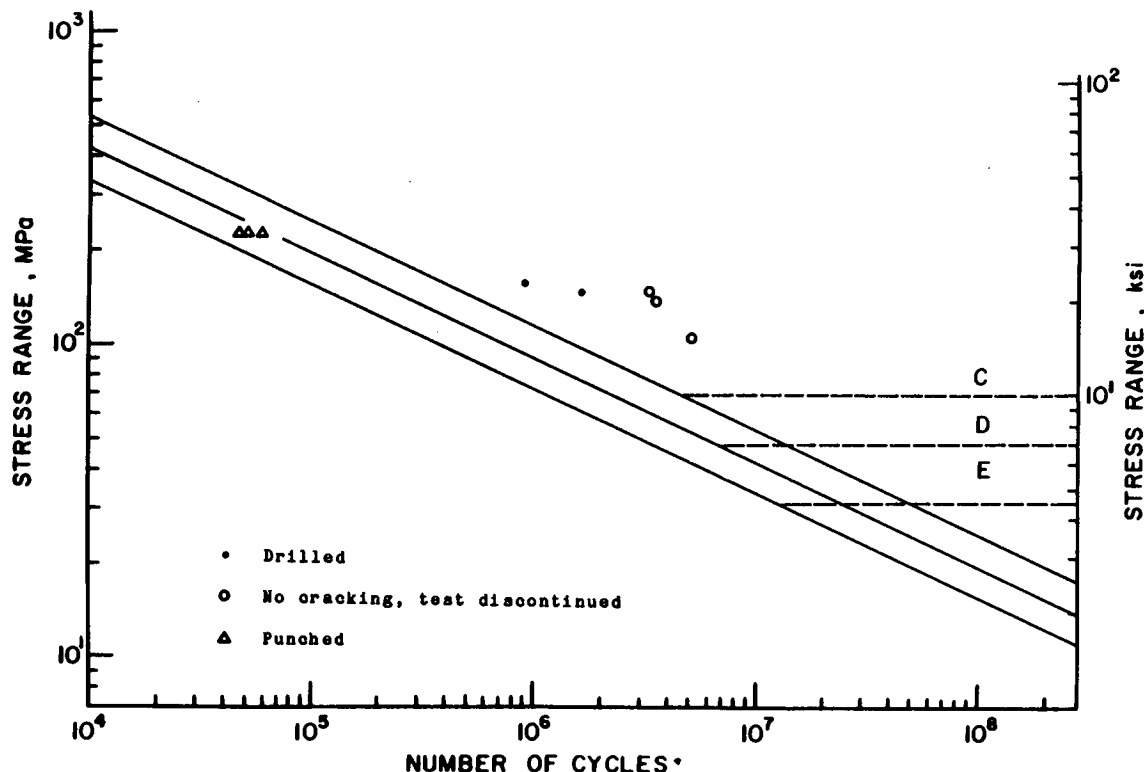
Figure 19. Fatigue resistance of steel plates with open drilled or punched holes.
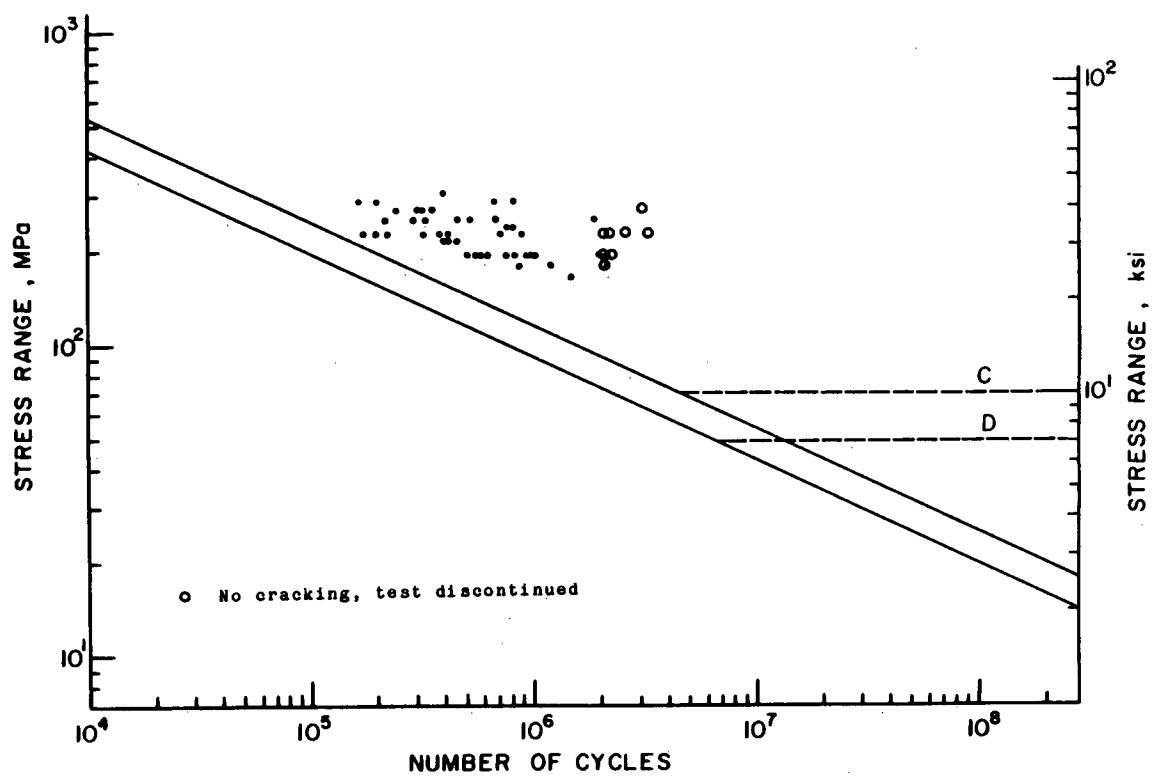
Figure 20. *Fatigue resistance of steel plates with open subpunched and reamed holes.*
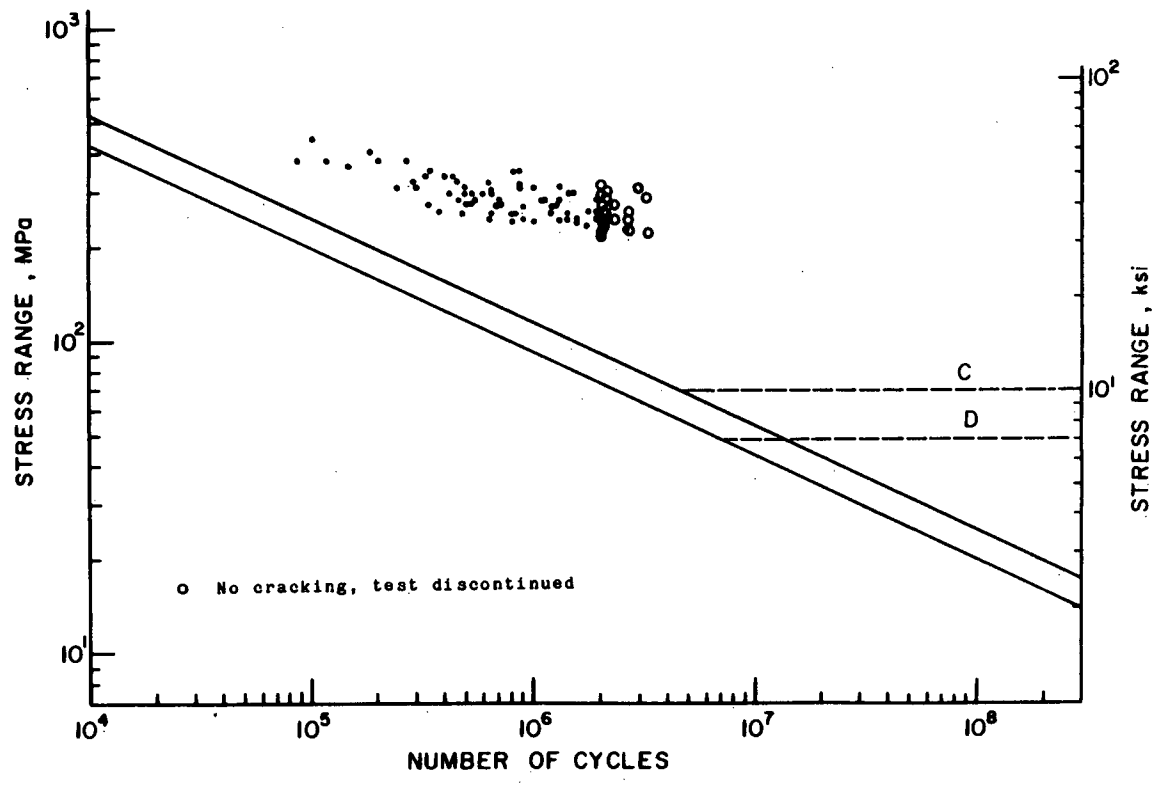
Figure 21. *Fatigue resistance of steel plates with open subdrilled and reamed holes.*
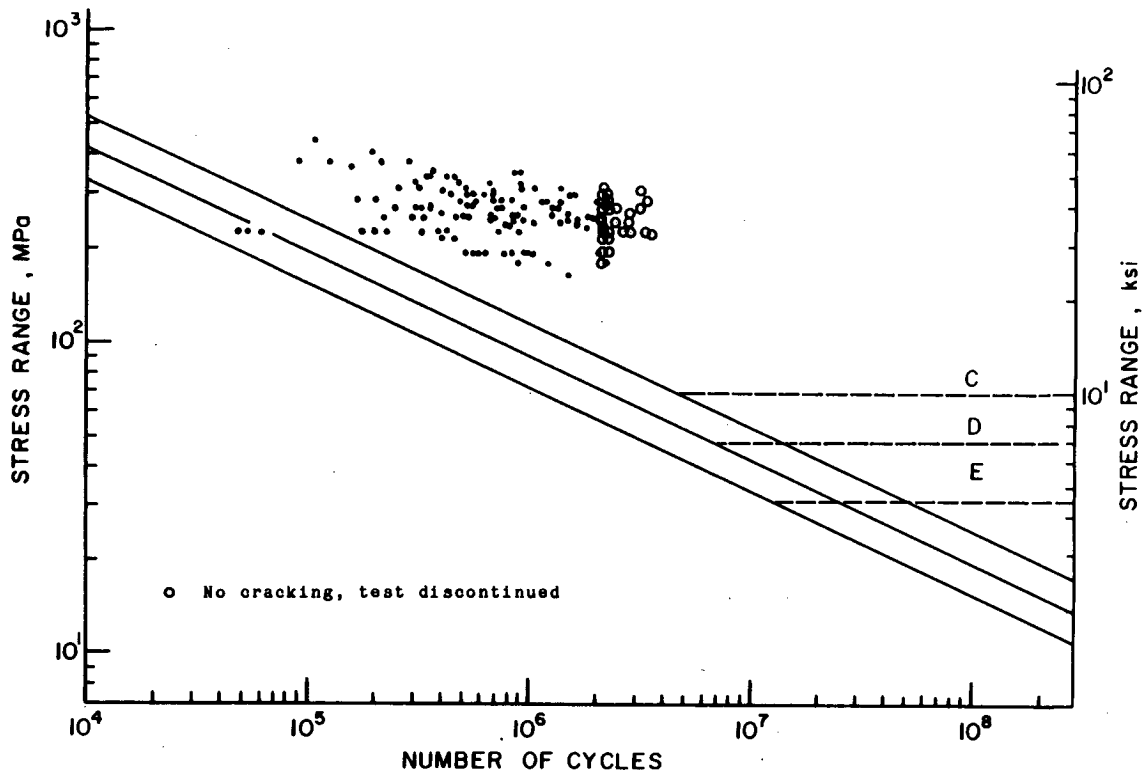
Figure 22. Fatigue resistance of steel plates with holes fabricated for laboratory tests.
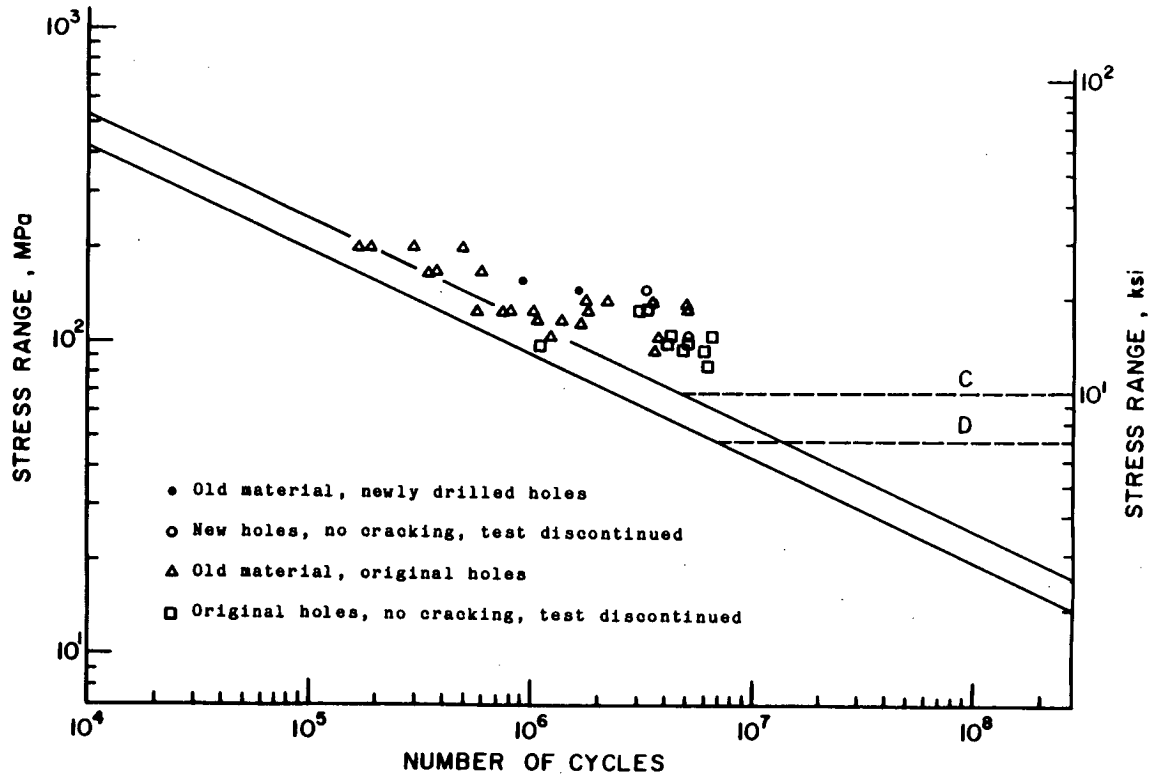
Figure 23. Fatigue resistance of steel plates with new or existing open holes, fabricated from existing structures.
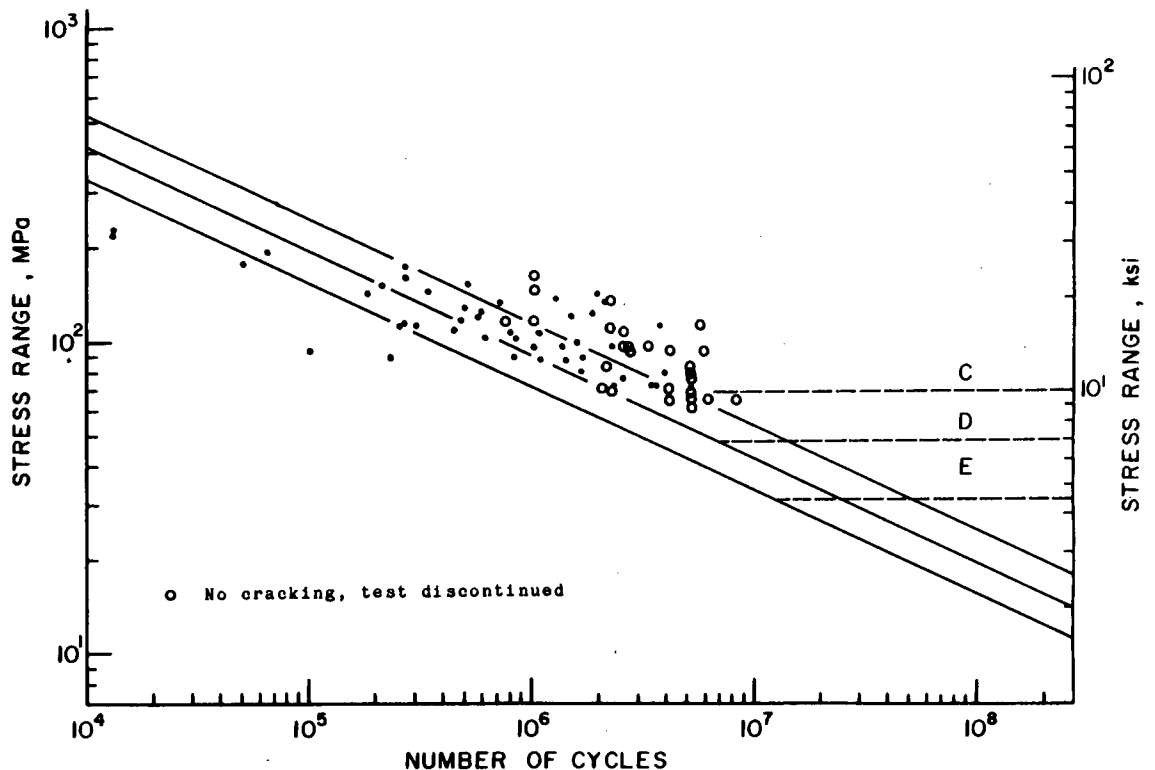
Figure 24. Fatigue resistance of wrought iron riveted connections.

ally, the vast majority of the specimens tested were oriented in the rolling direction of the material.

A comparison of Figures 24 and 25 indicates that there is no major difference between the behavior of riveted specimens and the plate specimens with open holes. The lower bound fatigue resistance falls between Categories D and E. A few specimens provided resistances below Category E, but the corresponding stress ranges tended to be high so as to induce low cycle fatigue phenomena. Two of the riveted specimens exhibiting a fatigue strength below Category E and tested at a stress range of 13 ksi (90 MPa) had been tested before at lower stress ranges and may have contained cracks hidden by the riveted head that were not reported (*18*).

A comparison of Figures 1 and 24 indicates that riveted wrought iron connections have a fatigue strength lower than riveted steel connections: between Categories D and E. Considering maximum stress limitations, it appears reasonable to use Category D for the fatigue resistance of wrought iron components.

3.3 FATIGUE TESTS ON FULL SIZE RIVETED MEMBERS AND CONNECTIONS

3.3.1 Review of Test Data

Fatigue tests on full scale steel members and connections are not very extensive. The first tests were carried out by Reemsnyder on truss connections from riveted ore bridges (*22*). The primary objective of these tests was to develop methods of fatigue life extension by replacing the rivets with preloaded high strength bolts. The tests were carried out at relatively high stress

range levels. Altogether, 18 tests were conducted on truss connections. The connection geometry is shown in Figure 26. Sixteen of the tests were on full scale models, and two tests were carried out on members taken from service. Also two test specimens were tested under a variable amplitude duty specimen.

Only six of the connections were tested to failure. The remaining connections were retrofitted with high strength bolts in order to extend their fatigue life. Small cracks were detected in the rivet holes of the connections, and cycle life at the time the connection was rehabilitated is shown in Figure 27. The test results show that the cracks that were detected in the connections of the rolled elements attached to the gusset plates were near the Category D design curve. The connections that failed provided a fatigue strength between Categories C and D. It should also be noted that the stress cycle for all of the tests varied between a negative minimum stress $= -6.5$ or -9.0 ksi (-45 or -62 MPa) to a positive maximum stress $= 11.6$ or 13.7 ksi (80 or 94.5 MPa). Hence, the R ratio was either from -0.56 or -0.66. The test results, based on the full stress range, are in reasonable agreement with other tests not subjected to partial reversal of the stress cycle.

The fatigue tests carried out by Kulak and Baker (*3*) were on portions of hanger angles removed from a highway truss bridge. Figure 28 shows the test specimen. The tests were carried out at a stress range of 24 ksi (165 MPa) and 27.2 ksi (188 MPa). Most of the failure occurred beyond the Category C resistance curve, as can be seen in Figure 27. All of the rivets in the test sections were tight, and there was no evidence of flaking paint or corrosions of the surfaces.

All of the fatigue cracks developed in the net section at the rivet hole and propagated toward the toe of the angle. The tests were stopped when one angle of the pair cracked in two.
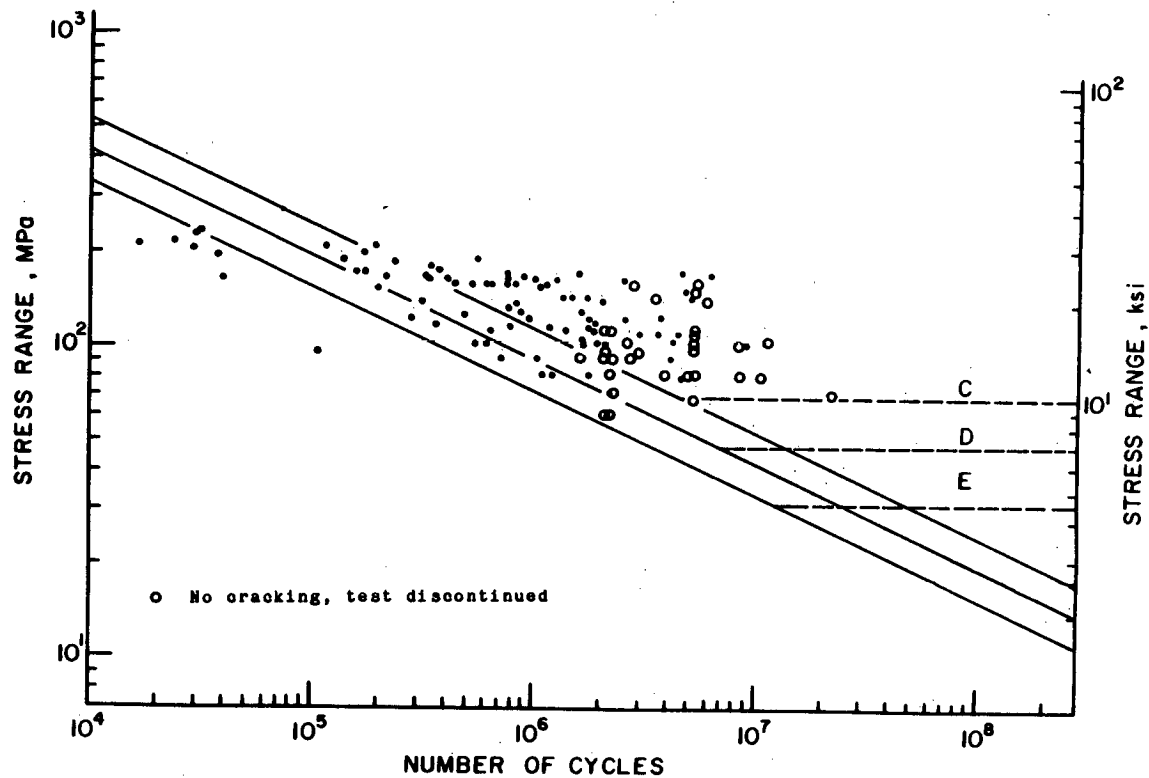
Figure 25. Fatigue resistance of wrought iron plates with open holes.

O   No cracking, test discontinued
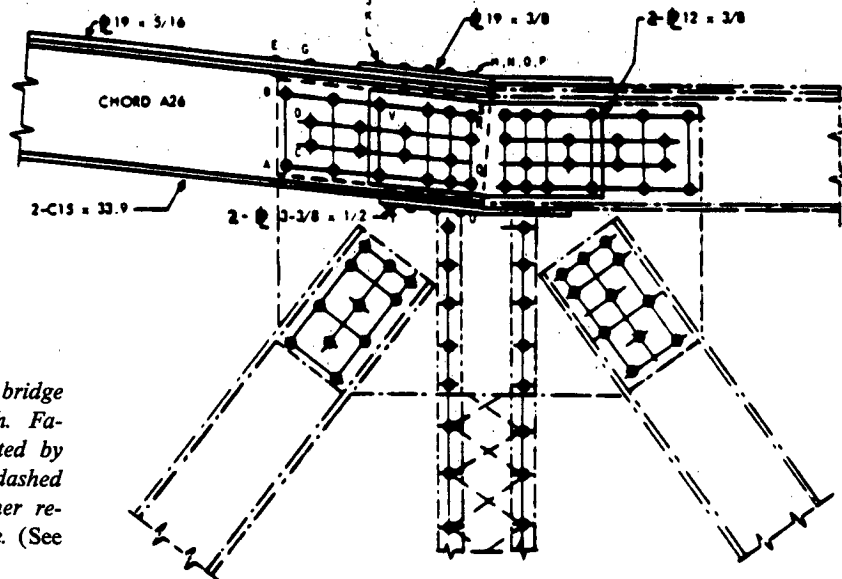
Figure 26. Details of one bridge tension chord connection. Fatigue specimen is indicated by solid lines; prototype, by dashed lines; and sites of fastener replacement, by solid circle. (See Ref. 22)
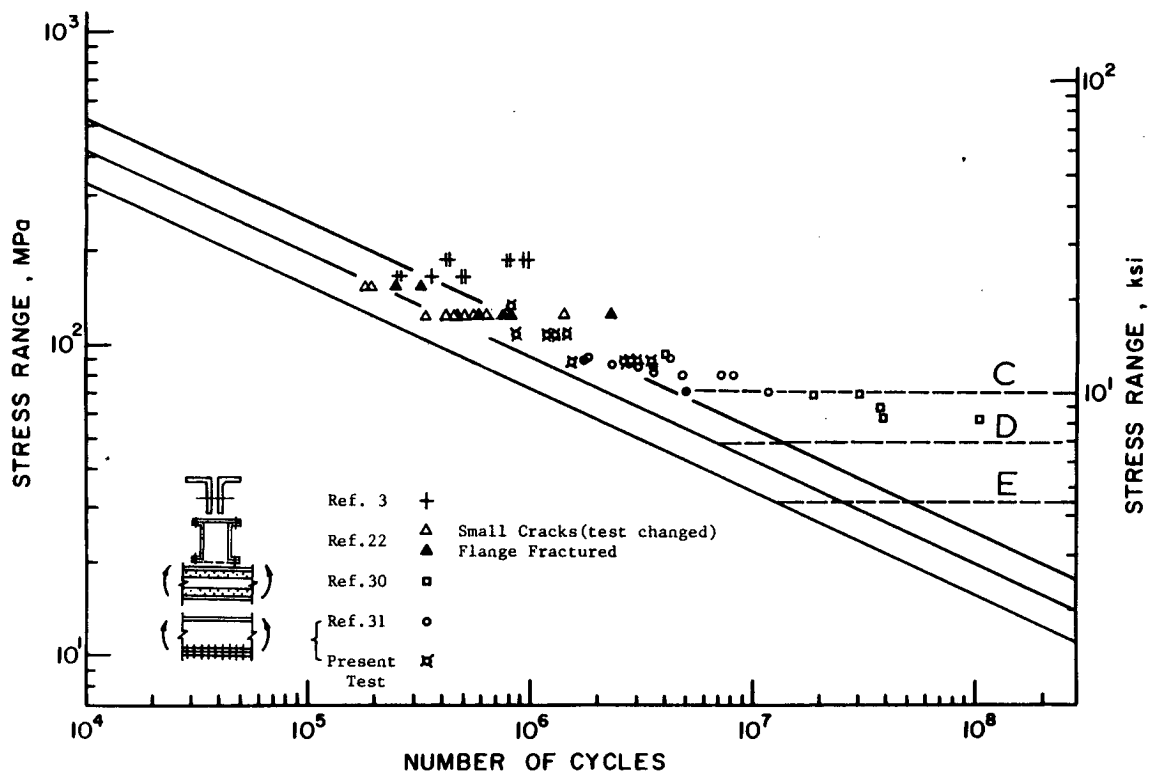
Figure 27. Fatigue test data for full-scale members taken from bridge structures.

Six riveted built-up stringers were tested by Out, Fisher, and Yen (30) with primary focus of the high cycle fatigue behavior under constant cycle stress ranges between 7 and 10 ksi (48 and 69 MPa). The fatigue tests were conducted on stringers which had been removed from riveted truss railroad bridges supporting a single track. Strain measurements made while the structure was in service indicated that about 1 percent of the stress cycles exceeded the Category D fatigue limit 7 ksi (48 MPa), so that the cumulative fatigue damage from service was negligible (12).

The six stringers were built-up I-shapes 39 in. (1 m) deep and consisted of a web plate and four angles, connected to the web by two rows of rivets, as shown in Figure 29. No evidence of initial cracks from prior service was observed at any of the cracks that formed at the riveted sections.

Fatigue cracks were observed to develop at the rivet holes at the net section of the riveted member. The test results are plotted in Figure 30 for the first observed crack in one of the riveted components based on the net section stress range. Failure of the flange angle developed in two stringers.

One stringer failed because of fatigue crack extension and the second stringer because of fracture at a reduced temperature. The fatigue cracks in the two flange angles were 3.54 in. (89 mm) and 6.0 in. (152 mm) long at fracture. The cracks in the other four beams developed in both angles and varied in length between 2 in. (51 mm) and 5 in. (127 mm) at the time the cross section was retrofitted, so that testing could continue.
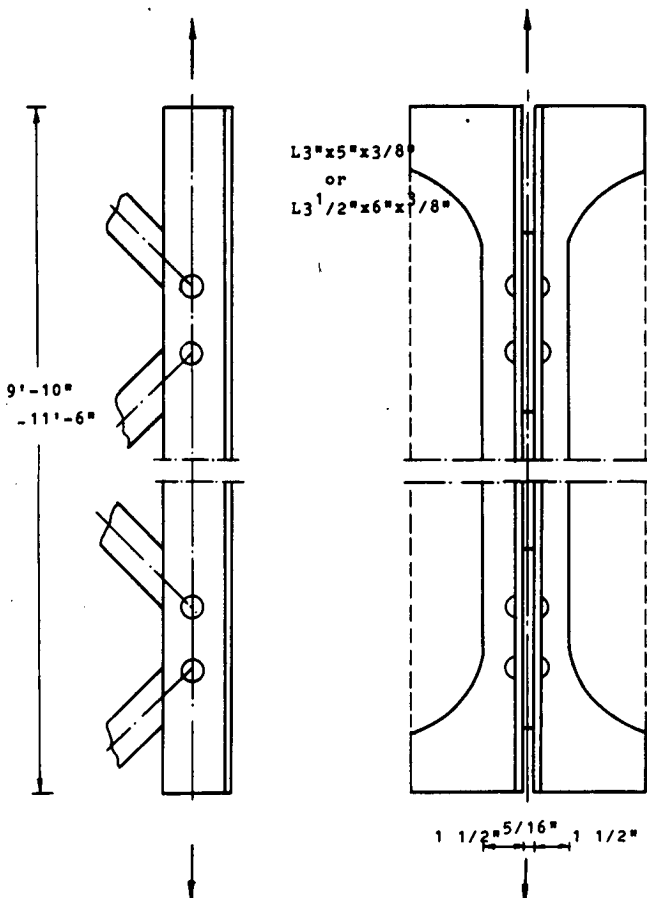
Figure 28. Riveted test specimen fabricated from highway truss bridge hangers. (See Ref. 3)

22
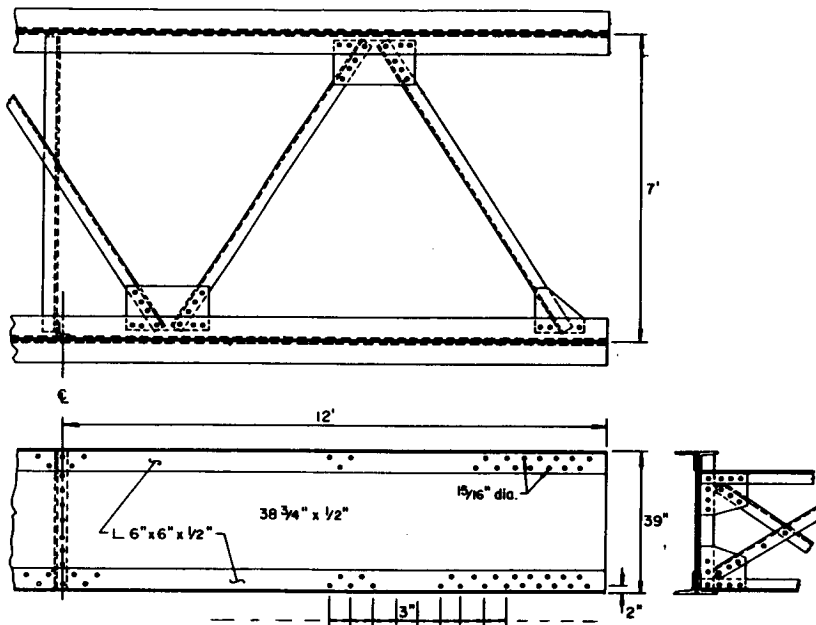
Figure 29. Stringers of the French Broad Ivy River Bridge. (See Ref. 30)
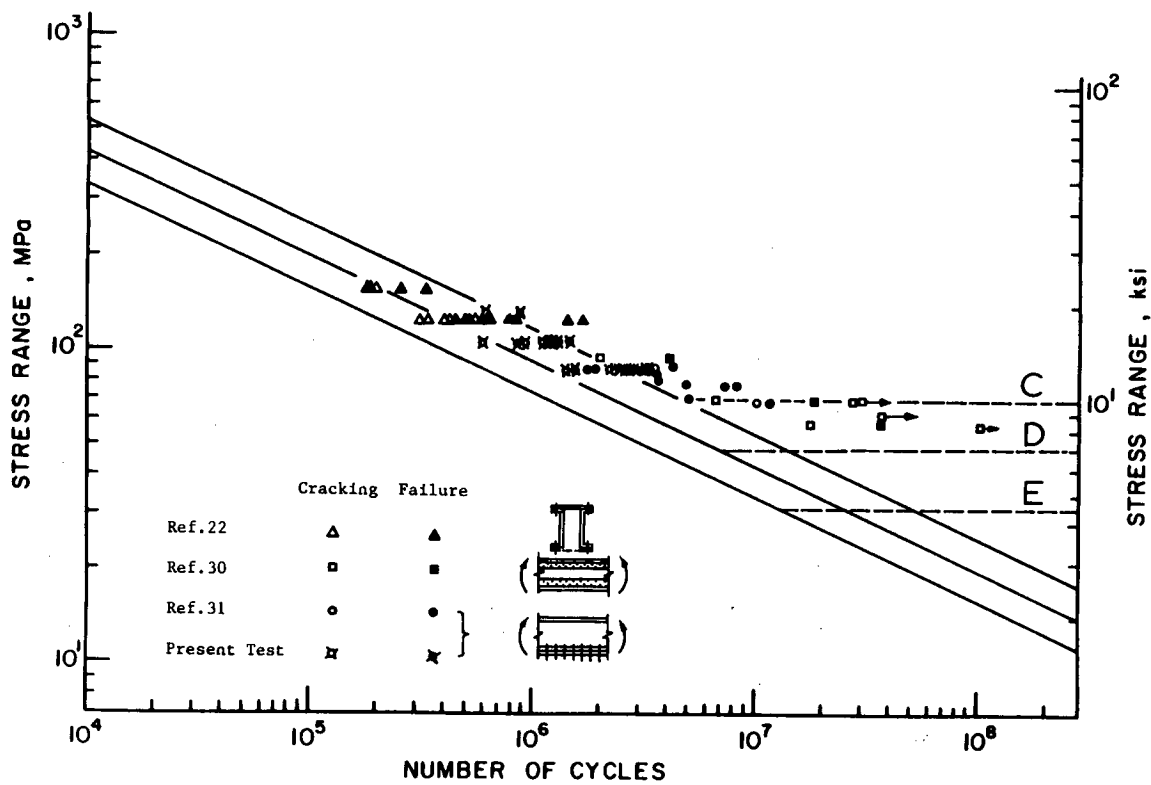
Figure 30. Comparison of first detectable cracking and failure of the sections of full-scale members.

Fatigue cracking was observed to occur below the fatigue limit for Category C = 10 ksi (69 MPa). Two cracks developed below the fatigue limit of Category D = 7 ksi (48 MPa). Both of these cracks were located in a shear span. The stress condition corresponding to bending and shear is slightly more severe than bending alone, if the rivets are in bearing.

The literature review demonstrated that clamping force and bearing ratio were the principal variables influencing the fatigue resistance of riveted joints. Most of the cracked rivet details in the test beams were located in a constant moment region. Hence, the rivets did not transmit a significant bearing force. This was a favorable condition. In addition, the rivets appeared to be tight, which is favorable as well.

Four large rolled steel sections with a full riveted coverplate were tested at ICOM, Lausanne, by Rabemanantsoa and Hirt (31). Two of the beams had the coverplate cut in each shear span so that a riveted coverplate termination was simulated. Figure 31 shows the riveted cross section and the geometry of the test section. Fatigue cracks formed first in the net section of the flange of the rolled section two times. Cracks formed first in the net section of the coverplate three times. Only one crack developed that was not at the net section. This occurred in the coverplate near a rivet head.

The tests were carried out under four point bending. The cyclic stress was applied under constant cycle loading with a minimum stress of 1 ksi (7 MPa). The stress range varied between 10.3 ksi (71.4 MPa) and 13.1 ksi (90.9 MPa).

The test results are summarized in Figure 27. The cracks that formed in the rolled section at the coverplate termination are identified as circles. The cracks that developed at other sections are identified by the solid dots. Two of the cracks that formed adjacent to the coverplate termination developed in the second row of rivets, not in the row adjacent to the coverplate terminations.

The test results do not indicate much difference in fatigue resistance of the coverplate termination and the continuously riveted coverplate.

3.3.2 Summary of Fatigue Test Results

The test results reviewed in Chapter Three have demonstrated that stress range provides a reasonable definition of fatigue resistance. Category D is seen to provide a lower bound estimate of net section fatigue strength for simple shear splices, riveted built-up girders, and complex truss connections.

The tests on large scale riveted members and connections summarized in Figures 27 and 30 are compared with the tests on simple shear splices in Figure 32. All tests at extreme bearing ratios $(F_b/F_a > 1.5)$ and with the clamping force reduced by removing the rivet head were eliminated from the data base for Figure 32.

The comparison demonstrates that various types of riveted members and connections are not significantly different. Stress range on the appropriate net section of each type of riveted detail can be seen to provide comparable fatigue resistance for the test data plotted in Figure 32.

The test results also indicate that failure of the cross section and loss of load-carrying capability only develop after Category C is exceeded. Small cracks were consistently detected near the lower bound provided by Category D.

The only extreme life data available are from the riveted beam
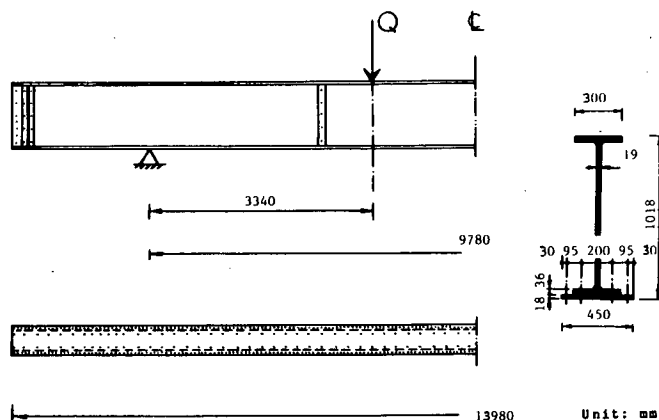
Figure 31. Schematic of riveted girder specimen. (See Ref. 31)

tests reported in Ref. 30. Fatigue cracks can be seen to develop at stress range levels between 7 and 10 ksi (48 and 69 MPa). Only one girder was able to achieve 10^8 cycles without cracking.

3.4 REDUCED TEMPERATURE TESTS

3.4.1 Summary of Test Results

Prior to this study, only two reduced temperature tests have been carried out on fatigue cracked riveted members (30). The objective was to establish whether or not brittle fracture would occur and how the fracture would affect the behavior of the riveted cross section. When the cracked section reached the desired test temperature of −40 F to −60 F (−40 C to −51 C), cyclic loading was resumed at a frequency of 250 cpm (4.33 Hz), and the crack front advanced in a stable, fatigue mode. The cyclic loading was continued for a period of ½ hour to 1 hour at the reduced temperature. Then the crack would be propagated at room temperature for an additional ½ in. (12 mm) to 1 in. (25 mm). This procedure was repeated until failure.

No unstable crack extension occurred in the cracked angle of one beam. During the process of crack extension, the net section stress increased by about 30 percent.

The second reduced temperature test was carried out with a pattern of fatigue cracking that was substantially different from that observed in the first beam as a crack front existed in each of the components. No crack instability developed during the first two low temperature −40 F to −60 F (−40 C to −51 C) fatigue crack extensions which are shown schematically in Figure 33. Cleavage crack extension occurred in each of the beam elements at failure when the fatigue crack fronts in the three cracked elements exceeded half the angle area and the web crack extended above the legs of the angles (see Fig. 33).

An indication of the fracture characteristics of the material was obtained by performing a series of Charpy V-notch impact tests on 18 specimens, taken from a tension flange angle of one of the stringers. Temperatures varied from 0 F (−18 C) to 150 F (66 C). Results are summarized in Figure 34.

A large variation in absorbed impact energy can be seen at test temperatures between 70 F (21 C) and 110 F (43 C). The estimated 15 ft-lb (20 J) transition temperature was about 70 F (21 C). Hence, the material would satisfy the impact energy
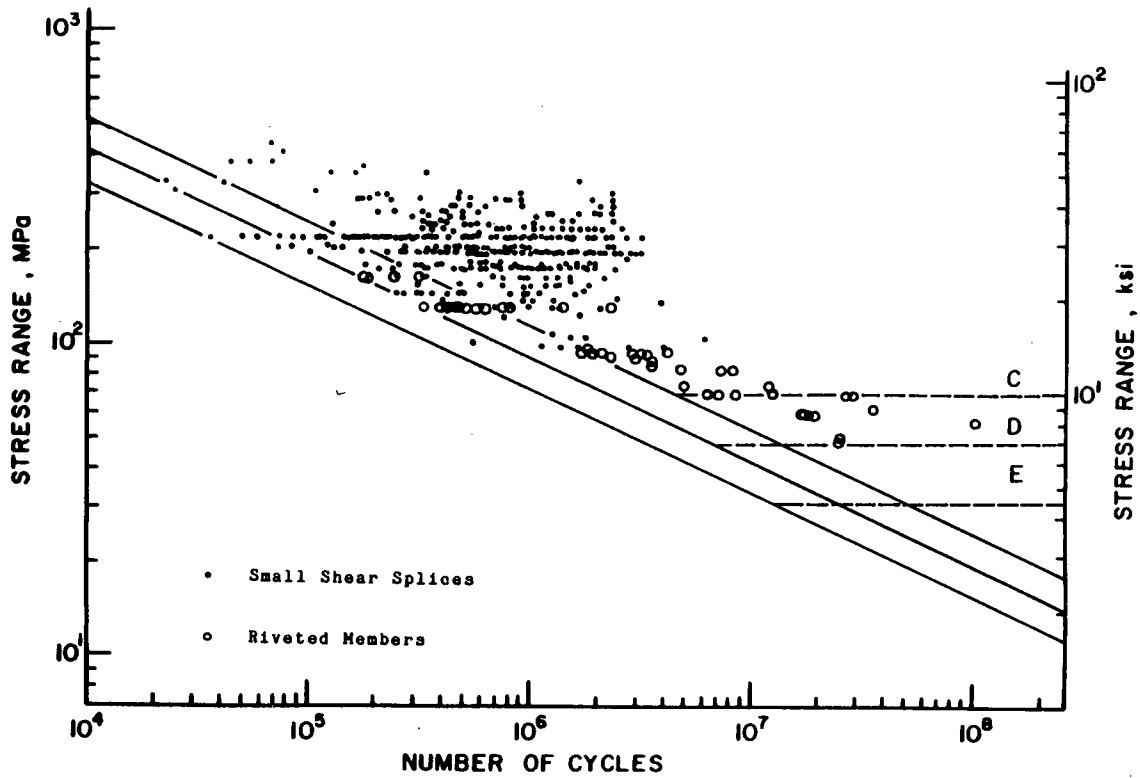
Figure 32. Comparison of fatigue resistance of full-size members with small shear splices.
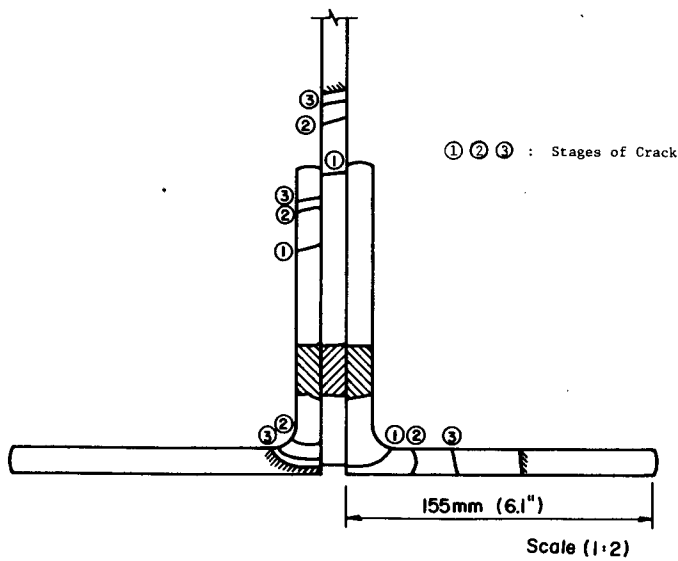
Figure 33. Schematic of beach-marked crack fronts in test beam.
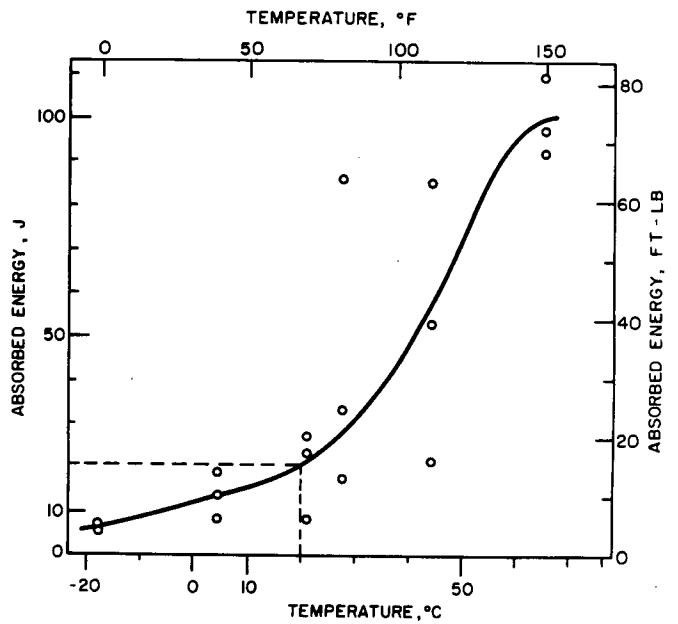
Figure 34. Charpy V-notch characteristics of the flange angle.
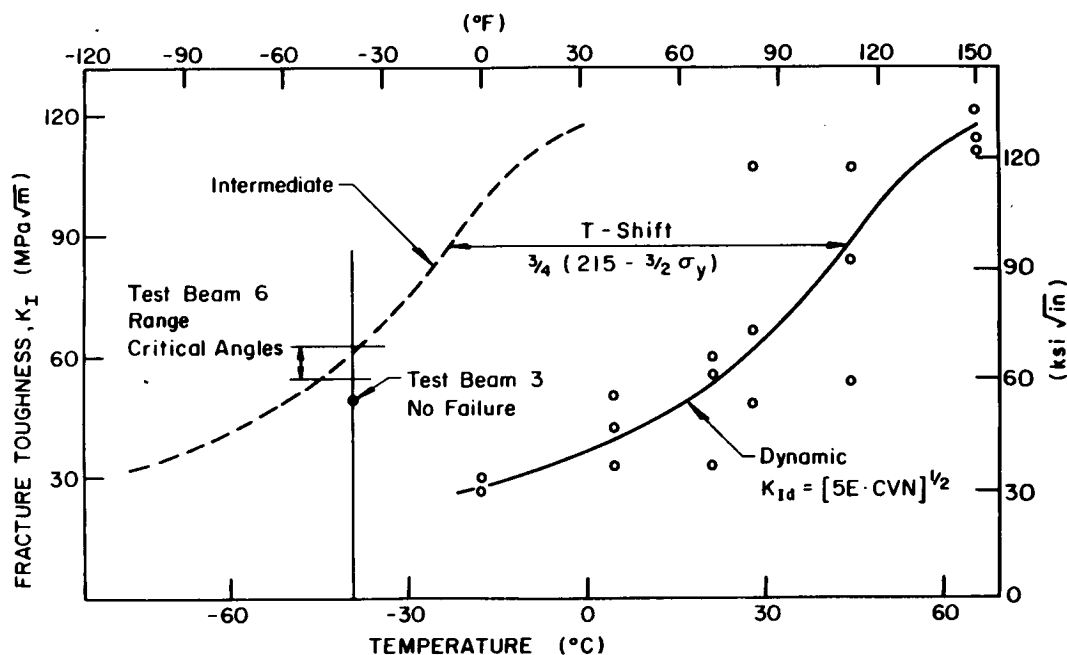
Figure 35. Fracture toughness of the flange angles.

requirement for Zone 2 of the AASHTO and AREA specifications based on average values of impact energy.

Correlations between Charpy V-notch data and K_{Ic} values have provided an empirical relationship between the two measures of toughness. This permits an estimate of the plane-strain (or high-constraint) fracture toughness of the material as a function of the temperature using the Charpy V-notch impact tests (23). The estimated dynamic fracture toughness curve given in Figure 35 and test points were developed from the Charpy V-notch test data. This curve estimates the fracture toughness K_{Id} under impact loading. For intermediate loading rates, corresponding to 1-sec loading, a temperature shift of 120 F (66 C) results from using the strain rate shift. The estimated critical stress intensity factor at failure for the flange angle was about 60 ksi$\sqrt{\text{in}}$. (66 MPa$\sqrt{\text{m}}$) and is compared with the fracture toughness data in Figure 35. When the stress intensity factor was below the intermediate strain rate fracture toughness, no failures occurred in the beams.

The two available fracture tests and the fatigue tests on riveted members demonstrate that alternate load paths are available even when cracks exist in more than one element. Significant cracks apparently have to exist in all elements before brittle fracture causes a loss in the member's ability to carry load. The fact that residual tensile stresses are significantly lower in riveted components also improves their fracture resistance.

3.4.2 Fracture Toughness of Riveted Bridge Steels

A summary of 1209 Charpy V-notch tests at 40 F (5 C) from about 90 riveted bridge structures built between 1890 and 1955 is given in Figure 36. It is apparent that most of the riveted bridge structures have material with fracture toughness characteristics that are similar to the two test beams reviewed in Section 3.4.1. At 40 F (5 C) the average absorbed energy is 10

ft-lb (13 J) (see Fig. 34) for the test beams. This level of absorbed energy permitted very large fatigue cracks to develop in the rolled elements of the girders. Only the beam with large cracks in both angles and the web developed cleavage fracture.

Figure 37 shows a summary of available fracture toughness test results from existing structures built between 1895 and 1958. These fracture toughness test results are compatible with the Charpy V-notch test results shown in Figure 36.

Additional tests are needed to better define the fracture resistance of riveted members and evaluate their ability to redistribute load once significant cracks develop in one or more components of the riveted section.

3.5 BEAM-END CONNECTIONS

Experience with the end connections of through-truss railroad bridges where stringers are connected to floor-beams by connection angles led to an investigation of the fatigue resistance of connection angles (32). It was noted that flexure developed in the outstanding legs of angles from the end rotation of the stringers. This occurred many times and resulted in fatigue cracking. The flexural stress was incidental to the shear capacity, so the connection could be constructed to permit movement without producing stress.

Only nine tests were carried out on simple Tee-connections where the gage between the rivets in the outstanding legs were varied. These specimens were 10 in. (254 mm) wide and simulated the distortion due to flexural rotation. The test results of the five specimens that cracked the angle or did not fail are plotted in Figure 38. For comparison, Category A for base metal is provided because the cracks originated in the fillet of the angle. The calculated flexural stress plotted in Figure 38 assumed that the outstanding leg was fixed at the heel and at the centerline of the rivets in the outstanding legs. Hence, the flex-
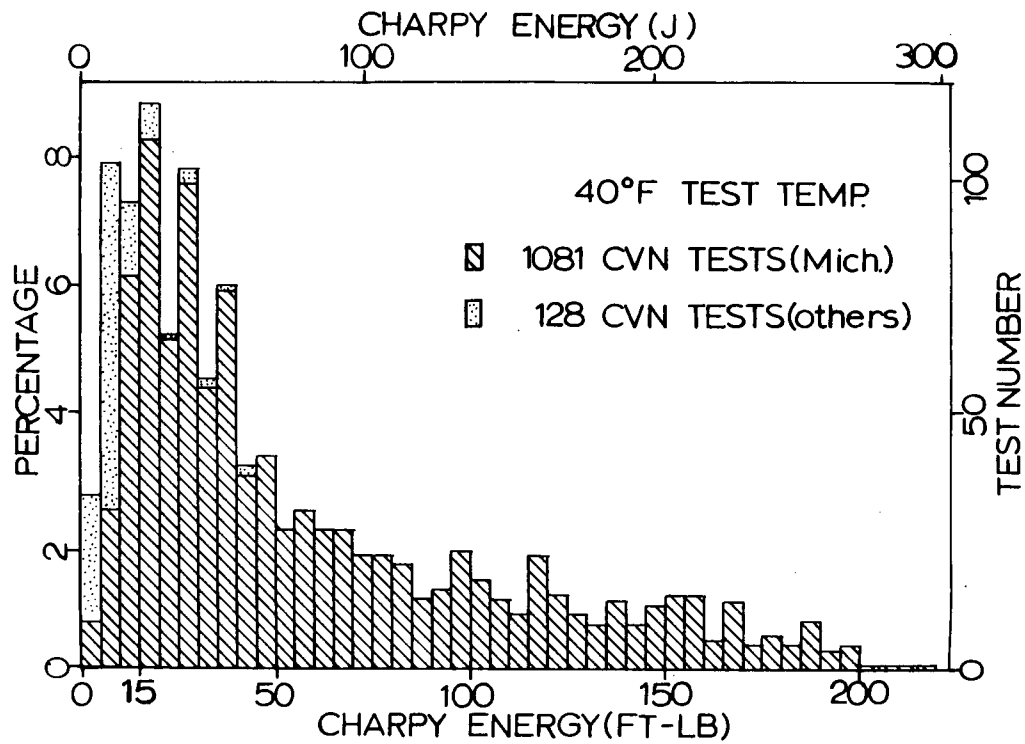
Figure 36. Summary of CVN test data at 40 F (4 C) from test samples removed from bridges.
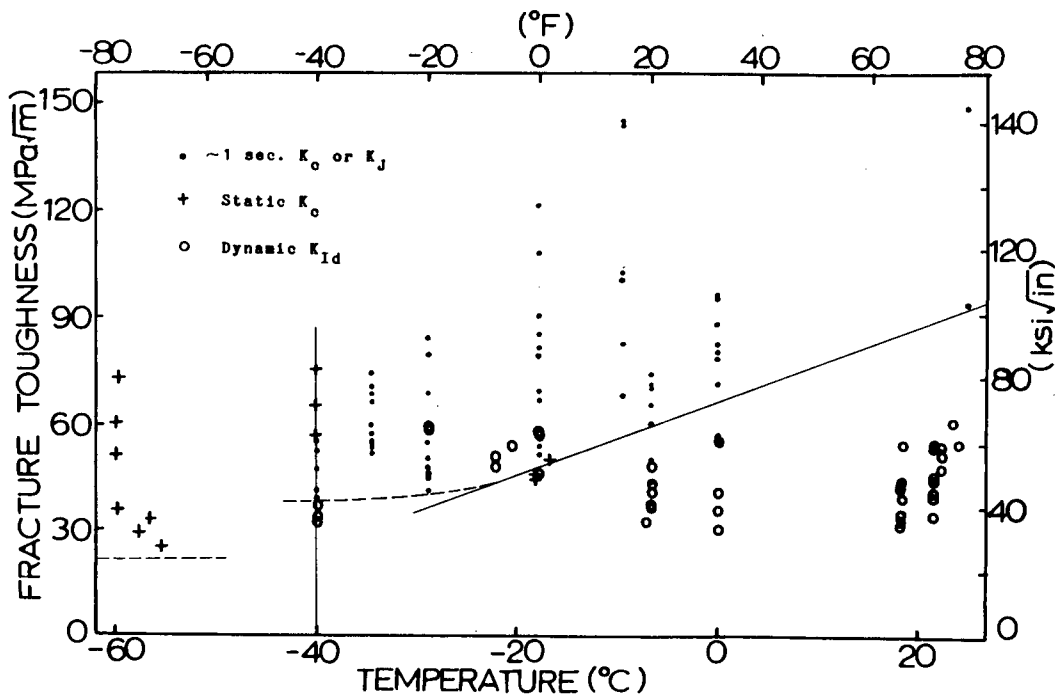
Figure 37. Summary of available fracture toughness test results from existing bridges (1895 to 1958).
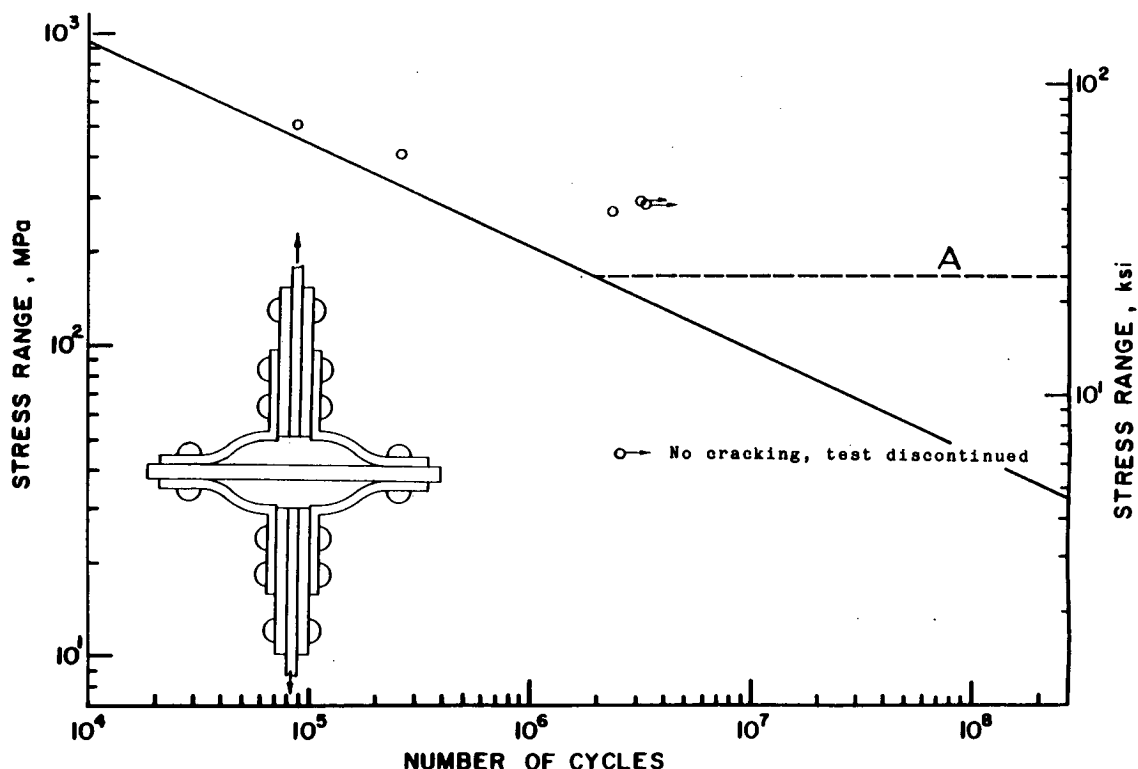
Figure 38. Results of riveted T-stub tests to simulate end connection distortion. (See Ref. 29)

ural stress is overestimated, and the actual stress range is somewhat less. Category A seems a reasonable lower bound fatigue resistance considering the small amount of test data.

To minimize the possibility of fatigue cracking, Wilson (*33*) proposed that the gage of the outstanding legs be governed by the rule

$$g = (Lt/8)^{1/2} \tag{1}$$

where L = span length, t = connection angle thickness, and g = gage of fasteners in the outstanding legs of the upper third of a member's depth. Wilson derived this rule considering the end rotation that occurred in a stringer during passage of a train.

Based on the same reasoning and criteria used by Wilson, a gage of

$$g = (Lt/12)^{1/2} \tag{2}$$

was suggested by Fisher (*34*) for highway bridge structures. Many highway bridges may not satisfy Eq. 2, particularly stringer end connections and diaphragms.

An assessment of the cyclic stress can be made by determining the end rotation and its effect on the angles based on Category A. THis will be conservative as the actual end rotation will be less than predicted for a "simple" end condition.

The known cases of such cracking have been mainly observed in railroad and mass transit rail structures. One system which has experienced this is New York City Transit Authority (*35*).

Cracking develops at or near the throat of the angle and occurs at the top or bottom of the connection. This same type of cracking has been observed in the end connection angles of at least one high strength bolted highway bridge.

3.6 REVIEW OF RIVETED DETAILS AND THE 1987 AASHTO RATING PROVISIONS

A detailed review was made of the riveted members and their details from 12 bridges. No incident of cracking was observed in any of these structures.

3.6.1 Design Details

The members and details were assigned to one of seven groups of classification summarized in Chapter Two. Following is a summary of the observations that were drawn from the evaluation of the design details used in the bridge structures that were examined.

a. Group I—Rivet Patterns for Built-up Flexural Members

(1) *Flange Angles to Web Connection.* Built-up members with web depths between 48 to 108 in. (1219 to 2743 mm), web thickness from $5/16$ to $5/8$ in. (8 to 16 mm), and flange angles 4×3 to 8×8 with thickness from $5/16$ to $7/8$ in. (8 to 22 mm) were considered.
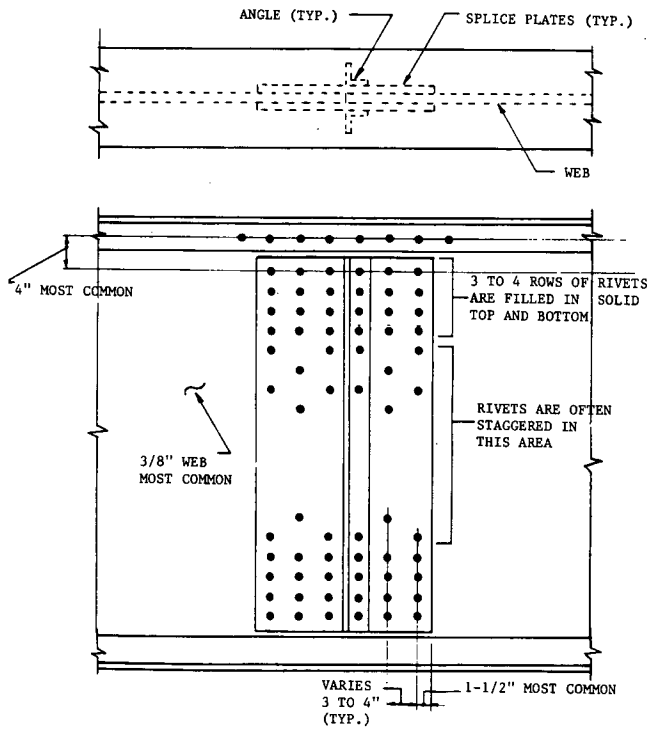
Figure 39. Typical web shear splice in girder.

There were no clear-cut patterns other than rivet spacing in the center of the span which is wider than at the ends. Spacing in the center of span ranges from 3⅝ to 5 in. (92 to 127 mm) and spacing near the ends from 1¾ to 3 in. (44 to 76 mm). These spaces will vary at the field splices (see Fig. 39) and at stiffener angles.

(2) Coverplate to Flange Angle Connections. These rivet spacings follow patterns similar to the flange angle to web connection, with mid-span spacing from 4 to 6 in. (102 to 152 mm) and end spacing 1½ and 3 in. (38 and 76 mm).

b. Group II—Coverplate Terminations

(1) Double Line of Rivets in Each Angle Leg (19 Examples). Coverplate thickness ranged from ⅜ to ¾ in. (10 to 19 mm). The first rivet space from end of plate to rivet ranged from 1½ to 2 in. (38 to 51 mm) with 1¾ in. (44 mm) being the most common, occurring 40 percent of the time. Ninety percent of the time the first rivet was on the outside line of rivets.

The first three rivet spaces ranged from 2¼ to 5½ in. (57 to 140 mm). The spacing of 3 in.-3 in.-3 in. (76 mm-76 mm-76 mm) occurred 60 percent of the time with others ranging from 1 to 10 percent of the time. It should be noted that about 15 percent of the time one or more spacings were relocated to avoid interference with a stiffener or angle. Without this relocation, the 3 in.-3 in.-3 in. (76 mm-76 mm-76 mm) spacing occurrence would be even higher.

*(2) Single Line of Rivets in Each Angle Leg (12 Examples).* Coverplate thickness ranged from ⅜ to ⅝ in. (10 to 16 mm). The space from end of plate to first rivet ranged from 1½ to 2

in. (38 to 51 mm) with spacing of 1¾ and 2 in. (44 and 51 mm) occurring most often. Again, the dominate spacing of the first three spaces is 3 in.-3 in.-3 in. (76 mm-76 mm-76 mm).

c. Group III—Stringer to Floor-Beam Connections

Stringer to floor-beam connections were always accomplished with one angle on each side of the stringer, as illustrated in Figure 40. Occasionally, a seat angle was also used. Spacing between rows of rivets varied according to the size of the angle, the thickness of the web of the stringer, and the rotation of the connection. No clear rivet spacing pattern was seen as typical. However, 3-in. (76-mm) spacing was used about 60 percent of the time on one or both legs of the angle. The gage on the outstanding legs varied from 3⅝ to 5½ in. (92 to 140 mm). The angle thickness varied between 5/16 and ½ in. (8 and 13 mm). All gages satisfied the equation $g > (Lt/8)^{1/2}$.

d. Group IV—Floor-Beam End Connections

Floor-beam connections (angle to web of floor-beam and angles to web of girder or hanger (see Fig. 40) were not found to have a common pattern of rivet spacing. Rivet patterns vary in accordance with the type of geometry and configuration of the connection of floor-beam to girder. The spacing of rows of rivets on the angle to girder connection is dependent on size of angles, thickness of floor-beam web, and use of filler plates or shear plates. The number of rows and gage between rows in the angle to floor-beam connection is dependent on the size of the angle used. (Usually double rows have staggered rivet pattern.)

The gage on the outstanding legs of the end connection angles was found to vary between 5½ and 8 in. (140 and 203 mm). The angle thickness varied from 7/16 to ⅝ in. (11 to 16 mm) with the thinner angles used on spans under 30 ft (9.14 m). All gages but one satisfied the equation $g > (Lt/8)^{1/2}$.

The one gage condition that did not satisfy $g > (Lt/8)^{1/2}$, did satisfy $g > (Lt/12)^{1/2}$.

In the angle to floor-beam connection, the spacing between rivets is usually determined by the spacing used on stiffeners, splices, flange angle to web (in other words, spacing already
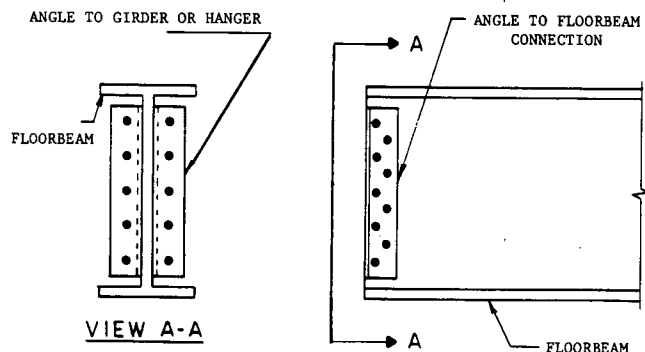

Figure 40. Typical riveted end connection.

used in the floor-beam member). In the angle to girder connection, the spacing between rivets is usually independent of the spacing used on angle to floor-beam.

For rolled section floor-beams, about 40 percent of the time spacing between rivets is the same on both the angle to floor-beam and angle to girder connection (see Fig. 40).

e. Group V—Rivet Patterns for Truss Members

Built-up members for trusses are often box-like sections with corner angles and plates or channels and plates and lacing, as shown in Figure 41. Plate thickness generally varies between ⅜ and 1 in. (10 and 25 mm). The corner angles are 4 × 3½ in. (25 × 90 mm) to 8 × 6 in. (203 × 152 mm) with thickness between ⁷⁄₁₆ and ¾ in. (11 and 19 mm). Channels vary from MC10 × 20 (254 × 508 mm) to MC18 × 58 (457 × 1473 mm) often with a plate attached to one pair of flanges and lacing on the other pair.

Spacing of rivets between the end connections varies from 3 to 13¾ in. (76 to 349 mm).

f. Group VI—Gusset Plate Connection (Truss)

Gusset plate thicknesses vary from ⅜ to ⅞ in. (10 to 22 mm) in the bridge structure examples. The gusset plate shapes vary depending on the number of members at the joint.

The only typical spacing detected is the distance from the edge of the plate to the first rivet. This dimension varies from 1½ to 2½ in. (38 to 64 mm), but 1¾ in. (44 mm) occurs the most often.

With respect to the spacing between rows and spacing between rivets, there seemed to be no recognizable pattern.

g. Group VII—Hanger Connection

Only two examples of hanger pin plate connections were examined. Because of the limited sample size, no pattern was identified. However, the edge of plate to first rivet is similar to other gusset connections with 1¾ in. (44 mm) being common.

The upper and lower connections of the vertical truss members that are only in tension were examined. Gusset plate sizes vary greatly depending on the size of the members and stresses involved. Rivet spaces and spaces between the rows of rivets varied greatly, and no clear pattern can be established. However, some plate edge to first rivet gages occurred often (see Fig. 42).

h. Steel and Rivet Types

The majority of the structures studied incorporate a combination of copper bearing carbon steel and copper bearing silicon steel. Basic allowable stresses were generally 18 ksi (124 MPa) for carbon steel and 24 ksi (166 MPa) for silicon steel.

Most rivets were ⅞ or 1 in. (22 or 25 mm) diameter, with a combination of those two sizes being used in several bridges. One structure incorporated 1 and 1⅛ in. (25 and 29 mm) rivets, with manganese steel used for the 1⅛ in. (29 mm) field rivets.

Rivets which are ¾ in. (19 mm) were specified for three smaller structures of 1890 to 1903 vintage.
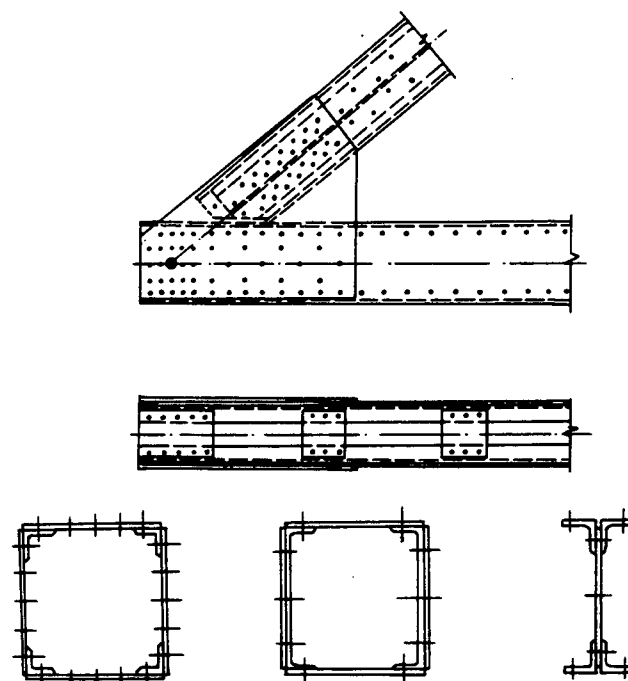
Figure 41. Typical built-up riveted truss members.
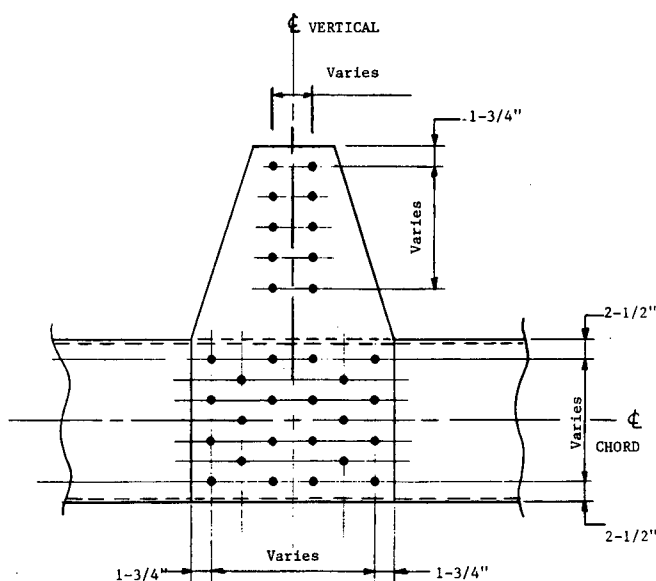
Figure 42. Typical truss hanger connection.

Material requirements for rivets were not generally shown on the drawings, with the exception of two references to carbon steel and manganese steel.

In one case a structure (fabricated in 1950) used ASTM material designations for the structural steel and rivets.

3.6.2 1987 AASHTO Rating Provisions Related to Fatigue and Fracture of Riveted Structures

Since most riveted bridge structures were designed and built prior to 1960, the specifications for checking their capacity are

provided in the AASHTO *Manual for Maintenance Inspection of Bridges* (*37*). The most recent version provides reference to allowable fatigue stresses in Article 5.5.2.5 under the "Load Factor Method." No reference is provided in Article 5.4 entitled "Allowable Stress Method." Section 5.5.2.5 states:

> 5.5.2.5 *Allowable Fatigue Stress.* Article 1.7.1 of the AASHTO *Standard Specifications for Highway Bridges* shall serve as a guide in determining the allowable fatigue stress, F_r. Special structural or operational conditions, policies of the owner or rating agency, and judgment of the Engineer shall likewise influence the determination of fatigue strength.

Article 1.7.2 refers to the 1977 specification. The 1983 edition (*1*) has the corresponding material in Article 10.3. The AASHTO fatigue design provisions assign Category D as the fatigue resistance for riveted connections. The allowable stress range, F_r, is applied to stresses computed on the net section.

The usual engineering practice for highway bridges is to determine the stress range on the net section using static analysis and design loads. The member is evaluated to determine if it is redundant (internally or externally). The assessment is made by following the AASHTO guidelines for new bridges provided in Article 10.3. Overstresses up to 10 percent are generally considered insignificant.

The AREA specification in Part 7 "Existing Bridges" (*2*) permits riveted connections to be considered as fatigue Category C when the rivets are tight (see 7.3.4.2b). This provision acknowledges the higher fatigue resistance of riveted joints with normal levels of clamping force which can be seen in Figure 9. This can also be observed in Figure 27 for stress range levels between 10 and 14 ksi (69 and 97 MPa).

It is also noted in AREA Section 7.3.4.2c that members, which do not satisfy the fatigue requirements of Category D, can have these requirements waived if the connection or the members will retain their structural adequacy should one of the elements crack. This recognizes the load redistribution and continued ability to carry load that is shown in Figure 30. The connection or member that has this waiver applied must have the capacity to carry the redistributed load and must also have a reasonable inspection interval which will permit discovery of a component crack.

No mention is made of the fracture toughness characteristics of the steel in riveted structures in either the AASHTO (*37*) or the AREA (*2*) rating provisions. It is apparent from the Charpy V-notch absorbed energy results plotted in Figure 36 that a substantial population of bridges can be expected to have impact energy levels that will not satisfy the notch toughness requirements of the AASHTO specification. No significant fracture problem has surfaced in either highway or railroad riveted bridge structures.

This fact is, in part, the reason for not imposing a penalty on these structures when they are found to have low levels of absorbed energy. As illustrated in Figure 37, a fracture toughness level of 50 ksi√in. (55 MPa√m) is not an unreasonable lower bound expectation for riveted structures. Since residual stresses in the rolled elements are relatively low, large fatigue cracks can form without crack instability even at reduced temperatures.

3.6.3 Live Load Stresses in Riveted Bridges

During the last two decades a number of stress history mea-

Table 1. Measured live load stresses in riveted bridges.

Bridge Type	Member	Length ft(m)	S_{rmax} ksi(MPa)	Reference
Girder-Floorbeam Continuous Spans 144'-180'-144' (44-55-44 m)	Long. Girder Floorbeam	144 (44) 21 (6.4)	6.0 (41) 7.1 (49)	Ref. 38
Girder-Floorbeam Continuous Spans 104-131-131-104' (32-40-40-32 m)	Long. Girder Floorbeam	104 (32) 43 (13)	4.7 (32) 3.3 (23)	Ref. 39
Girder-Floorbeam Continuous Spans 20@ 149' (20x45 m)	Long. Girder Stringer	149 (45) 30 (9.1)	3.0 (21) 6.0 (41)	Ref. 39
Multiple Girder Simple Spans 85' (26 m)	Ext. Girder Int. Girder Int. Girder	41 (12) 32 (10) 27 (8.4)	2.3 (16) 2.8 (19) 4.2 (29)	Ref. 40
Multiple Girder Simple Span 85' (26 m)	G1 G2 G3 G4 G5	85 (26) 85 (26) 85 (26) 85 (26) 85 (26)	3.8 (26) 5.8 (40) 6.2 (43) 5.4 (37) 3.2 (22)	Ref. 41
Multiple Girder Simple Span	G1 G2 G3 G4 G5	85 (26) 126 (38) 126 (38) 126 (38) 126 (38)	6.2 (43) 5.8 (40) 6.2 (43) 5.0 (34) 6.2 (43)	Ref. 41
Truss 200 ft. Span (61 m Span)	Stringer Floorbeam	25 (7.6) 30 (9.2)	2.8 (19) 2.2 (15)	Ref. 42
Riveted Hanger	Hanger	29 (8.7)	4.5 (31)	Ref. 43

surements have been carried out on riveted bridge structures (*38–43*). These included continuous plate girder bridges with floor-beams and stringers, simple span multiple girder bridges, and riveted trusses. Table 1 summarizes the length, type of member, and the magnitude of the maximum stress range observed during the field measurements. Only one maximum stress range in these riveted bridge members slightly exceeded the estimated fatigue limit for Category D. This occurred for the top flange of one floor-beam (7.1 ksi) that was also susceptible to out-of-plane bending (*38*). Hence, it does not appear likely that riveted highway members will experience fatigue crack growth unless significant secondary restraint or out-of-plane distortion stresses are developed. These possibilities are discussed in greater detail in Section 3.6.4.

The measurements summarized in Table 1 cover a wide range of span lengths and member types. The effective stress range for the stress spectrum was between 1 and 2 ksi for nearly every member. This combination of low effective stress range and the condition that the maximum stress range does not exceed the constant amplitude fatigue limit indicates that riveted members in highway bridges are not likely to experience fatigue cracking.

Exceptions to this observation occur as a result of unanticipated local cyclic stress from connection restraint or out-of-plane distortion in small gaps of girder webs and connection angles.

3.6.4 Distortion and Restraint Cracking in Riveted Bridges

Just as is the case for welded bridges, distortion can introduce secondary out-of-plane bending stresses in small gaps created

by the rivet or bolt patterns. Most often, the distortion develops in a connection angle. This can be the angles used to connect diaphragms to girder webs or connections between stringers and cross-girders.

Figure 43 shows a diaphragm in a skewed highway bridge. Cracking developed in the transverse connection angle, as shown in Figure 44, because of the small gap between the heel of the angle and the rivet restraint line. This is directly related to the behavior experienced at beam end connection discussed in Section 3.5. If Wilson's assumption of fixity along the rivet line and at the outstanding leg of the angle is used (32), the cyclic stress from movement is $S_r = (6Et/2L^2) * D_r = 22$ ksi, where the distance, L, is about 1 in.; the angle thickness is $\frac{1}{4}$ in.; and the out-of-plane movement, D_r, is 0.001 in. Hence, very small movements that result from the relative vertical deflection of adjacent girders causes stress range magnitudes above the fatigue limit.

Figures 45a and 45b show examples of end connection angle cracking as a result of end rotation of the longitudinal members. Eventually, complete failure of the end connection is possible as illustrated in Figure 45b. Girder end connections (whether
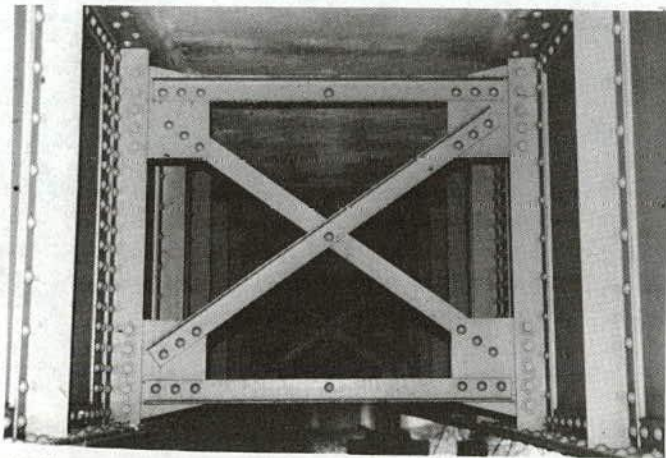

Figure 45a. Crack in stringer connection angle.
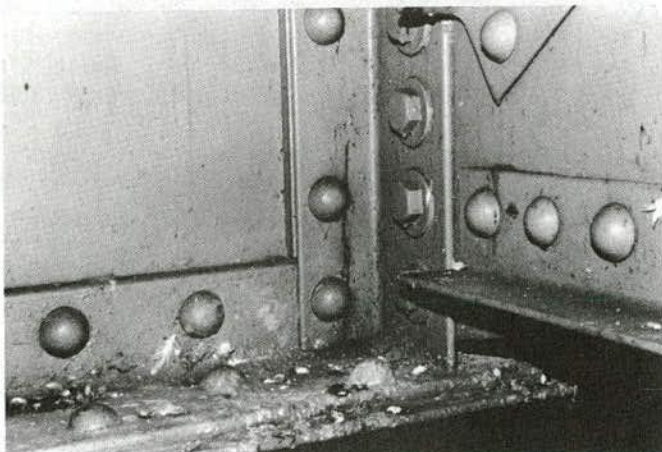

Figure 43. Transverse diaphragm in skewed bridge.
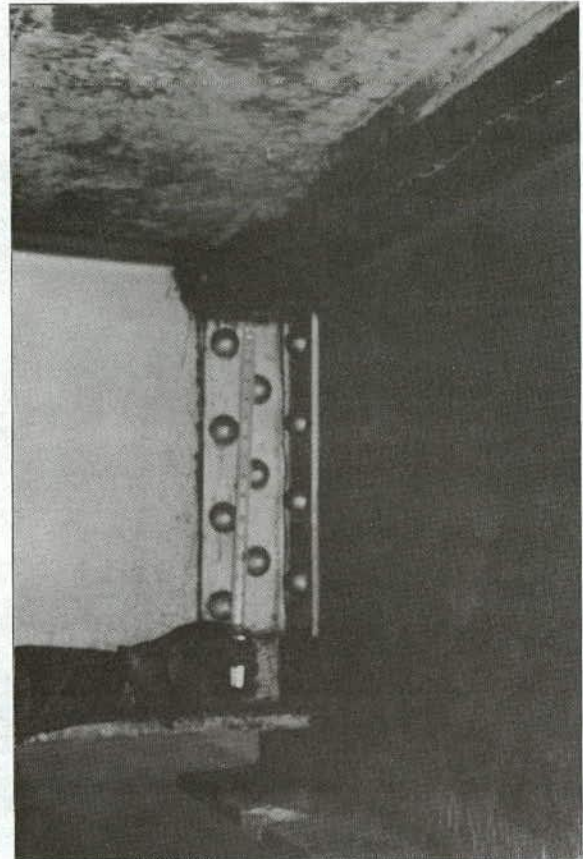

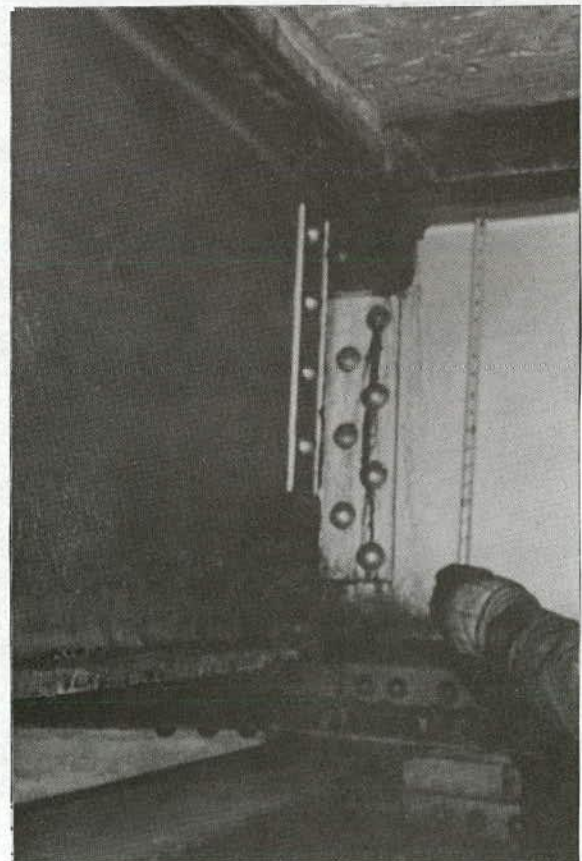Figure 44. Cracking along rivet restraint line.
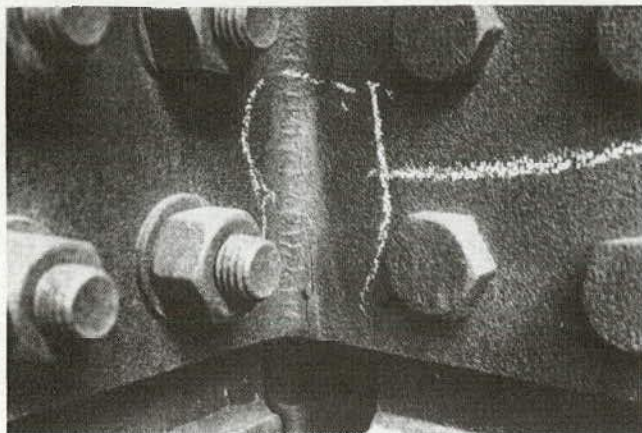

Figure 45b. Failure of stringer connection angle.

Figure 46. Cracking along angle fillet on compression side of end connection.
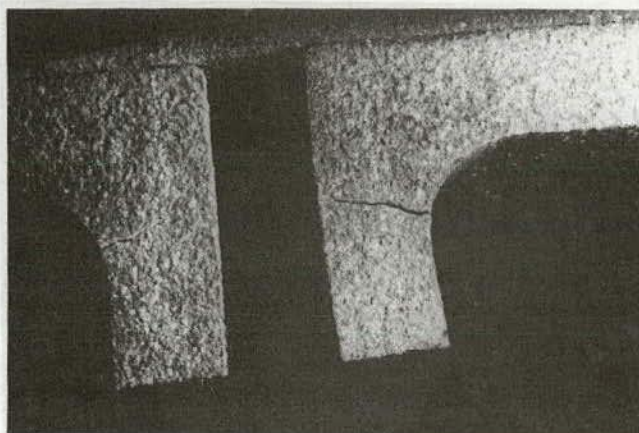
Figure 47. Crack viewed from bottom of connection—note preload deformation.
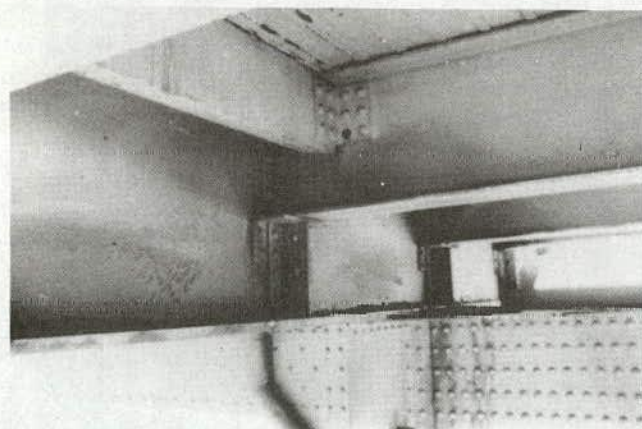
Figure 48. Cracked riveted head in outstanding leg of diaphragm end connection.
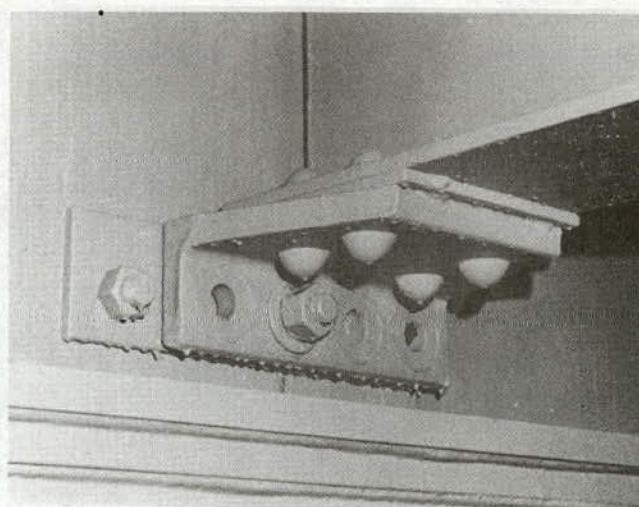
Figure 49. Cracked bolts with cracks forming in the threads under the nut.

riveted or bolted), as illustrated in Figure 46, can also result in cracking of the angle on the "compression side." In the bolted connection shown in Figure 46, construction tolerances resulted in the angles being preloaded so that the portion on the compression side of the girder was also susceptible to cyclic tensile stress. Section 3.5 reviews the available test data on connection angles. Figure 47 shows a view of the ends of the angles, and the deformed outstanding legs resulting from construction preloading can be seen. Apparently, the tolerance of the holes in the cross-girder resulted in the deformed shape and caused the angle to become more susceptible to cyclic end rotation of the longitudinal girder.

Depending on the angle thickness and the gage length of the rivet or bolt lines, the distortion can also result in the cracking of the rivet head or bolt. Figures 48 and 49 show the head of a rivet and several cracked bolts at two diaphragm end connections. In both instances out-of-plane movement of the outstanding angle leg has caused the fasteners to crack because of the axial stress and bending in the fastener.

This type of cracking has also been observed at stringer to floor-beam connections. An example is shown in Figure 50. In this instance, the expected compression region of the end connection has resulted in distortion and prying of the rivet heads. This can occur with flexible floor-beams or from construction tolerances that preload the angle and permit movement under repeated loads.

The restraint provided by end connection can also result in high stresses at coped flanges. This can be further aggravated if any lateral movement occurs. Figures 51 and 52 show cracking in the web at a coped stringer flange. Frequently these copes were formed by flame cutting which results in a residual tensile stress at the flame cut edge. Physical notches often exist as well, and these conditions result in fatigue susceptible details.

A third condition that can result in cracking occurs at blocked flanges or at similar conditions where flame cut notches are introduced at end connections. Figures 53 to 55 show cracks that have developed at flame cut notches as a result of restraint at the end connection.

Figure 50. Cracked rivet heads in outstanding legs of stringer-floor-beam end connection.

Figure 51. Cracks at coped stringer end connection.

Figure 52. Cracking at coped stringer web.

Figure 53. Blocked end connection.

Figure 54. Crack originating at notch from flame cut blocked flange.

Figure 55. Floorbeam flange coped to clear hanger at end connection.
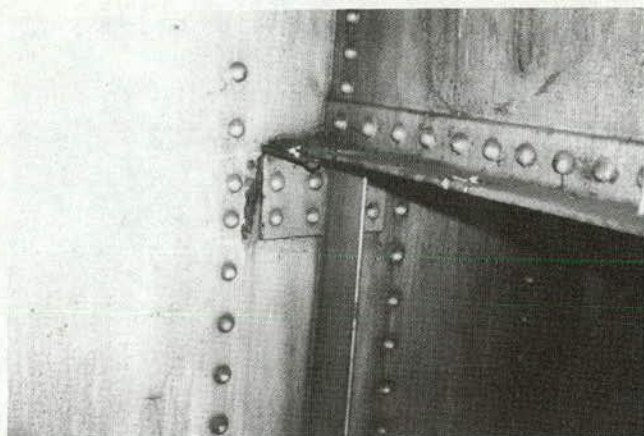
Figure 56. Stringer end seat with crack in floor-beam web.
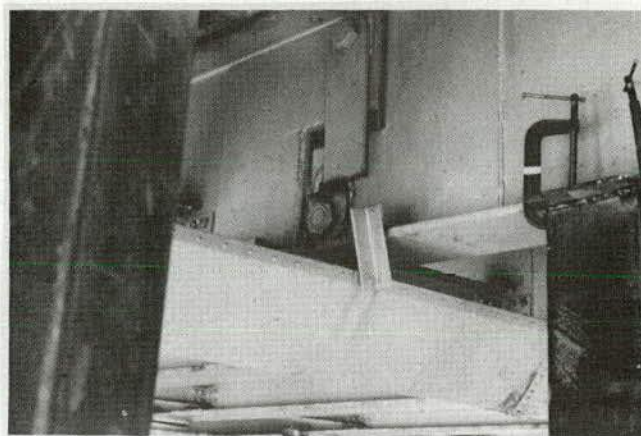
Figure 59. Cracked hanger plate under roadway relief joint.

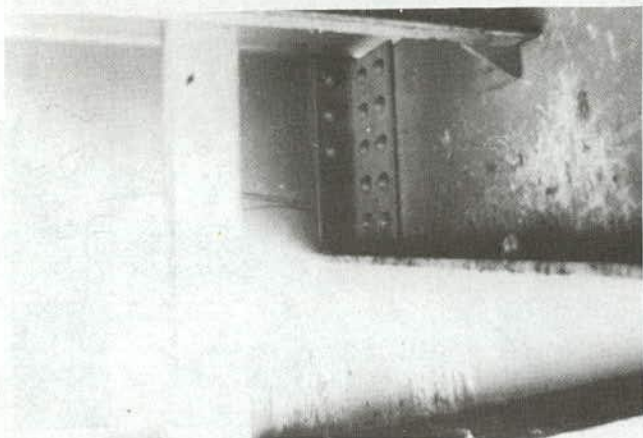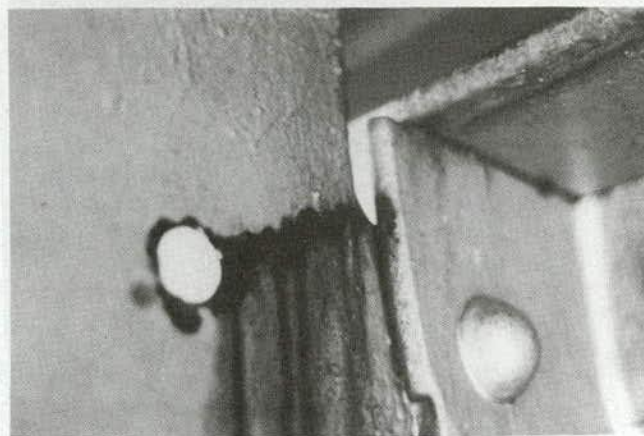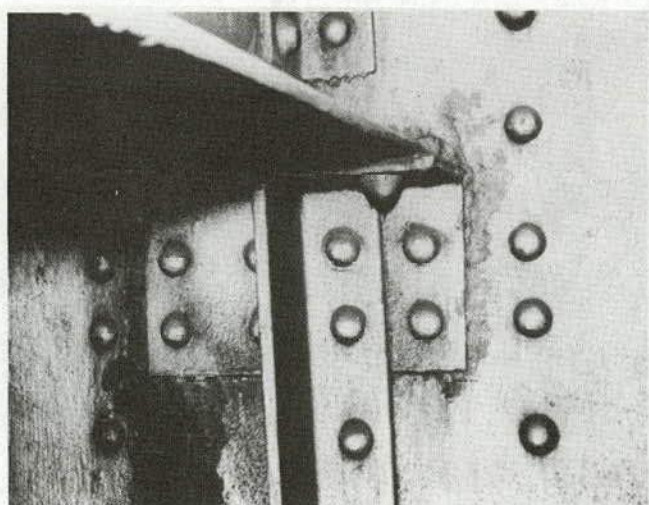Figure 57. Close-up view showing crack in web gap.

Figure 58. Transverse stiffeners behind the beam seat create small web gap.

Small gaps at end connections can also result in web cracking, as shown in Figures 56 to 58. A stringer framing into a floor-beam has its beam seat opposite transverse stiffeners on the backside of the floor-beam, as shown in Figure 58. This creates a small web gap susceptible to the stringer end rotation between the beam seat and the transverse stiffener angles. As a result, the vertical cracking seen in Figures 56 and 57 developed.

Cracks have also developed in plate and riveted hangers and eyebar straps as a result of fixity developing at pinned connections. Frequently water, dirt, and salt are directed onto the pin-hanger assembly because of the joints' proximity to the roadway. This causes corrosion cells to develop between the hangers and web or gusset plates and can eventually create nearly complete fixity at the "pinned" ends (39,43,44). Some degree of fixity has been observed on a wide variety of bridges with pin-hanger assemblies.

Examples of the types of cracking that have been observed in the hangers of several types of bridges are shown in Figures 59 to 63. In Figure 59, a cracked hanger plate can be seen with the crack developing in the gross section of the plate. Strain measurements on a number of these types of members have indicated that the corrosion packout (expansion of the corroded material) glues the components together to provide a rigid connection. As a result, the hanger experiences in-plane bending, and the maximum cyclic stress develops at the plate edge and initiates a fatigue crack.

Occasionally, as can be seen in Figures 60 and 61a, dirt accumulation results in a corrosion cell and extensive notching of the steel component. In the case shown in Figures 50 and 61a, dirt accumulation on the pier notched the eyebar, and fixity in the riveted built-up pin link subjected the anchor bar to significant in-plane bending. This resulted in fatigue crack growth from the edge of the eyebar at the corrosion notch. The crack surface is shown in Figure 61b.

Fatigue cracking can also develop in built-up hangers when fixity occurs because of corrosion. Figures 62 and 63, show cracking in a riveted member that resulted when the corrosion restraint was overcome by joint rotation forces causing sudden release and large dynamic bending stresses. These were found to occur a few times an hour and generated a sufficient number of cyclic stresses to induce cracks.

Figure 60. Cracked eyebar at pinned link.

Figure 61a. View of corrosion notch at edge of eyebar and corrosion fixity between faying surfaces.

Figure 61b. Cleaned crack surfaces and corrosion notches.

Figure 62. Crack in riveted deck truss hanger.

Figure 63. Close-up view of crack extending from rivet head into arrest hole.

3.6.5 Welding on Riveted Bridges

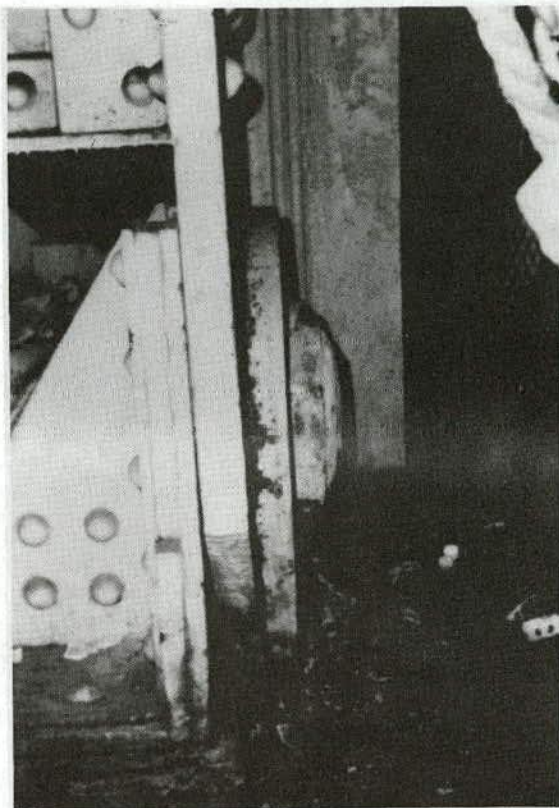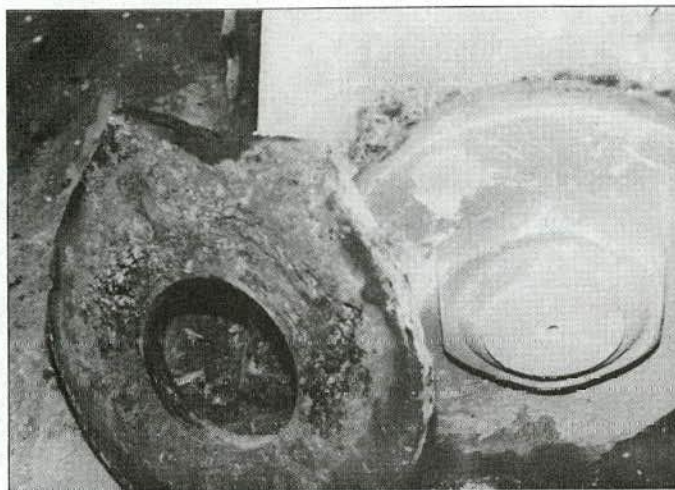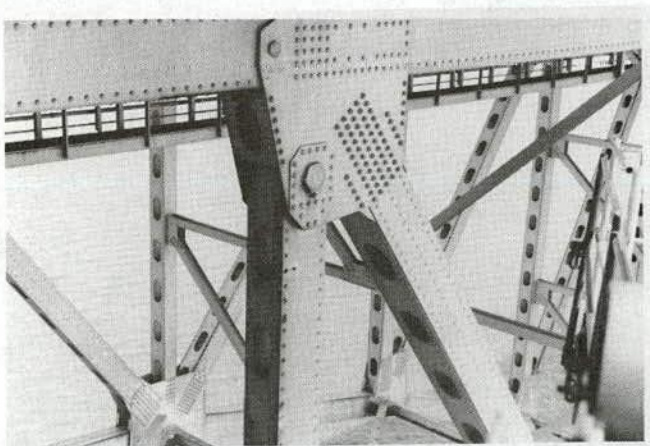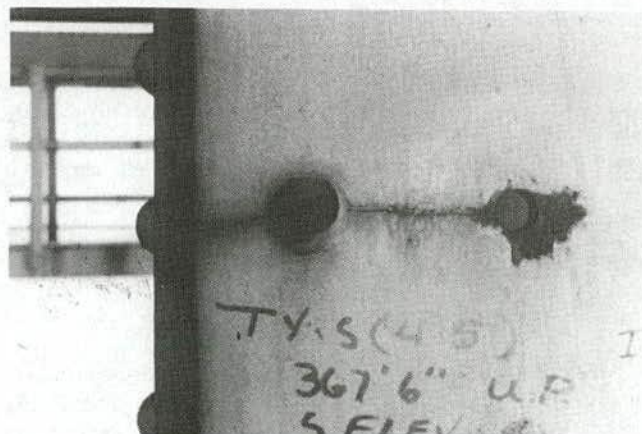Often weld repairs have been carried out on members and components of riveted bridges. These repairs have resulted because of corrosion, cracking, or the need to reinforce the section. The quality of weld repairs on existing members is often questionable. It is frequently undertaken by maintenance forces and quality control has often been lacking. Furthermore, access is often difficult, which results in poor welded joint details that are more severe than the details found on shop-fabricated bridge sections.

Following are examples of the types of welded repair that have been carried out and the cracking that has resulted from these repairs.

a. Corrosion Reinforcement

Severe corrosion of girder webs has often resulted in the addition of welded splice plates. Figures 64, 65, and 66 show reinforcement plates added to corroded web of riveted built-up girders. These reinforcement plates result in transverse welds with a high probability of lack of fusion at the weld root. The lack of fusion becomes susceptible to crack propagation at low stress range levels as can be seen in Figure 66. The growth of the crack in the transverse weld permits the crack to enter the girder web and flange angles via the longitudinal welds. Hence, the weld reinforcement provides a condition more susceptible to cracking than the original corroded regions.

A similar condition often exists when reinforcement is added to flange angles as shown in Figure 67. Again a combination of longitudinal fillet welds and transverse partial penetration groove welds results. Crack growth can be seen in the transverse groove weld shown in Figure 68. The longitudinal fillet welds that cross the transverse weld permit the crack to enter the flange angles.

b. Reinforcement at Web Gap Cracks

Cracks forming in web gaps have often led to reinforcement plates attached by welding. Figure 69 shows a triangular plate welded to the web and angles of a floor-beam. This type of repair often transfers the problem to an adjacent weld termination as shown in Figures 70 and 71. The reinforcement locally strengthens the web gap area, but does not prevent the distortion from continuing. Hence, high stress cycles are transferred to the plate boundaries and crack growth continues to develop elsewhere as the distortion results in high stress cycles at the weld terminations. In addition, weld quality is not very high because the weldments are produced in the field under awkward conditions.

c. Reinforcement Plates

On occasion, splice plates have been welded to truss members in order to reinforce the structural member or to aid in tightening loose members. Figure 72 shows splice plates welded to the surfaces of eyebar diagonals. These were used to splice the eyebar after it was cut and tightened. Fatigue cracks can be seen to develop at the ends of the splice plates as shown in Figure 73.

Figure 64. Web reinforcement plates welded to flange angles and stiffeners.
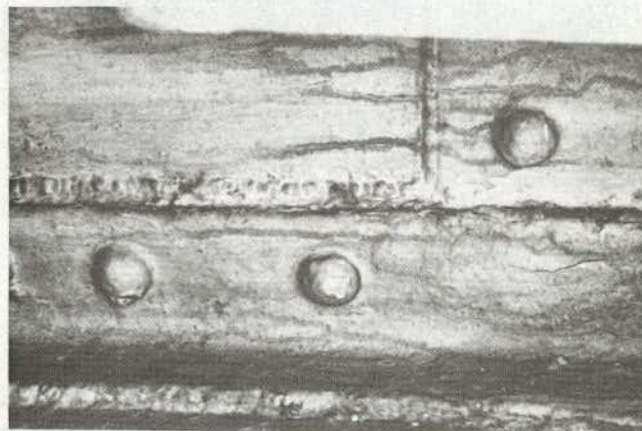
Figure 65. Close-up view showing longitudinal weld to flange angle and transverse weld to stiffener angle.

Figure 66. Crack originating in transverse weld between web reinforcement plates.
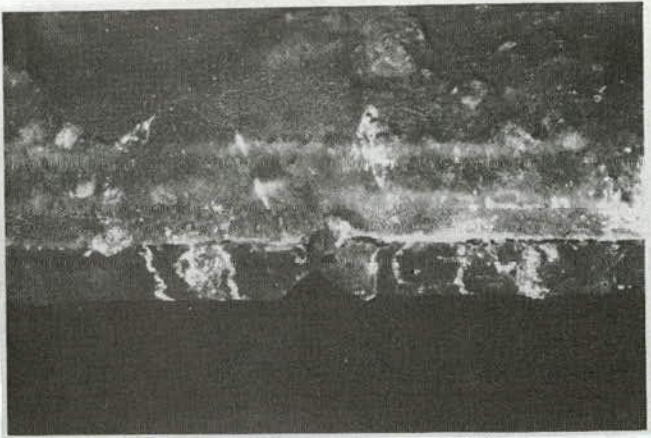
Figure 67. Lack of fusion in coverplate reinforcing added to flange angles.

Figure 68. Crack forming from lack of fusion in coverplate.
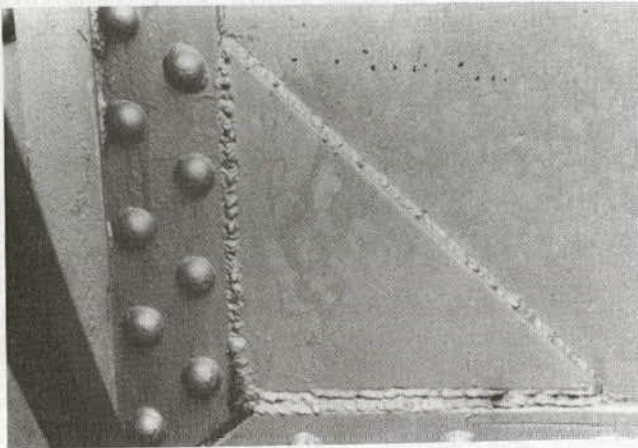
Figure 69. Welded reinforcement at cracked web gap between flange and connection angles.
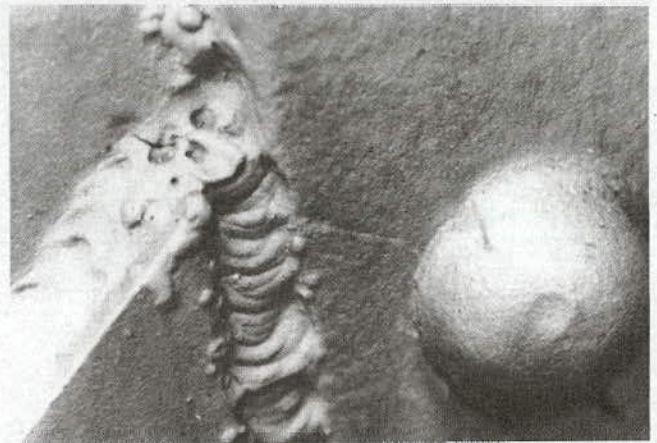
Figure 70. Crack forming in connection angle at weld termination.
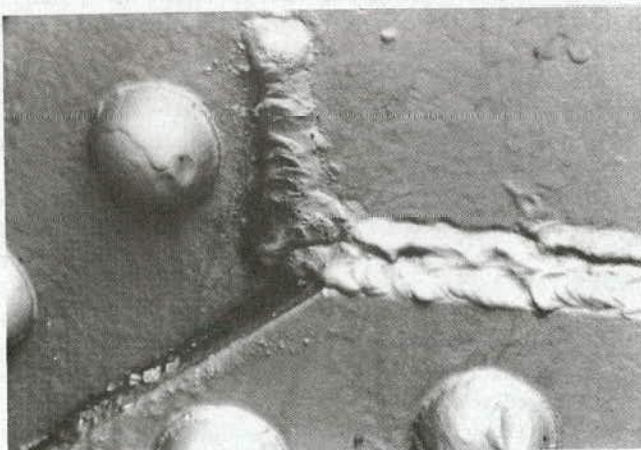
Figure 71. Crack forming in weld at gap.
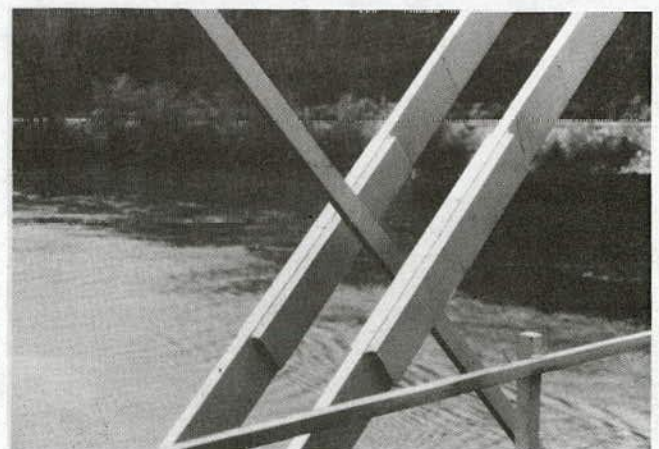
Figure 72. Welded splice plates added to truss eyebars.

Figure 73. Crack forming at weld toe of welded splice plate.

Weld toe cracking exists along the length of the transverse end weld.

The addition of the welded splice details has created a Category E detail. This resulted in fatigue cracking because the cyclic stresses exceeded the fatigue limit.

If welded details are found on riveted members, they should be carefully examined. Their resistance can be estimated from the fatigue provisions for welded details. Poor quality welding should be down-graded at least one detail category, i.e., a Category C detail should be treated as Category D for fatigue resistance.

d. Tack Welds

Tack welds have been frequently found on riveted members. These welds were often used to temporarily connect components together pending installation of the rivets. They are often located on gusset plates and their connecting members. When these tack welds are at the ends of the gusset, they are more severe because the stress range is often higher and the end of the gusset is like a long attachment with a fatigue strength near Category E.

Cracking has been observed in truss members with tack welds at the ends of the gusset plate at the member end.

Tack welds on floor-beam-bracket tie plates resulted in fatigue cracks developing in the tie plates (*38*). Category D was found to be the appropriate fatigue resistance for this type of connection. The stress range in these structures was higher than anticipated because distortion produced secondary bending stresses that were not predicated by the design process.

Tack welds are often removed by grinding when they are detected on riveted members.

CHAPTER FOUR

FULL-SCALE LABORATORY TESTS ON RIVETED GIRDERS

Fourteen full-scale riveted girders, all removed from riveted steel bridges, were tested during this study to evaluate their fatigue and fracture resistance. Each beam provided one or more cracked details.

4.1 PURPOSE OF THE TESTS

The review of previous work provided in Chapter Three demonstrated that the type of detail was not a major variable influencing the fatigue resistance of riveted connections and members. Category D was seen to provide a lower bound for initial cracking for most of the test data when the stress range was calculated on the net area. Continuous riveted web-flange angle connections, coverplate terminations and truss tension members all provided comparable fatigue resistance at a given level of stress range.

Although the test data are limited, the review also indicated that fatigue cracking and/or fracture of a component does not lead to complete fracture of the section and loss of load-carrying capability of the cross section. Significant additional life was observed once a component of the cross section developed a crack and eventually fractured.

Because only a limited number of full size tests have been carried out at stress ranges between 12 ksi (83 MPa) and 18 ksi (125 MPa), all of the girders were tested in this range. Table 2 shows the factorial arrangement of the test series. Three levels of minimum stress were examined—2 ksi (14 MPa), 8 ksi (55 MPa), and 14 ksi (96 MPa). Only one beam was tested at 14-ksi (96 MPa) minimum stress level because the maximum stress exceeded the static design limits.

It was the intent of this study to provide fatigue test data which supplemented the data available from previous research. Beams with less corrosion were sought in order to examine their fatigue behavior at stress ranges above 12 ksi (83 MPa). This would provide fatigue and fracture data at stress range levels mainly defined from simple shear splices (*45,46*). It would permit more fracture test data to be acquired as well as extend the stress range level examined.

The primary focus of the low temperature tests was to assess fatigue crack extension at reduced temperature and the consequences of fracture of an element on the capacity of the girder.

Table 2. Factorial arrangement of test series.

S_{min} \ S_r	12 ksi (83 MPa)	15 ksi (103 MPa)	18 ksi (124 MPa)
2 ksi (14 MPa)	T3,T4,T9	T1,T2	T7,T12
8 ksi (55 MPa)	T5,T6,T13	T8,T10,T14	----
14 ksi (97 MPa)	T11	----	----

Note: Sources of Specimens

T1 - T8: From Santa Fe Railroad

T9 - T12: From Ocean County, New Jersey

T13, T14: From Minsi Trail Bridge, Pennsylvania

4.2 TEST SPECIMENS

The test girders were obtained from three different sources. Girders 1 to 8 were obtained from the Santa Fe Railroad. Girders 9 to 12 were supplied from an Ocean County, New Jersey, highway bridge that was dismantled. Girders 13 and 14 were removed from the Minsi Trail bridge in Bethlehem, Pennsylvania, at the time it was dismantled. Figures 74 and 75 show the geometry and profiles of the test girders. Except for Ocean County girders, which were heavily corroded, the girders were generally in good condition. No fatigue cracks were detected in any of the test girders before the laboratory tests.

In order to examine the behavior of coverplate terminations, both existing and simulated coverplate terminations were evaluated during the tests. Simulated coverplate ends were developed by cutting the continuous coverplate as shown in Figure 76.

The large depth girder sections shown in Figure 75 were geometrically altered in order to reduce their section modules. The section was split longitudinally and a new compression flange was fillet-welded to the web plate as shown in Figure 77. This process worked satisfactorily inasmuch as no fatigue cracks were detected in the welded compression flanges.

4.3 MATERIAL TESTS

Material test samples were cut from the test girders after the fatigue and fracture tests were completed. These samples were taken from regions without significant corrosion and where no cracks existed in the flange angles and coverplates.

Tensile tests were conducted for each of the different types of girders (Table 3). The results show that all of the test girders were fabricated from mild steel with yield strength between 29 ksi (200 MPa) and 42 ksi (290 MPa). The test results indicate that the flange angles and coverplates for each set of girders were similar.
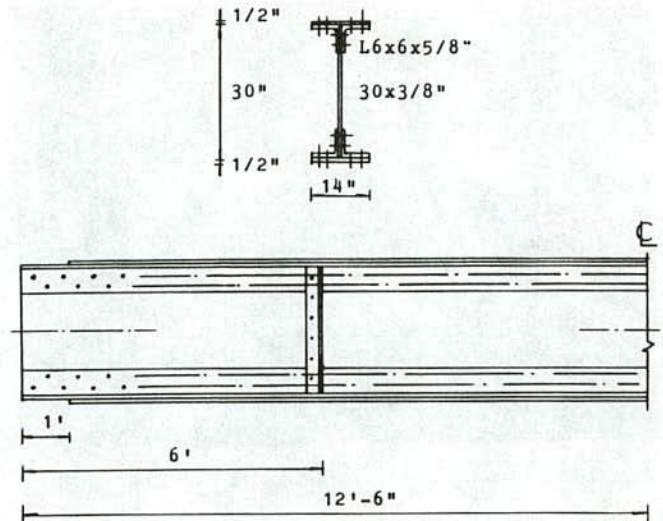
Figure 74. Geometry and profile of test girders for direct testing (beam specimens from Santa Fe Railroad).
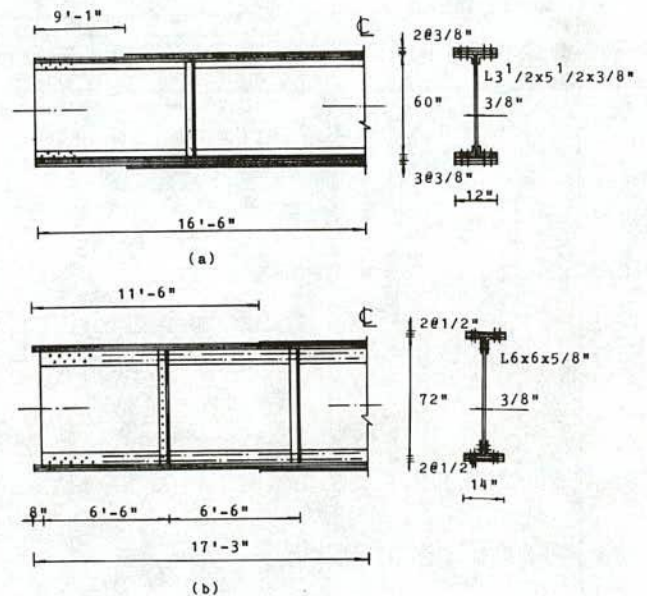
Figure 75. Geometry and profile of test girders requiring fabrication: (a) girder sections from Ocean County, N.J.; (b) girder section from Minsi Trail Bridge, Bethlehem, Pa.

Charpy V-notch tests were also fabricated and tested for each girder group. The results are given in Table 4. These results are directly comparable to the larger test sample summarized in Figure 37. The Charpy data were transformed to dynamic fracture toughness values, K_{Id}, using Barsom's correlation equation. These results are summarized in Figure 78. The tests were carried out at an intermediate strain rate equivalent to the 1-sec loading used for bridge components. The test results are also plotted in Figure 78 and compared with the fracture toughness estimated from the Charpy V-notch test results.
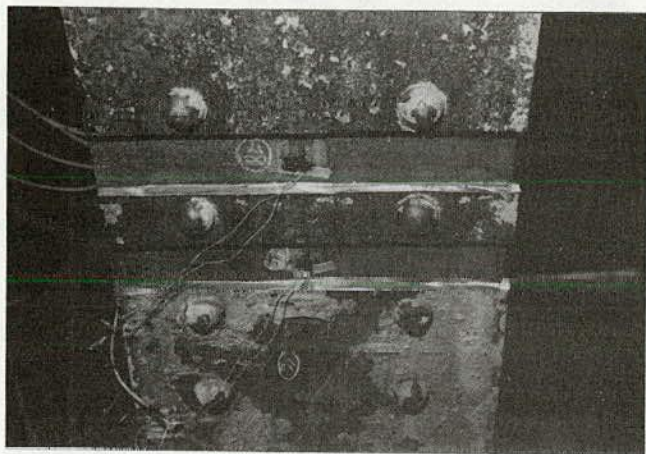
Figure 76. Simulated coverplate termination by grind cuts.
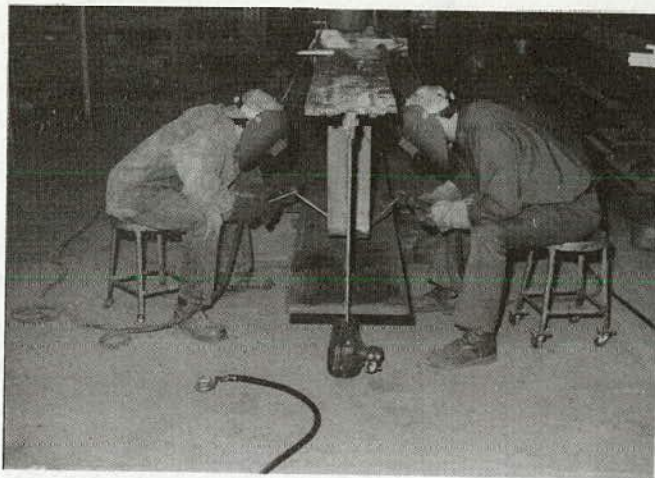
Figure 77. Fabrication of test girder.
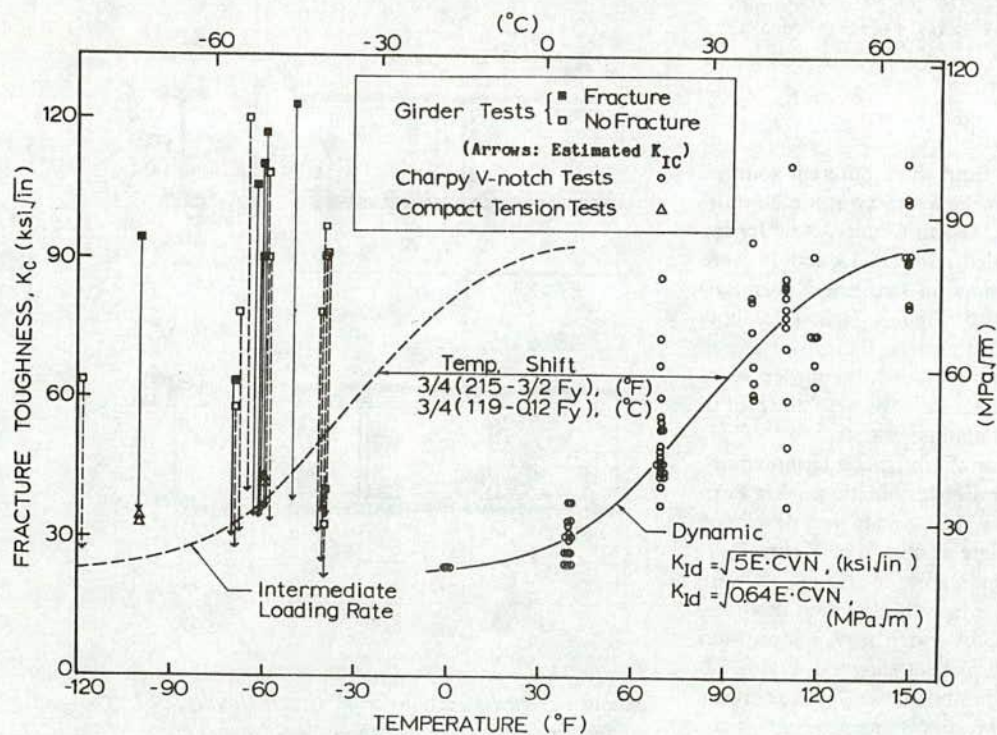
Figure 78. Comparison of girder fracture tests with estimated material fracture toughness.

Compact tension tests were also carried out on specimens fabricated from the Santa Fe girder angles, and the results are presented in Table 5. These tests were carried out at a 1-sec loading rate to simulate the test condition (36). The results are also plotted in Figure 78, showing reasonable agreement with the fracture toughness predicted by CVN tests.

Chemical analyses were obtained from the web and an angle of Ocean County girder 9. This girder had fractured during the static test when the flange angle stress at a net section was more than 30 ksi (207 MPa). The results are summarized in Table 6 and show high levels of phosphorous and sulfur. This indicates that these steel components were likely made by "Acid Bessemer Process" (47). This seems consistent with the erratic Charpy V-notch values obtained at 70 and 100 F (21 and 38 C).

Table 3. Tensile test results of test girder components.

Source	Girder No.	Component	Yield Strength ksi (MPa)	Ultimate Strength ksi (MPa)	Elongation of 8" gage Length %
Santa Fe	1-8	Angle	28.7 (198)	53.8 (371)	30.8
		Coverplate	31.6 (218)	57.8 (399)	29.5
Ocean County	9-12	Angle	41.2 (284)	64.4 (444)	25.3
		Coverplate	41.7 (288)	57.7 (398)	23.1
Minsi Trail	13,14	Angle	38.7 (267)	67.8 (467)	29.3
		Coverplate	34.5 (238)	62.9 (434)	28.2

Table 4. Charpy V-notch test results in ft-lb (J).

Santa Fe, Girder 1-8

Component	0°(-18°)	40°(4°)	70°(21°)	100°(38°)	120°(49°)
Angle		5 (7)	31 (42)	38 (52)	
		4 (5)	22 (30)	45 (61)	
		5 (7)	16 (22)	24 (33)	
		4 (5)	15 (20)	30 (41)	37 (50)
		5 (7)	12 (16)	28 (38)	30 (41)
		4 (5)	12 (16)	25 (34)	27 (37)
Coverplate	4 (5)	8(11)	21 (28)	184(250)	56 (76)
	4 (5)	7 (9)	13 (18)	60 (81)	37 (50)
	4 (5)	10(14)	14 (19)	46 (62)	37 (50)

Ocean County, Girder 9-12

Component	70°(21°)	110°(43°)	150°(66°)
Angle	18 (24)	17 (23)	45 (61)
	12 (16)	10 (14)	45 (61)
	10 (14)	26 (35)	56 (76)
Coverplate	16 (22)	80(114)	
	51 (69)	50 (68)	
	26 (35)	49 (66)	
	37 (50)		

Minsi Trail, Girder 13,14

Component	40°(4°)	70°(21°)	110°(43°)	150°(66°)
Angle	7 (9)	20 (27)	35 (47)	56 (76)
	7 (9)	20 (27)	40 (54)	57 (77)
	10(14)	14 (19)	43 (58)	57 (77)
Coverplate	6 (8)	15 (20)	51 (69)	85(115)
	8(11)	15 (20)	42 (57)	72 (98)
	7 (9)	14 (19)	47 (64)	74(100)

Table 5. Compact tension test results of Santa Fe girder flange angles (1-sec loading rate).

Specimen No.	B in. (cm)	W in. (cm)	a in. (cm)	a/W	P_{max} lbs. (N)	K_{max} ksi√in (MPa√m)	Temperature °F (°C)
3-1	0.569 (1.445)	1.992 (5.060)	1.223 (3.106)	0.61	2406 (10701)	42.5 (46.7)	-60 (-51)
3-2	0.569 (1.445)	1.990 (5.055)	1.202 (3.053)	0.60	1939 (8625)	33.0 (36.3)	-100 (-73)
4-1	0.576 (1.463)	1.991 (5.057)	1.205 (3.061)	0.61	1950 (8674)	34.5 (37.9)	-100 (-73)
4-2	0.576 (1.463)	1.991 (5.057)	1.196 (3.038)	0.60	2422 (10773)	41.2 (45.3)	-60 (-51)

Table 6. Chemical analysis results of steel from Ocean County girder 9 (%).

	Sample from the Angle	Sample from the Web
C	0.090	0.490
Mn	0.420	0.330
P	0.090	0.084
S	0.083	0.044
Si	0.020	0.013
Cu	-----	0.012

4.4 TEST PROCEDURE

The girders were tested under four-point bending as shown in Figures 79 and 80. Two 110-kip (490-kN) Amsler jacks were used to load each test girder. A 5-ft (1.52-m) constant moment length between the jacks permitted a significant length of beam to be subjected to the same stress range. On some girders, depending on the test conditions and the load and stroke capacity of the jacks, coverplate ends and/or simulated coverplate terminations (Fig. 76) were placed in the shear spans.

In order to provide lateral stability of the girder compression flange, two lateral bracing bars were attached to the compression flanges as can be seen in Figure 80. Because the fatigue cracks developed in a bottom flange angle, the resulting eccentricity of the flange force caused the girder to move sideways. Two lateral bracing bars were connected to the bottom flange as shown in Figure 81. This simulated the restraint of the bracing system in the bridges and minimized the lateral movement of the tension flange.

Wooden blocks were used as stiffeners at points of support and concentrated loads to minimize local yielding and buckling

as can be seen in Figure 81. An automatic-shut-down displacement control device (Fig. 82) was used to prevent excessive deflection and stop the test should failure occur.

Figure 83 shows the set-up used to cool the fatigue cracked section. The cross section was enclosed and cooled by liquid nitrogen. Thermal gages were used to control and stabilize the temperature during the reduced temperature tests when the fatigue crack was advanced under the lowered temperature.

4.5 SUMMARY OF TEST RESULTS

The test results of the fatigue cracks for the 14 girders tested in this study are summarized in Table 7. The summary provides the nominal test conditions at the failure section in terms of the
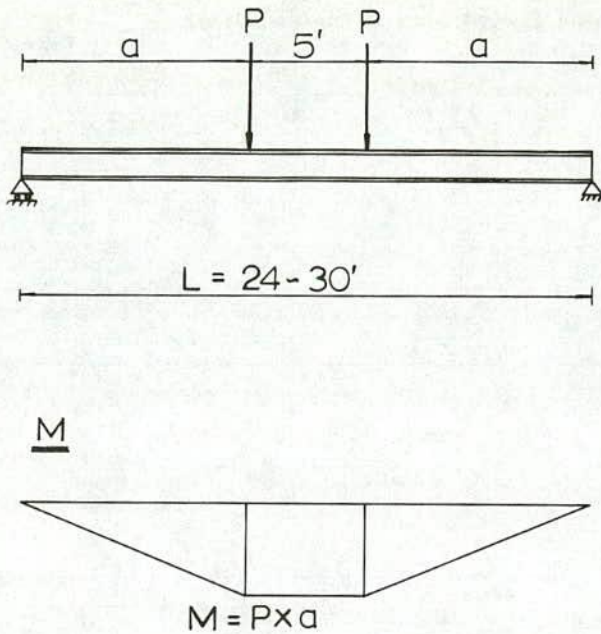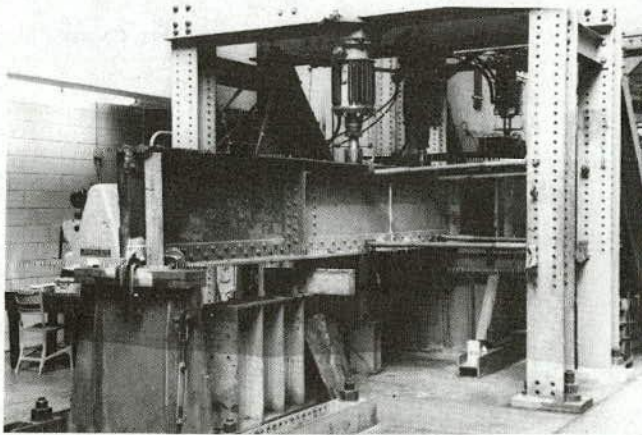
Figure 79. Schematic of the test set-up.

Figure 80. General set-up of test girders.

Figure 81. Test set-up and lateral bracings added at the tension flange after cracking.
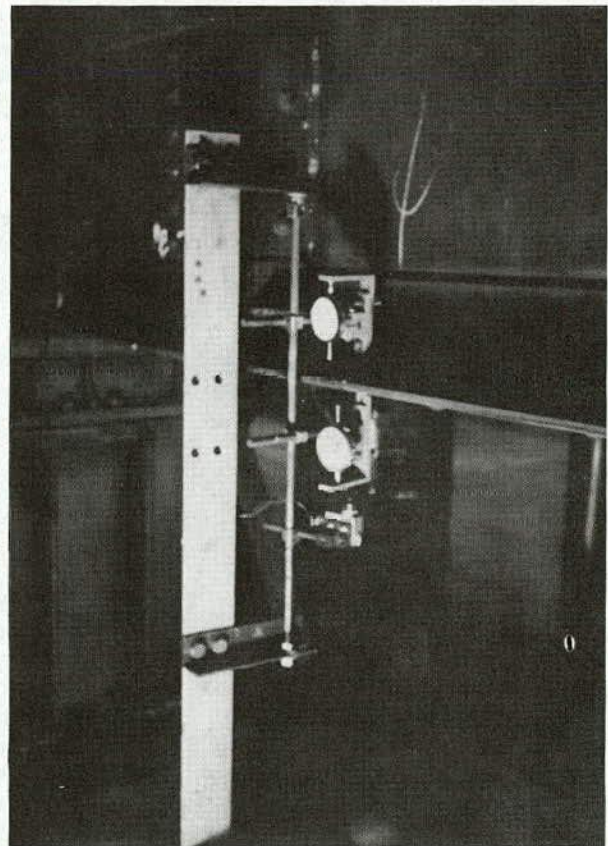
Figure 82. Automatic-shut-down displacement control device.

net section stress range and minimum stress. The fourth column shows the cycles to which the girders were subjected at the time the first crack(s) was detected. The fifth column shows the additional stress cycles that the girder was subjected to before the test was discontinued. Also shown is the detailed location of the cracks. A description of the cross section at which the critical cracks formed is provided in the last column. Most of the specimens failed at the riveted web-flange angle connection. The cracks generally formed at a rivet hole at the net section. Three beams developed cracks at a severely corroded section because of the corrosion notch effect. These cracks developed in the gross section and were not significantly influenced by the net section.

At various stages of crack growth, the cracked section was cooled and the crack tip extended under a cyclic load. The conditions that existed when crack instability finally resulted are summarized in Table 8. The table shows the nominal maximum stress at the failed section, the fatigue crack condition, the temperature, the estimated maximum stress intensity factor, and the residual static capacity of the girder in terms of the previous loading.

Figure 83. Set-up of liquid nitrogen ice box for reduced temperature tests.

Table 7. Summary of full-scale test results on riveted steel beam specimens.

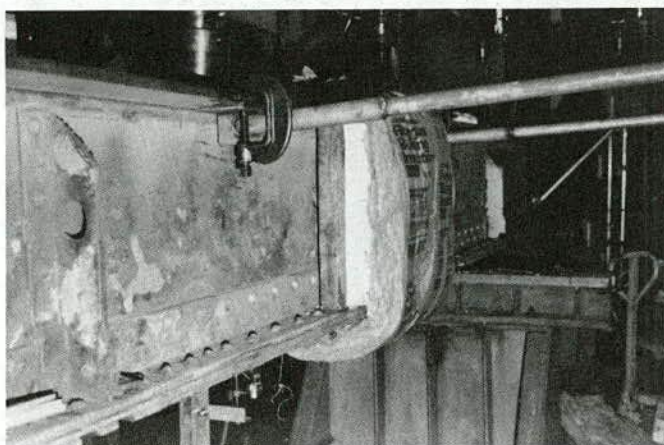| Beam ID	Stress Range ksi (MPa)	Minimum Stress ksi (MPa)	Cycles to Detection of Fatigue Cracks x10⁶cycles	Additional Cycles to Failure of Cross-section* x10⁶cycles	Detailed Condition of Cracks**
3	12 (83)	2 (14)	1.410	0.213	W-F, Hole
4	12 (83)	2 (14)	2.630	0.208	W-F, Hole
9	12 (83)	2 (14)	0***	0.415	C-T, Hole
5	12 (83)	8 (55)	2.344	0.384	W-F, Hole
6	12 (83)	8 (55)	2.575	0.430	W-F, Hole
13	12 (83)	8 (55)	3.040	0.573	W-F, Hole
11	12 (83)	14 (97)	0.522	0.135	W-F, Corrosion
1	15 (103)	2 (14)	0.588	0.328	C-T, Hole
2	15 (103)	2 (14)	1.094	0.143	W-F, Hole
8	15 (103)	8 (55)	0.923	0.393	W-F, Hole
10	15 (103)	8 (55)	0.471	0.040	C-T, Corrosion
14	15 (103)	8 (55)	1.446	0.117	C-T, Hole
7	18 (124)	2 (14)	0.601	0.172	W-F, Hole
12	18 (124)	2 (14)	0.827	0	W-F, Corrosion

Note: *   This was influenced by the reduced temperature tests.

   ** "W-F": Cracking at web-flange angle connection with continuous coverplate(s)
       "C-T": Cracking at coverplate termination
       "Hole": Crack initiation at rivet hole
       "Corrosion": Crack initiation at corrosion reduced section

   *** Fatigue tested after both angles had fractured during static test.

Table 8. Summary of full-scale test results at failure.

Beam ID	Nominal Maximum Stress ksi (MPa)	Sketch of Fatigue Cracked Section	K_{max}* ksi√in. (MPa√m)	Temp. °F (°C)	Residual Static Strength at Room Temp. (% of S_{max})
3	14 (97)		68 (75)	-70 (-57)	>100
4	14 (97)		-- (--)	Room Temp.	40
9	14 (97)		83 (91)	Room Temp.	64
5	20 (138)		94 (103)	-100 (-73)	30
6	20 (138)		110 (121)	-60 (-51)	50
13	20 (138)		97 (107)	-40 (-40)	>100
11	26 (179)		174 (191)	Room Temp.	**
1	17 (117)		98 (108)	Room Temp.	>100
2	17 (117)		120 (132)	Room Temp.	>100
8	23 (159)		122 (134)	-50 (-46)	80
10	23 (159)		151 (166)	Room Temp.	70
14	23 (159)		90 (99)	-60 (-51)	57
7	20 (138)		106 (116)	-60 (-51)	48
12	20 (138)		122 (134)	Room Temp.	84

Note:

   *   Estimated stress intensity factors

   ** Not measured

More extensive information on each of the test girders is provided in Appendix B. This includes the location of the cracked sections, the history of crack development in the girder components at the critical section, and several photographs of the cracked condition and crack surface.

For all of the test girders without significant corrosion loss of section, cracks formed at the net section in a rivet hole. Figure 84 shows typical fatigue cracks extending beyond the rivet head. As these cracks continued to propagate, as shown in Figure 85, a powder generally formed under the rivet head at the hole and was extruded because of fretting. This was a general indication of the increased movement of the connected

Figure 84. Typical fatigue crack extending beyond rivet head.
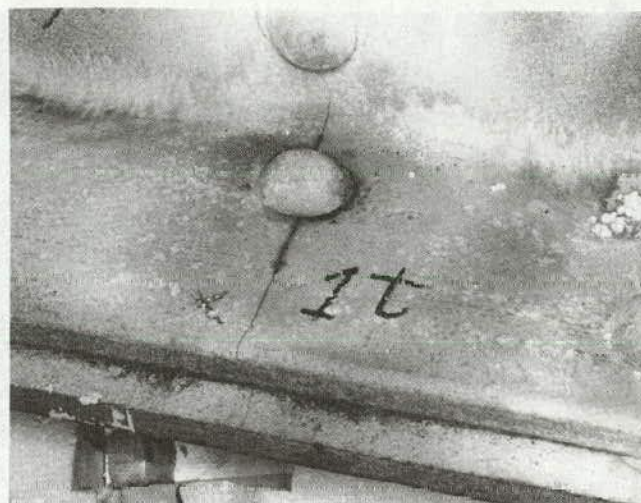
Figure 85. Powder formed under rivet head and extruded because of fretting (girder 2).
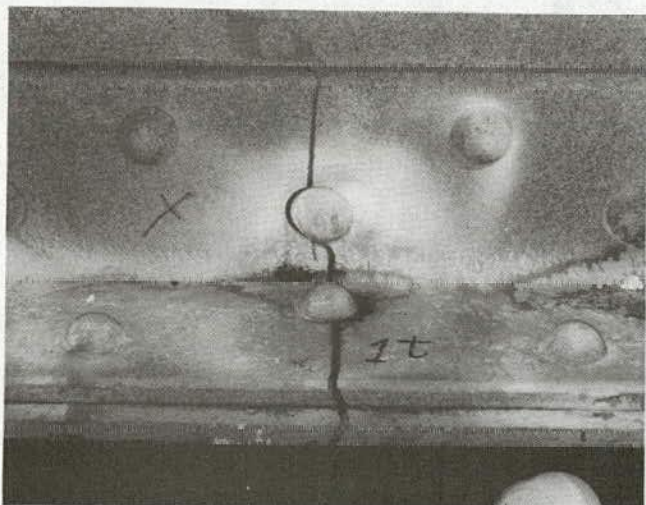
Figure 86. Cracked tension flange components: angle and coverplate (girder 2, south side).
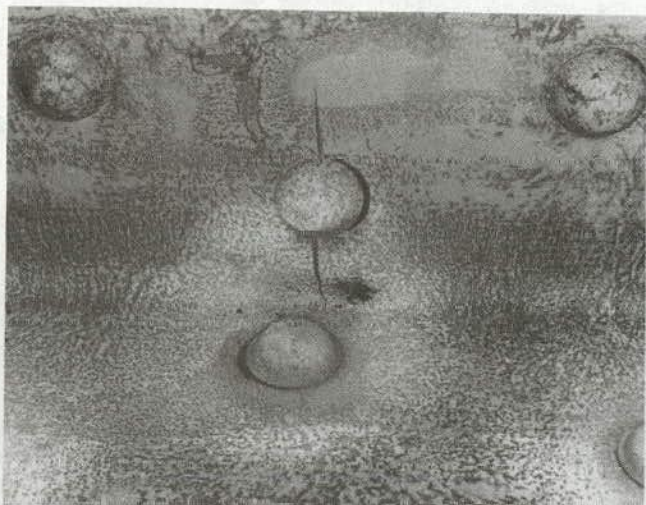
Figure 87. Plasticity and crack opening at component not fractured (girder 2, north angle).

parts caused by cracking. For the continuous web-flange and continuous flange coverplate connection shown in Figures 84 and 85, eventually one or more of the components cracked in two, as shown in Figure 86 for girder 2. Those components that did not fracture exhibited significant plasticity and in some cases substantial crack opening displacement as shown in Figure 87.

When cracks formed at the ends of coverplates, they often formed at the net section of the last row of rivets connecting the terminating plate to the angles and continuous plate. Figure 88 shows the final cracks that developed in girder 14. Both flange angles and the continuous coverplate were fractured during the final reduced temperature test.

Further details of the individual tests are given in Appendix B. For example, the tests on girder 2, which resulted in the cracks shown in Figures 84 to 87, examined the crack conditions at seven different increments of life that are detailed on the summary sheets and sketches in Appendix B. A similar description of crack development at the coverplate termination, shown in Figure 88, is provided for girder 14.

The other condition that caused cracking was corrosion notching, as shown in Figure 89. As can be seen from the figure, extensive corrosion loss of the flange angle outstanding leg resulted in the fatigue crack forming at the gross section. Similar behavior was reported in Ref. 30 on other corrosion notched members.

After the tests were completed, several sections were saw-cut along the longitudinal length in order to examine the net section of riveted sections that had not experienced visible cracking. Figure 90 shows a typical rivet cross section for a flange-angle coverplate connection. It can be seen that the rivets were in general well driven and filled the rivet holes.

All of the test results for the first detectable fatigue cracks are plotted in Figure 91. Only girder 9 was excluded from this plot, because the girder had experienced fracture of both flange angles during a static overloading of the net section at the coverplate termination. The estimated net section stress was 32 ksi at the critical section for girder 9. All other girders that developed fatigue cracks at the riveted net section equalled or exceeded the fatigue resistance provided by Category D at

detection of the first fatigue crack. Substantial variation in the size of these cracks was apparent, as can be seen in Appendix B.

4.6 CRACKING AT RIVET HOLES OF WEB-FLANGE ANGLE CONNECTIONS WITH CONTINUOUS COVERPLATE(S)

Eight of the test girders developed their failure sections at the riveted web-flange angle connections with continuous coverplate(s). Cracks generally formed simultaneously in the flange angles and the continuous coverplate. These crack developments are shown schematically in Appendix B for girders 2 to 8 and 13. Generally between 5 and 15 percent of the net section area was cracked when these fatigue cracks were discovered. Once the fatigue cracks were visible, stable fatigue crack extension was observed in the cracked elements. At the high stress range levels used for these tests—12 to 18 ksi (83 to 125 MPa)—the crack growth rates were relatively high, so only 100,000 to 400,000 additional stress cycles were needed to significantly enlarge the cracks that formed in the individual components.

Table 8, as noted earlier, summarizes the crack conditions that existed in the various elements at the time of failure. This table shows the level of maximum stress, the cracked section, the temperature at failure, an estimate of the stress intensity factor at the time of failure, and the residual static capacity of the cross section after crack instability or plastic hinging of the section.

All of the tests resulted in significant resistance to crack instability even at reduced temperatures as low as -100 F (-73 C). As can be seen in Table 8, between 30 and 90 percent of the tension component area was cracked at the time of failure. The smaller percentages were a result of the reduced test temperatures and the high value of the stress intensity factor in the cracked components.

4.7 CRACKING AT COVERPLATE TERMINATIONS

Although seven of the test girders (1 and 9 to 14) had coverplate terminations, only four of these girders developed fatigue
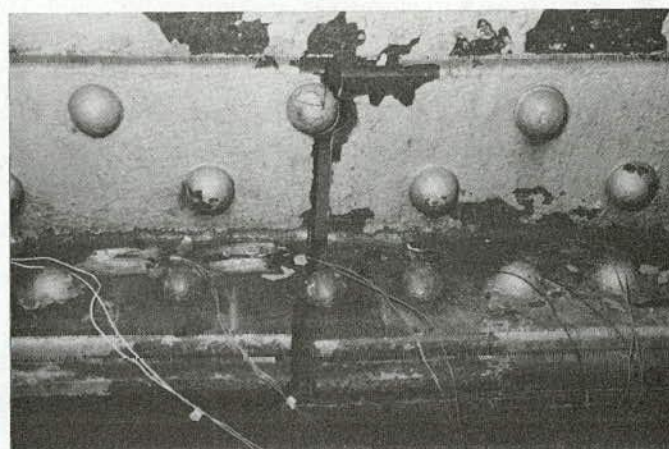

Figure 88a. Final cracks at coverplate termination (girder 14, north side).
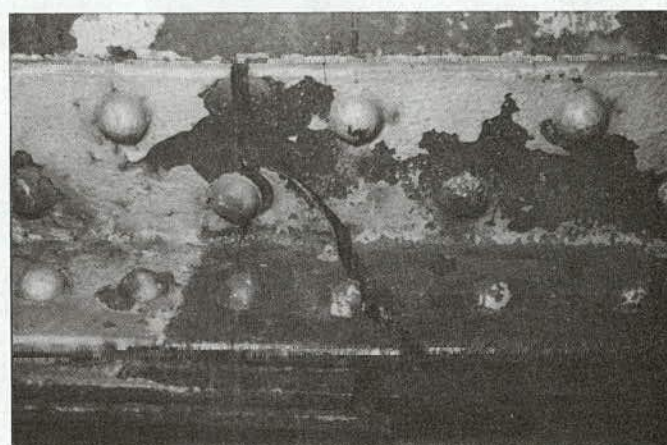
Figure 88b. Final cracks at coverplate termination (girder 14, south side).

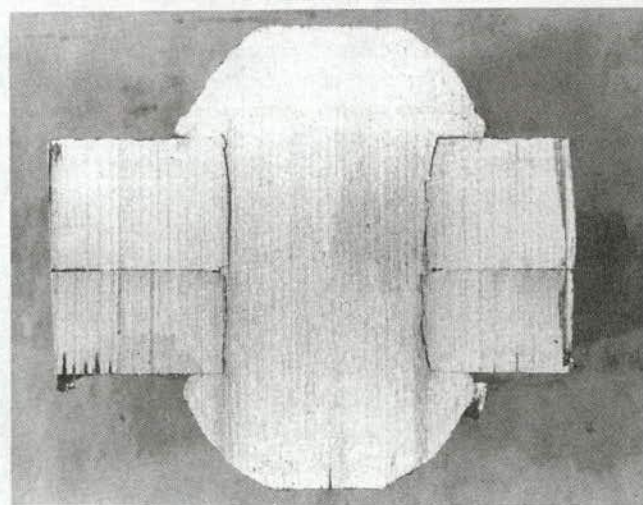Figure 89. Extensive corrosion loss of tension flange outstanding leg (girder 11, north side).

Figure 90. A typical rivet cross section for a flange-angle coverplate connection.
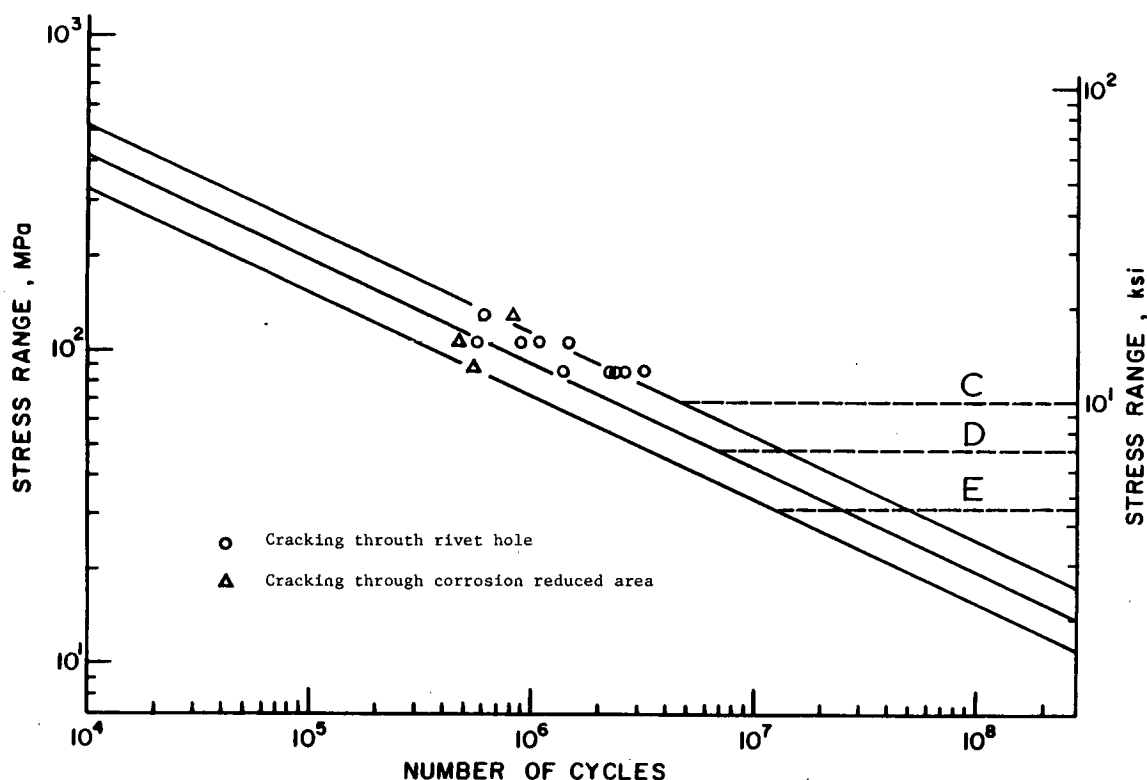
Figure 91. First crack detecting of full-scale steel bridge girders tested in this study.

cracks at the termination (girders 1, 9, 10, and 14). The stress range in the net section at the coverplate termination was about equal to the stress range in the net section of the constant moment region with continuous coverplate(s). For girder 9, an overload at the coverplate termination during the initial static test resulted in fracture of the two flange angles. This occurred when the nominal stress on the net section was about 32 ksi.

Girder 10 developed fatigue cracking in the gross section of one of the corroded flange angles at the coverplate termination. Cracking in the other angle and the continuous coverplate occurred at the rivet hole net section in a corroded region. Corrosion notching of the bottom flange angles governed the fatigue resistance of girder 10. About 85 percent of the tension flange area was cracked at the time of failure (see Table 8).

The fatigue resistance of the coverplate termination details was not significantly different from the fatigue resistance of the continuous riveted connections. Several of the girders had the coverplate termination located so the nominal stress range was about the same as the constant moment region. Nevertheless, in girders 11, 12, and 13, the critical section was in the constant moment region and not the coverplate termination. For girders 11 and 12, the corrosion notching of the flange angles influenced this behavior.

4.8 CRACKING AT CORROSION NOTCHED SECTIONS

Three of the girders developed fatigue cracks at corrosion notches (girders 10, 11, and 12). One of the girders (No. 10) cracked at the end of a coverplate as can be seen in Figure B23.

The other two developed cracks in the constant moment region at corrosion notches in the continuous section as can be seen in Figures B28 and B31. From Figure 91, it is noted that two of the corrosion notched girders provided a fatigue resistance best characterized by Category E, similar to the test results reported by Out, Fisher and Yen (30). One of the girders (No. 12) provided a fatigue resistance comparable to the other riveted girders.

The corrosion notching resulted in fatigue cracks forming nearly simultaneously in all of the member components. This resulted in 85 to 90 percent of the tension components cracking before failure of the section at room temperature (see Table 8).

4.9 FRACTURE RESISTANCE

Failure developed in the test girders because of brittle fracture of one or more of the fatigue cracked elements or because of plastic deformation of the cracked components, which sometimes exceeded the tensile strength of the net section. The test results are summarized in Table 8 for the failure condition.

Seven of the 14 girders were failed at reduced temperatures between -40 F and -100 F (-40 C and -73 C). These tests simulated the lowest levels of fracture resistance likely to exist in riveted members. As the material fracture toughness characteristics shown in Figures 37 and 78 illustrate, a lower bound fracture toughness of about 50 ksi$\sqrt{\text{in}}$. (55 MPa$\sqrt{\text{m}}$) is representative of the lowest toughness of riveted bridge members down to -50 F (-46 C).

Figure 78 compares the estimated stress intensity factor for the test girders with the estimates of material fracture toughness.

Also shown are the tests carried out at reduced temperatures that did not result in crack instability.

The test results indicate that reduced temperatures did not significantly affect the fatigue and fracture resistance of the test girders. The maximum level of stress intensity at failure was comparable because failures at reduced temperature (68 ksi$\sqrt{\text{in.}}$ to 122 ksi$\sqrt{\text{in.}}$, or 75 MPa$\sqrt{\text{m}}$ to 134 MPa$\sqrt{\text{m}}$), overlapped the spread observed at room temperature (83 ksi$\sqrt{\text{in.}}$ to 120 ksi$\sqrt{\text{in.}}$, or 92 MPa$\sqrt{\text{m}}$ to 134 MPa$\sqrt{\text{m}}$). Two of the corroded members failing at room temperatures corresponded to

higher levels of stress intensity (151 to 174 ksi$\sqrt{\text{in.}}$, or 166 to 191 MPa$\sqrt{\text{m}}$). These estimates of stress intensity reduce to values close to the lower bound of 50 ksi$\sqrt{\text{in.}}$ (55 MPa$\sqrt{\text{m}}$) when the test results are adjusted using the β_{Ic} correction (49,50).

After failure, two of the reduced temperature tests (girders 3 and 13) and two of the room temperature tests (girders 1 and 2) were capable of supporting the maximum test load without significant distortion. The maximum nominal stress for these girders varied from 14 to 20 ksi (98 to 138 MPa).

CHAPTER FIVE

RECOMMENDATIONS AND APPLICATIONS

The findings of this study will be of value to bridge engineers involved in the evaluation of riveted bridge structures, researchers working in the subject area, and members of specification-writing bodies. A procedure is presented that can be incorporated into the AASHTO *Manual for Maintenance Inspection of Bridges*. The results and findings of this study are also applicable to other specifications, such as those of the American Railway Engineering Association for rating riveted railway and mass transit bridges.

5.1 FATIGUE BEHAVIOR OF RIVETED MEMBERS

1. This study has shown that fatigue cracking of a riveted built-up steel member can be detected and observed in one or more elements of the riveted member when the stress range exceeds 7 ksi. The Category D fatigue curve was found to provide a good estimate of the cycles for fatigue crack development.

2. The fatigue strength of riveted steel members was best characterized by the Category C fatigue curve. This resistance can be achieved under all service conditions. Reduced temperatures did not significantly affect the resistance of the fatigue cracked member having three or more tension components (including the web plate). All of the members tested were able to retain their structural adequacy when one or two components of the tension-carrying components cracked. The sections were all found to be able to redistribute the load without adverse effect. As can be seen in Table 8 and Appendix B, failure only occurred when more than 50 percent of the tension area was fatigue cracked.

3. Fatigue cracks can be readily detected in riveted members because of their tolerance to crack growth. It is relatively easy to detect a cracked component, and significant residual life exists between cracking of a component and failure of the section. It was not possible to develop fast fractures from small fatigue cracks.

5.2 RECOMMENDED SPECIFICATION FOR FATIGUE AND FRACTURE EVALUATION OF RIVETED BRIDGE MEMBERS AND CONNECTIONS

(*This section would be inserted into the AASHTO* Manual for Maintenance Inspection of Bridges. *Examples of the use of this evaluation procedure are given in Appendix C. Reference* 48 *provides details of the fatigue damage estimate procedures developed in* NCHRP Report 299.)

5.2.1 General

The development of the procedures in this section is based on the experimental evaluation and detailed study of riveted steel bridge members given in this report.

5.2.2 Fatigue Resistance

Riveted steel members composed of rolled plates or shapes that have their tensile stresses resisted by three or more components (e.g., the web plate, each flange angle or coverplate as one component of the tension flange of a flexural member) shall be checked for fatigue crack development using detail Category C. This shall apply to the net section stress at the applicable section and detail.

5.2.3 Toughness Considerations

Riveted members which have tensile stresses resisted by three or more components (including the web) need not satisfy the Charpy V-notch impact requirements of Article 10.3.3 of the AASHTO *Standard Specifications for Highway Bridges* if the connection or member retains structural adequacy with one of the components cracked.

5.2.4 Stress Range

5.2.4.1 Members shall be investigated for the stress range produced by placing a single HS-20 truck on the bridge distributed to the girders as designated in the AASHTO *Standard Specifications for Highway Bridges,* Article 3.23.2, for one traffic lane loading. The impact required in the specifications Article 3.8 shall be used to increase the stress range. Where the section is corroded, the net section area must be reduced to account for the loss of section.

5.2.4.2. If the stress range determined from Article 5.2.4.1 does not exceed 7 ksi, the member is not susceptible to crack growth and no further check is required. If the stress range determined from Article 5.2.4.1 exceeds 7 ksi, the evaluation procedure provided in *NCHRP Report 299* should be followed as amended in Article 5.2.5.

5.2.5 Evaluation Procedure Adjustments

5.2.5.1 Reliability Factor.—The basic reliability factor R_{so} (*48*) shall be taken as 1.35 for all riveted members satisfying the conditions of Article 5.2.2.

5.2.5.2 Remaining Life.—When assessing the remaining safe life in accord with the provisions of the evaluation procedure in Article 6.3 of Appendix A in *NCHRP Report 299,* the detail constant K shall be used corresponding to detail Category C.

5.2.6 Inspection

When the remaining life estimated from Article 5.2.5.2 is inadequate, normal periodic visual inspections of the particular details are necessary to permit discovery of a cracked component.

CHAPTER SIX

CONCLUSIONS

6.1 SMALL-SCALE SHEAR SPLICES AND TENSILE SPECIMENS

A detailed review was carried out on available fatigue test data on riveted steel and wrought iron joints and on steel and wrought iron plates with open holes. Approximately 1,200 test results were examined and evaluated. Following are the findings of that review.

1. The major variables observed to affect the fatigue resistance of riveted joints are the rivet clamping force and the rivet bearing ratio.
2. The variation in fatigue strength of small-scale specimens was found to be large. It is possible that this stems from the fact that the sources associated with these test data provided very diverse test conditions. In addition, many tests were discontinued before developing fatigue cracks and without accumulating a sufficient number of stress cycles to determine the fatigue limit. It was customary to discontinue testing after two or three million cycles. All of the fatigue tests on small steel specimens were conducted at stress ranges above 13.3 ksi (92 MPa). Hence, the fatigue limit was not defined because failures were observed to occur at all levels of applied stress range.
3. Plates with open holes tended to provide greater fatigue resistance than riveted joints. All plates yielded fatigue strengths that exceeded the Category C fatigue resistance curve.
4. The effect of different methods of hole preparation did not result in major differences in fatigue strength. Drilling, punching, subpunching and reaming, and subdrilling and reaming provided fatigue resistances that did not differ appreciably. How-

ever, the amount of test data on punched holes is very limited and does not represent the wide variation that is likely to exist in practice, as a result of punch wear, plate thickness, and material. The tests on plates and joints with punched holes were carried out at relatively low bearing ratios (1.25 to 1.75). Reamed holes, whether subpunched or subdrilled, seemed to provide better performance than drilled holes.

5. The lower bound fatigue resistance of simple riveted shear connections is reasonably well represented by the Category D fatigue resistance curve, as it was exceeded by nearly all the test data. Exceptions were specimens with reduced clamping and high bearing ratios. These results apply primarily to simple connections and do not reflect the additional life observed for built-up members because of their inherent load redistribution capacity.
6. Steel connections with good clamping force and normal bearing ratios, i.e., smaller than 1.5, have a lower bound fatigue strength that is defined by Category C. A number of tests at high stress range levels fell below Category C probably because of yielding.
7. Small specimens subjected to stress reversal provided a fatigue resistance significantly greater than other test specimens. The stress range is overestimated using the full stress amplitude, and part of the compression stress cycle does not appear to cause damage.
8. Although only limited test data are available for wrought iron riveted members or plates with open holes, their fatigue resistance is affected by the same factors that influence steel specimens. Clamping force and bearing ratio are the main factors, while the state and age of specimens and holes play a part.

9. Wrought iron riveted connections exhibit a lower bound fatigue strength represented by Category E. A few test data fell below Category E, possibly as a result of their previous load history and the level of maximum stress in the stress cycle.

6.2 TESTS ON LARGE-SCALE RIVETED MEMBERS AND CONNECTIONS

The experimental studies carried out on large-scale riveted members provided information on their behavior. Following are the principal findings.

1. The high cycle life fatigue resistance of the net section of riveted members and connections appears to be close to the Category D fatigue limit. Several fatigue cracks were found to develop in the riveted details at stress ranges between 6.7 and 9.5 ksi (46 and 66 MPa) after 8 to 36 million cycles.

2. Tests on truss-type connections and built-up flexural members with wide variations of geometry provided about the same fatigue behavior. Hence, the type of riveted member and connection does not appear to be a significant factor. Gusset connections, coverplate ends, and web-angle and angle-coverplate continuous connections yielded similar test results on the net section. Category D was found to provide a reasonable lower bound for crack development and detection in an individual component. Also, the full stress cycle appeared to be effective for those members subjected to partial reversal.

3. Severing a component of the built-up section did not immediately impair the capacity of the members. Between 200,000 and 1,000,000 additional cycles of stress range were required before the load-carrying capacity was completely destroyed. Cracks formed slowly in the other angle, the coverplate, and the web plate of the girders. All test beams exhibited redundant behavior after cracks developed that severed a flange angle or coverplate.

4. Significant bond was often observed to exist between the angles and web plate of the beam tests as a result of their painted and corroded condition. This reduced the opening of the crack and extended the fatigue life.

5. Reduced temperature tests at periodic intervals of extension of a crack grown from a rivet hole into the legs of the angle did not result in unstable crack growth until large cracks developed. Even with 50 percent of the angle section cracked, the crack extension mode was stable. Beams with large cracks in all tension elements were able to resist significant maximum stress.

6. The test results indicate that low Charpy V-notch absorbed energy levels are not critical in riveted built-up members. The fracture toughness requirements of the AASHTO design specifications need not be applied to riveted bridge members.

7. Category C was found to provide a reasonable lower bound estimate of the fatigue strength of riveted members.

8. Limited tests on end connection angles indicated that their fatigue resistance was in agreement with Category A for base metal. The bending stresses caused by end rotation were estimated from a simple flexural model, assuming that double curvature was introduced into the outstanding legs.

9. Distortion of small web gaps and restraint at end connections or of pinned-ended members were found to be the major causes of cracking in riveted structures.

6.3 RIVETED DETAILS AND RATING PROVISIONS

1. An examination of a wide range of riveted members and details indicated that they could be grouped into seven classes. These involved the rivet patterns for flexural and axially loaded members, stringer and girder end connections, and gusset plate connections.

2. Rivet sizes were found to correspond to $7/8$ in. (22 mm) or 1 in. (25 mm).

3. Plate thickness varied from $5/16$ in. (8 mm) up to 1 in. (25 mm).

4. Rivet spacing near the ends of beams, or coverplates was found to vary between $1\frac{1}{2}$ in. (38 mm) and 3 in. (76 mm).

5. The gage length between rivets in the outstanding legs of connection angles was generally equal to, or greater than, the gage suggested by Wilson $(g > [Lt/8]^{\frac{1}{2}}$.

6. Fatigue cracks detected in highway bridge structures are in general related to distortion and unanticipated restraint.

7. Very conservative guidance for checking the fatigue capacity of existing steel highway bridges is provided in the AASHTO *Manual for Maintenance Inspection of Bridges.* This indicates that the standard fatigue design provisions can serve as a guide to determine allowable fatigue stress.

8. The general practice is to ignore the possibility of fatigue damage in riveted highway bridge structures as a result of the positive experience without significant cracking.

9. Available studies on riveted highway bridge members have demonstrated that the maximum stress range will seldom if ever exceed the fatigue limit applicable to riveted members (7 ksi, or 48 MPa). Hence, fatigue damage will not likely develop in most structures.

10. A procedure was developed to assist assessment of the likelihood of fatigue damage in riveted bridge members (see Section 5.2).

CHAPTER SEVEN

RECOMMENDATIONS FOR FURTHER RESEARCH

The experimental work available in the literature and the tests carried out in this study have pointed out the need for additional research on riveted built-up members. It is recommended that consideration be given to the following.

1. Additional tests are needed for the extreme life behavior of riveted steel and wrought iron members. The limited studies reported by Out, Fisher, and Yen (30) are all that exist. Also needed are tests with random variable loading with only a few cycles exceeding the constant cycle fatigue limit. No tests are available for this condition which is critical to the assessment of riveted members.

2. Studies are needed for conditions of partial stress reversal. Although small specimen tests indicate that the compression portion of the stress cycle is not fully effective, the tests on large-scale truss members are not conclusive. No partial reversal tests have been carried out on flexural members. Because stress reversal members are common, it is highly desirable to ascertain whether or not stress reversal provides higher fatigue resistance in full-scale members.

3. Additional tests are needed on corrosion notching so that rational fatigue resistance relationships can be developed. The available test data demonstrate that the fatigue resistance can be decreased to Category E. Corrosion notch factors to adjust fatigue resistance can only be developed with additional experimental results.

4. Work is needed on repair and retrofit procedures for corrosion notched components. Such procedures as surface peening with shot or multiple point tools need to be evaluated.

5. Additional studies are needed on secondary distortion of connection angles so that rational gages and details can be developed. These tests would be equally applicable to the bolted connections in common use today. No criteria now exist for highway bridge details.

REFERENCES

1. American Association of State Highway and Transportation Officials, *Standard Specifications For Highway Bridges,* 13th Edition (1983).
2. American Railroad Engineering Association, "Steel Bridges." *Manual for Railroad Engineering,* Ch. 15, (1984).
3. BAKER, K. A., and KULAK, G. L., "Fatigue of Riveted Connections." *Canadian J. Civ. Eng.,* Vol. 12 (Mar. 1985) pp. 184–191.
4. BARON, F., and LARSON, E. W., JR., "The Effect of Certain Rivet Patterns on the Fatigue and Static Strength of Joints." Technical Report, Dept. of Civil Engineering, Northwestern University, Evanston, Illinois (Feb. 1952).
5. BARON, F., and LARSON, E. W., JR., "Comparative Behavior of Bolted and Riveted Joints." *Research Report C109,* The Technological Institute, Northwestern University, Chicago, Illinois (Sept. 1952).
6. BARON, F., and LARSON, E. W., JR., "The Effect of Grip on the Fatigue Strength of Riveted and Bolted Joints." *Research Report C110,* The Technological Institute, Northwestern University, Chicago, Illinois (Sept. 1952).
7. BARON, F., and KENWORTHY, K. J., "The Effect of Certain Rivet Patterns on the Fatigue and Static Strengths of Joints." Part 2, Technical Report, Dept. of Civil Engineering, Northwestern University, Evanston, Illinois (Feb. 1954).
8. BARON, F., LARSON, E. W., and KENWORTHY, K. J., "The Effect of Certain Rivet Patterns on the Fatigue and Static Strength of Joints." Report on RCSJ, Research Council on Riveted and Bolted Structural Joints of the Engineering Foundation, New York, New York (Feb. 1955).
9. CHEESEWRIGHT, P. R., "Analysis of Fatigue Data from Riveted Wrought-Iron Girders Using the Method of Maximum Likehood." *Technical Memorandum TM FM 26,* British Rail—Research and Development Div. (Mar. 1982).
10. European Convention for Constructional Steel Work, "Recommendations for the Fatigue Design of Structures." Technical Report, ECCS (Oct. 1982).
11. Research Council on Riveted and Bolted Structural Joints of the Engineering Foundation, "The Effect of Grip on the Fatigue Strength of Riveted and Bolted Joints," Technical Report, Research Council on Riveted and Bolted Structural Joints of the Engineering Foundation, New York, New York (Dec. 1953).
12. FISHER, J. W., YEN, B. T., FRANK, W. J., and KEATING, P. B., "An Assessment of Fatigue Damage in the Norfolk and Western Railway Bridge 651 at Hannibal, Missouri, Technical Report 484-1(83), Fritz Engineering Laboratory (Dec. 1983).
13. GRAF, O., "Experiments on the Fatigue Behavior of Punched and Drilled Holes in I30 Girders" (ST37), Die Stahlbau (19/2):9–16, January 1937, Additional Publication to Die Bautechnik.
14. Deutschen Ausschusses fuer Stahlbau, "Versuche Mit Nietverbindugen," Julius Springer, Berlin, W. Germany, 1941, Berichte der D.A.S. Vol. 12.
15. HANSEN, N. G., "Fatigue Tests of Joints of High-Strength Steel," American Society of Civil Engineers, Transactions ASCE, Vol. 126, pp 750–763 (1961).
16. KLOEPPEL, K., "Gemeinschaftsversuche Zur Bestimmung Der Schwellzugfestigkeit Voller, Gelochter Und Genieteter Staebe Aus St. 37 Und St. 52," Der Stahlbau, 9(13/14):97–112, June 1936, Additional Publication to Die Bautechnik.
17. LENZEN, K. H., "The Effect of Various Fasteners on the Fatigue Strength of a Structural Joint," American Railroad Engineering Association, *AREA Bulletin,* Vol. 51, No. 481 (1949).
18. Nederlandse Spoorwegen, "Various Fatigue Tests on Steel and Wrought-Iron Specimens," Test Reports, Nederlandse Spoorwegen (1974–82) (Not published).
19. OWENS, G. W., DRIVES, P. J. and KRIGE, A. J., "Punched Holes in Structural Steel Work," *Journal of Constructional Steel Research 1(3)* (May 1981).

20. PAROLA, J. F., CHESSON, E. and MUNSE, W. H., "Effect of Bearing Pressure on Fatigue Strength of Riveted Connections," *Engineering Experiment Station Bulletin,* Vol. 481, University of Illinois (1965).

21. Research Council on Riveted and Bolted Structural Joints of the Engineering Foundation, "New Concepts in Structural Joint Design." Technical Report, Research Council on Riveted and Bolted Structural Joints of the Engineering Foundation, Chicago, Illinois (Dec. 1953).

22. REEMSNYDER, H. S., "Fatigue Life Extension of Riveted Connections." ASCE *J. Struct. Div.* 101:2591 (Dec. 1975).

23. ROLFE, S. T., and BARSOM, J. M., *Fracture and Fatigue Control in Structures—Application of Fracture Mechanics.* Prentice-Hall (1977).

24. SBB-GD, Bauabteilung Bruckenbau, *Wrought Iron Bridges.* PART 4: "Fatigue Strength," Technical Report, Schweizerische Bundesbahn, Bern, Switzerland (March 1979). (In German, not published)

25. SEONG, C. K., "Fatigue Resistance of Riveted Steel Truss Members and Joints." Ph.D. Dissertation, Lehigh University (Sept. 1983).

26. STOUT, R. D., TOR, S. S., and RUZEK, T. J., "The Effect of Fabrication Processes used in Pressure Vessels." *Welding J.* (Sept. 1951).

27. TADA, H., PARIS, P. C., and IRWIN, G. R., *The Stress Analysis of Cracks Handbook.* Del Research Corporation, Hellertown, Pennsylvania (1973).

28. WILSON, W. M., and THOMAS, F. P., "Fatigue Tests of Riveted Joints." *Engineering Experimental Station Bulletin,* Vol. 32 302, University of Illinois (1938).

29. WILSON, W. M., "Flexural Fatigue Strength of Steel Beams." *Engineering Experiment Station Bulletin,* Vol. 377, University of Illinois (1948).

30. OUT, J. H., FISHER, J. W., and YEN, B. T., "Fatigue Strength of Weathered and Deteriorated Riveted Members." *Final Report DOT/OST/P-34/85/016,* U.S. Dept. of Transportation (Oct. 1984).

31. RABEMANANTSOA, H., and HIRT, M. A., "Comportement a la Fatigue de Profiles Lamines avec Semelles de Renfort Rivetees." *Publication ICOM 133,* Swiss Federal Institute of Technology, Lausanne (Sept. 1984).

32. WILSON, W. M., and COOMBE, J. W., "Fatigue Tests of Connection Angles." *Engineering Experiment Station Bulletin,* Vol. 317, University of Illinois (1939).

33. WILSON, W. M., "Design of Connection Angles for Stringers of Railway Bridges." *Proc., AREA,* Vol. 41 (1940).

34. FISHER, J. W., "Bridge Fatigue Guide—Design and Details." AISC (1976).

35. Ammann & Whitney, "Elevated Lines Structural Survey." Phase I and Phase II reports to New York City Transit Authority (Sept. 1975 and Aug. 1978).

36. ROBERTS, R., FISHER, J. W., IRWIN, G. R., BOYER, R. D., HAUSAMMANN, H., KRISHNA, G. V., MORF, U., and SLOCKBOWER, R. E., "Determination of Tolerable Flaw Sizes in Full Size Welded Bridge Details." *Report No. FHWA-RD-77-170* (Dec. 1977).

37. AASHTO, *Manual for Maintenance Inspection of Bridges.* AASHTO, Washington, D.C. (1983).

38. FISHER, J. W., YEN, B. T., and DANIELS, J. H., "Fatigue Damage in the Lehigh Canal Bridge from Displacement-Induced Secondary Stresses." *TRB Record 607,* Transportation Research Board (1976).

39. FISHER, J. W., BELLENOIT, J. R., DANIELS, J. H., and YEN, B. T., "High Cycle Fatigue Behavior of Steel Bridge Details." Final Report, *Fritz Engineering Laboratory Report 386-13,* Lehigh University (1982).

40. CUSTEN, A. M., and GOLDSMITH, R. H., "Queens Boulevard Bridge over Sunnyside Yards." Bridge Rehabilitation Project Program, AMMANN & WHITNEY preliminary report to New York City DOT and New York State DOT (Apr. 1982).

41. DANIELS, J. H., WILSON, J. L., LAI, L. Y., ABBASZADEH, R., and YEN, B. T., "WIM + Response Study of Four in Service Bridges." Final Report Draft of DTFH61-83-C-00091, Lehigh University (Mar. 1986).

42. SVOTELIS, R. A., HEINS, C. P. JR., and LOONEY, C. T. G., "Analytical and Experimental Study of a Through Truss Bridge." Progress Report, University of Maryland (June 1967).

43. FISHER, J. W., "Report on Susquehanna River Bridge." Letter Reports to Maryland Transportation Authority (May 1986 and Aug. 1986).

44. FISHER, J. W., *Fatigue and Fracture in Steel Bridges,* John Wiley & Sons (1984).

45. KULAK, G. L., FISHER, J. W., and STRUICK, J. H. A., *Guide to Design Criteria for Bolted and Riveted Joints.* John Wiley & Sons, 2nd Ed., New York City (1987).

46. MUNSE, W. H., and GRUVER, L. M., "Fatigue of Welded Steel Structures." Welding Research Council, New York City (1964).

47. SAMANS, C. H., *Engineering Metals and Their Alloys.* The Macmillan Company, New York (1950).

48. MOSES, F., SCHILLING, C. G., and RAJU, K. S., "Fatigue Evaluation Procedures for Steel Bridges." *NCHRP Report 299* (Nov. 1987).

49. IRWIN, G. R., "Linear Fracture Mechanics—Fracture Transition and Fracture Control." *Engineering Fracture Mechanics,* Vol. 1 (1968).

50. MERKLE, J., "Construction Research for Materials Engineering Branch." U.S. Nuclear Regulatory Commission *Report NUREG-0975,* Vol. 1 (Mar. 1983).

APPENDIX A

FORMAT OF DATA BASE

<u>Example:</u>

<u>NS70W</u>10.150<u>03.340</u>+0.500<u>31.620</u>03.250<u>01.300</u> 1 2 1 2 2 -1 2 2

   <u>ID</u>   S_r   <u>N</u>   R   <u>F_Y</u>   BR <u>GL</u> N<u>GTMRDHCC</u>F<u>HP</u>TC<u>SS</u>

Where:

ID = Identification

S_r = Stress range

N = Cycles at failure $(\times 10^6)$

R = Stress ratio $(= S_{min}/S_{max})$

F_Y = Yield strength of material

BR = Bearing ratio

GL = Grip length

NG = Nominal stress calculation (Net section/Gross section)

TM = Type of material (Steel/Wrought iron)

RD = Rolling direction (Parallel/Transverse)

HC = Hole condition (Open hole/With rivet)

CF = Clamping force (Reduced/Normal)

HP = Method of hole preparation (Punched/Drilled)

TC = Type of connection (Simple shear splice/Coverplate end/Built-up girder)

SS = Specimen state (Virgin material/Existing structure)

APPENDIX B

DETAILS OF TEST RESULTS

<u>Terminology</u>

A_c	Lost area due to cracking or corrosion	N	Fatigue test cycles
A_n	Net area at the critical section without loss	Rm.T.	Room temperature (70°F or 21°C)
F_Y	Yield strength of the steel	$S_{max,net}$	Estimated net section stress at the cracked section
F_u	Ultimate strength of the steel		

Girder No. 1: S_r=15 ksi (103 MPa), S_{min}=2 ksi (14 MPa)
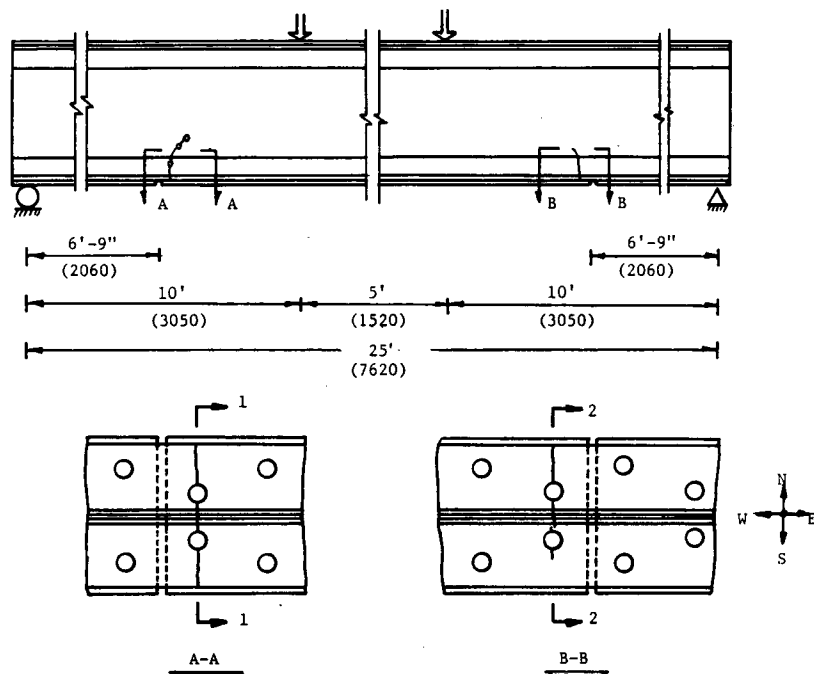
Fatigue crack initiation: at coverplate termination, through rivet holes.

Load redistribution: As one of the component cracked, the other took over the load, and the girder moved sideways. Bottom flange lateral bracing prevented lateral movement and increased fatigue life.

At failure: More than 80% net section area lost; all components failed; deflection increment indicated plastic deformation; girder still took full fatigue loading.

Girder No. 1

Section 1-1

Staggered crack surfaces

Coverplate-cut

Girder No. 1

Section 2-2

Staggered crack surfaces

Coverplate-cut
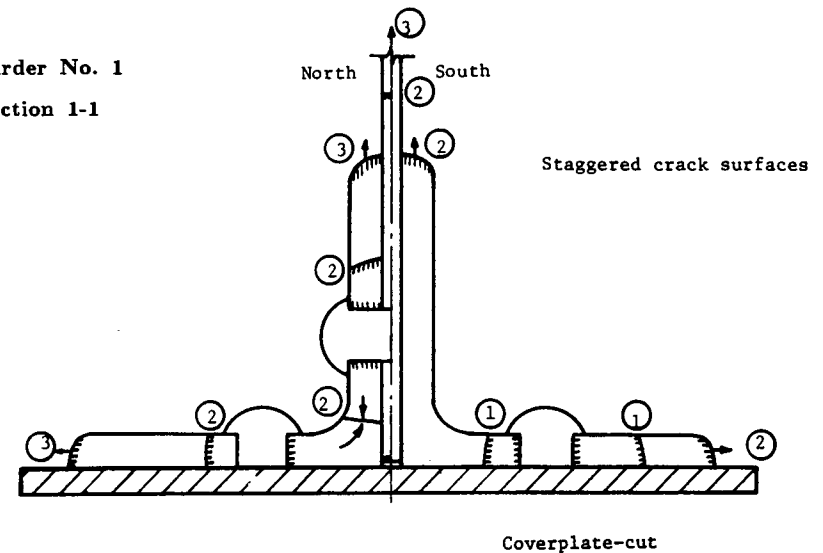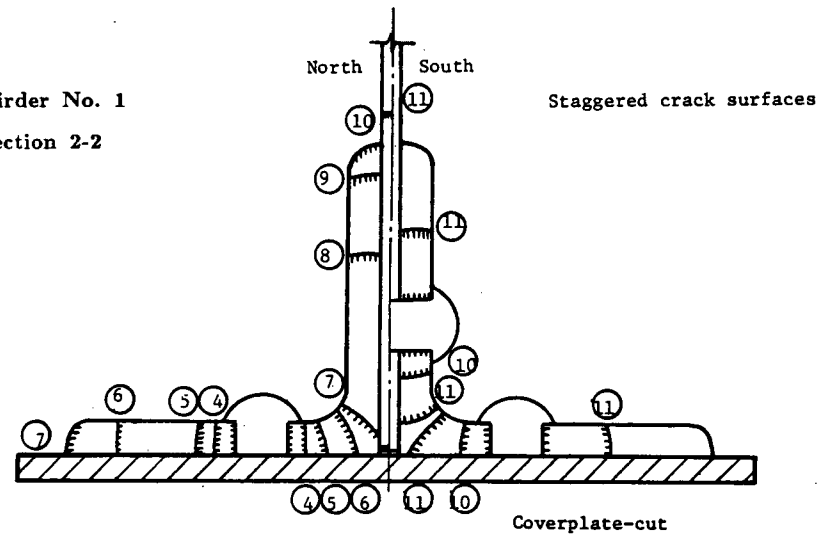
Girder No. 1

Stage	Cycles $\times 10^6$	A_c/A_n %	Temp. °F (°C)	P_{max} kip (KN)	$S_{max,net}$ ksi (MPa)	Note
1	<0.588	9	Rm.T. (1-1)	80 (356)	18.6 (128)	Crack initiated at cover-plate termination, through riveted holes.
2	0.588	81	Rm.T. (1-1)	80 (356)	>F_u	Section 1-1 cracked in most of the components, and was retrofitted by C-clamping reinforcing plates. Holes were drilled at crack tips.
3	0.647	100	Rm.T. (1-1)	80 (356)	>F_u	Section 1-1 components cracked completely, Web cracks were arrested by drilling holes.
4	0.686	3	Rm.T. (2-2)	80 (356)	17.6 (121)	New cracks were detected at section 2-2.
5	0.730	6	Rm.T. (2-2)	80 (356)	18.1 (125)	Stable crack growth
6	0.813	15	Rm.T. (2-2)	80 (356)	20.1 (139)	Stable crack growth
7	0.818	22	Rm.T. (2-2)	80 (356)	21.7 (150)	Stable crack growth
8	0.847	36	Rm.T. (2-2)	80 (356)	26.4 (182)	Stable crack growth
9	0.864	42	Rm.T. (2-2)	80 (356)	29.4 (202)	Stable crack growth
10	0.911	49	Rm.T. (2-2)	80 (356)	33.4 (230)	Crack reinitiation at south angle and web.
11	0.916	83	Rm.T. (2-2)	80 (356)	>F_u	Machine stopped by displacement control device. No cracks were found in constant moment region. The girder still took full fatigue load.

Figure B1. Girder 1 at 647,800 cycles (section 2-2, north side).
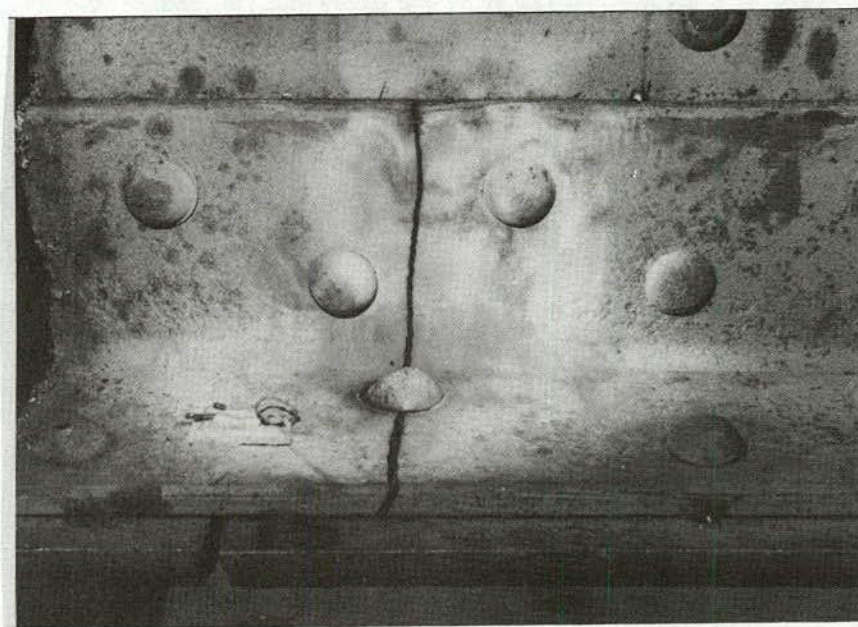
Figure B2. Girder 1 at 916,000 cycles (section 2-2, north side).
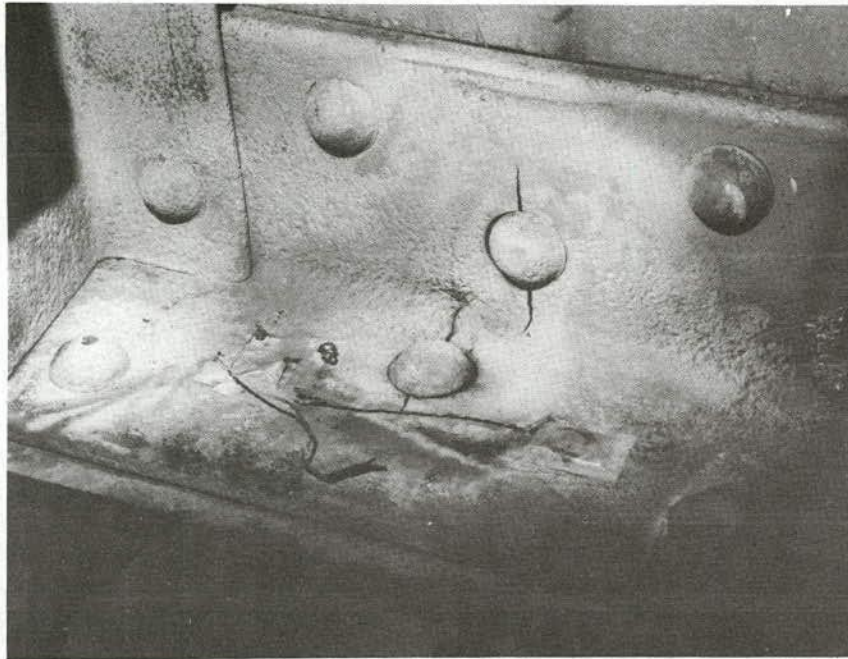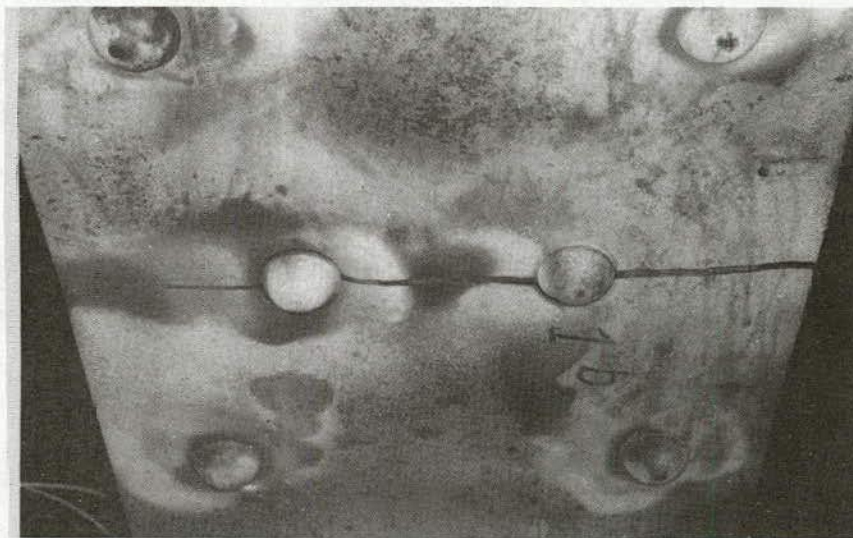
Figure B3. Girder 1 at 916,000 cycles (section 2-2, south side).
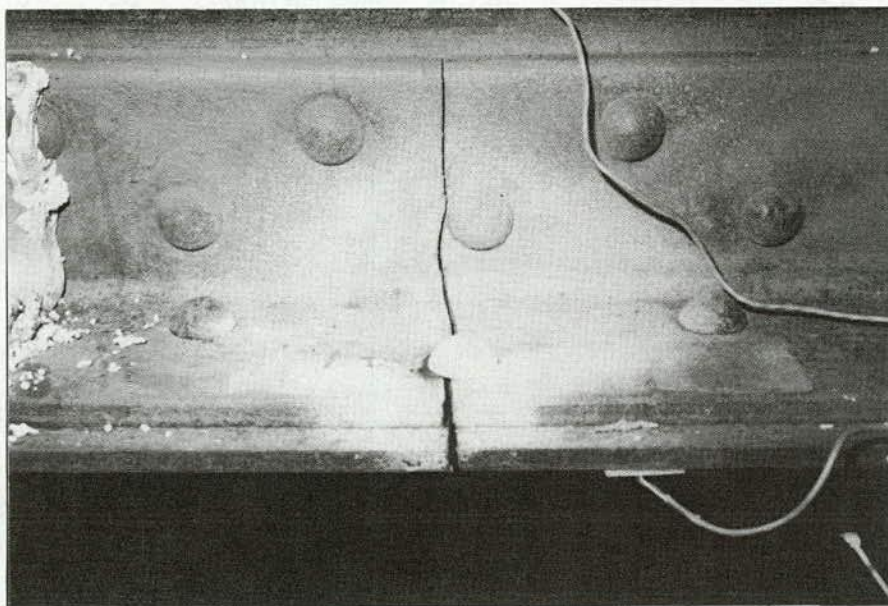
Girder No. 2: S_r=15 ksi (103 MPa), S_{min}=2 ksi (14 MPa)
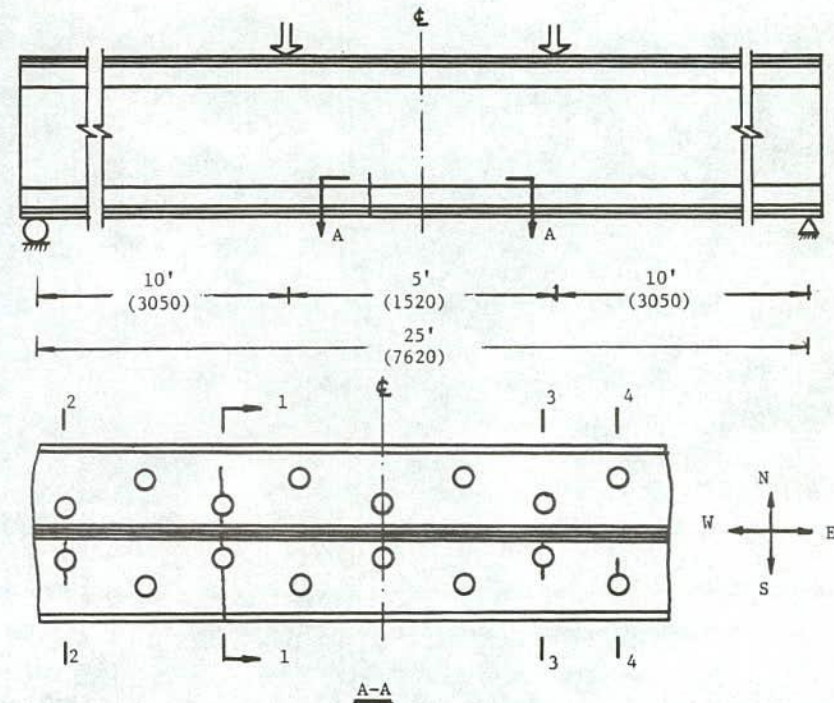
A-A

Fatigue crack initiation: within constant moment region, through rivet holes.

Load redistribution: Four cross-sections cracked at 1.094 million cycles. Section 1-1 became the critical section while the others were arrested. As one component cracked, the others took up the load and the girder moved sideways. Bottom flange lateral bracing increased fatigue life.

At failure: About 90% net section area lost; all components failed; increasing deflection indicated plastic deformation; girder still took full fatigue load.

Girder No. 2

Section 1-1
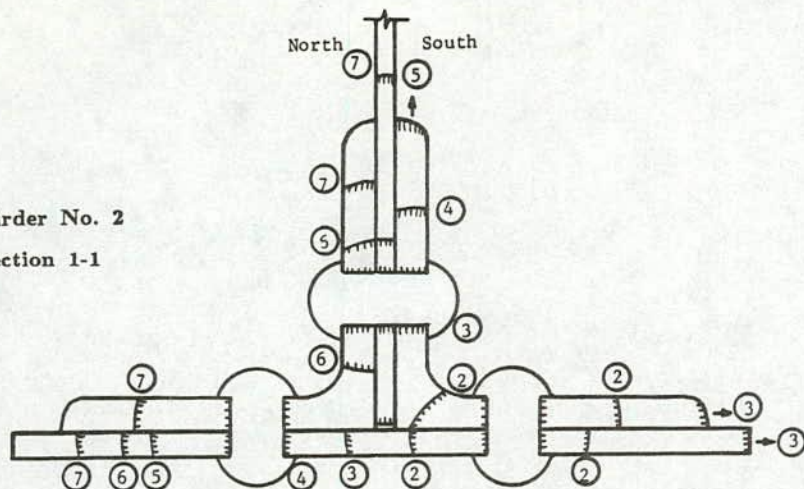
Girder No. 2

Stage	Cycles x10^6	A$_c$/A$_n$ %	Temp. °F (°C)	P$_{max}$ kip (KN)	S$_{max,net}$ ksi (MPa)	Note
1	1.056	–	Rm.T.	89 (396)	17.0 (117)	Powder was seen at section 1-1, around south flange rivet head.
2	1.094	15	Rm.T.	89 (396)	20.0 (138)	Cracks initiated at four net-sections in constant moment region.
3	1.214	38	-40 (-40)	89 (396)	27.2 (188)	A sharp noise was heard and girder moved sideways when angle and coverplate cracks extending to the tips.
4	1.228	45	Rm.T.	89 (396)	30.9 (213)	Stable crack growth
5	1.234	57	Rm.T.	89 (396)	>F$_Y$	Stable crack growth
6	1.236	70	Rm.T.	89 (396)	>F$_u$	Fast crack extension on north angle.
7	1.237	90	Rm.T.	89 (396)	>F$_u$	Machine stopped by displacement control device. The girder still took full fatigue load.

Figure E4. Girder 2 at 1,214,000 cycles (section 1-1, south side).

Figure B5. Girder 2 at 1,237,000 cycles (section 1-1, bottom view).

Girder No. 3: S_r=12 ksi (83 MPa), S_{min}=2 ksi (14 MPa)
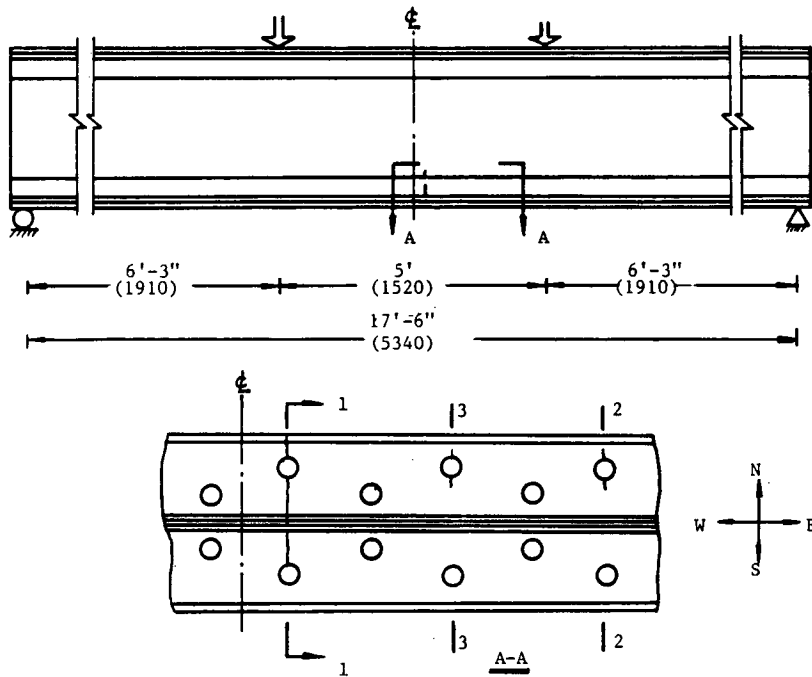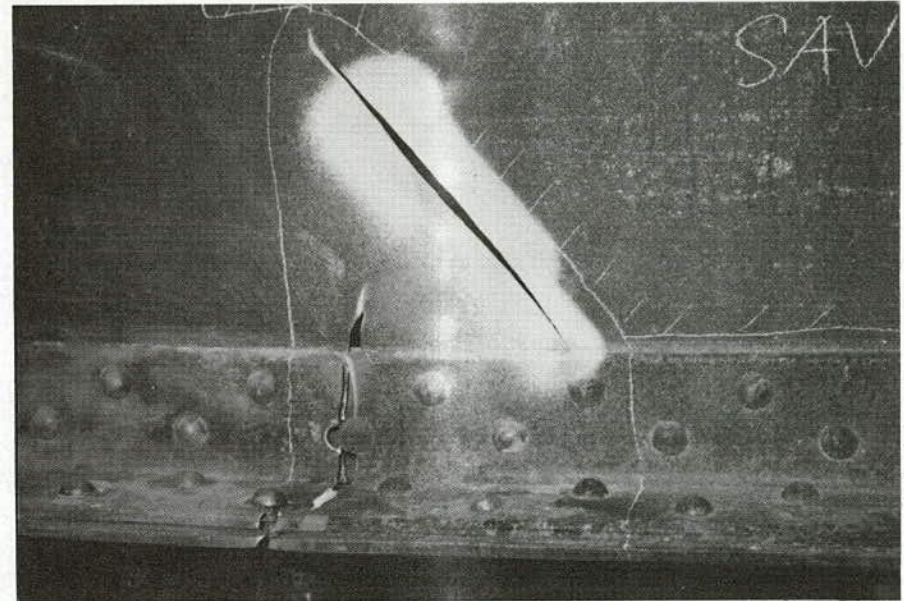

Girder No. 3

Section 1-1

Staggered crack surface

Fatigue crack initiation: within constant moment region, through rivet holes.

Load redistribution: Cracks initiated at three cross-sections between 1.410 and 1.500 cycles. Section 1-1 became critical while the others were arrested. As one component cracked, the others took up the load and the girder moved sideways. Adding bottom flange lateral bracing increased fatigue life.

At failure: More than 80% net section area lost; most components failed completely; no big deflection increment occurred; the girder still took maximum fatigue loading.

Girder No. 3
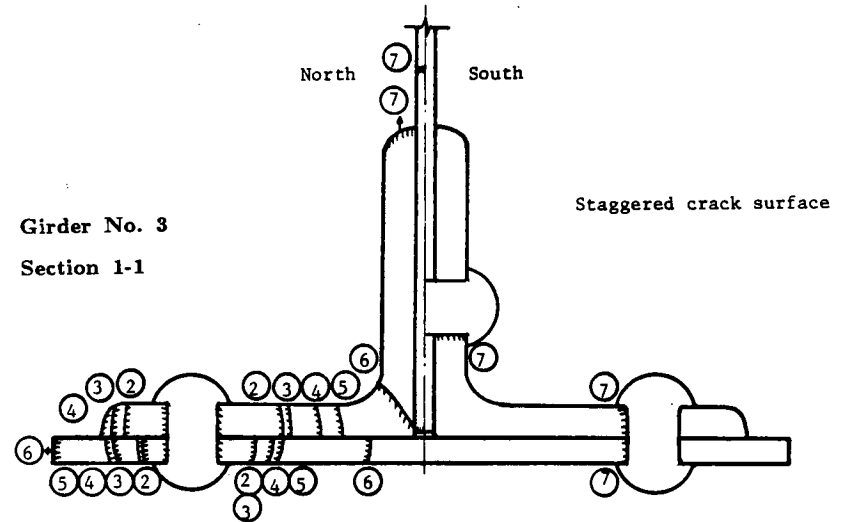
Stage	Cycles x10⁶	A_c/A_n %	Temp. °F (°C)	P_{max} kip (KN)	$S_{max,net}$ ksi (MPa)	Note
1	1.410	–	Rm.T.	105 (467)	14.0 (97)	Strain gage reading change indicated crack initiation.
2	1.435	9	Rm.T.	105 (467)	15.4 (107)	Cracks were detected at two net-sections in constant moment region.
3	1.509	12	-40 (-40)	105 (467)	15.8 (109)	Reduced temperature test did not cause fracture. A third crack was detected.
4	1.548	15	Rm.T.	105 (467)	16.6 (114)	Stable crack growth
5	1.575	17	-70 (-57)	105 (467)	16.9 (116)	Reduced temperature test did not cause fracture.
6	1.599	30	Rm.T.	105 (467)	20.1 (138)	Stable crack growth
7	1.623	82	-70 (-57)	105 (467)	>F_u	Reduced temperature test caused fracture.
8	1.623	82	Rm.T.	110 (489,static)	>F_u	No overall failure was observed.

Figure B6. Girder 3 at 1,623,000 cycles (section 1-1, north side).

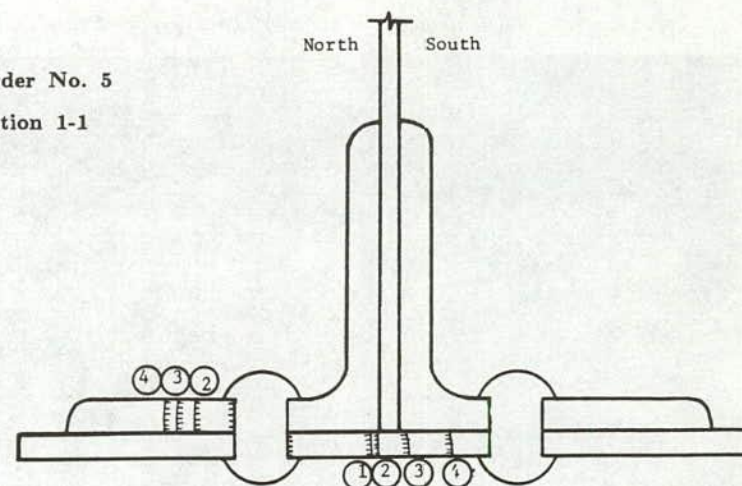Girder No. 4: S_r=12 ksi (83 MPa), S_{min}=2 ksi (14 MPa)
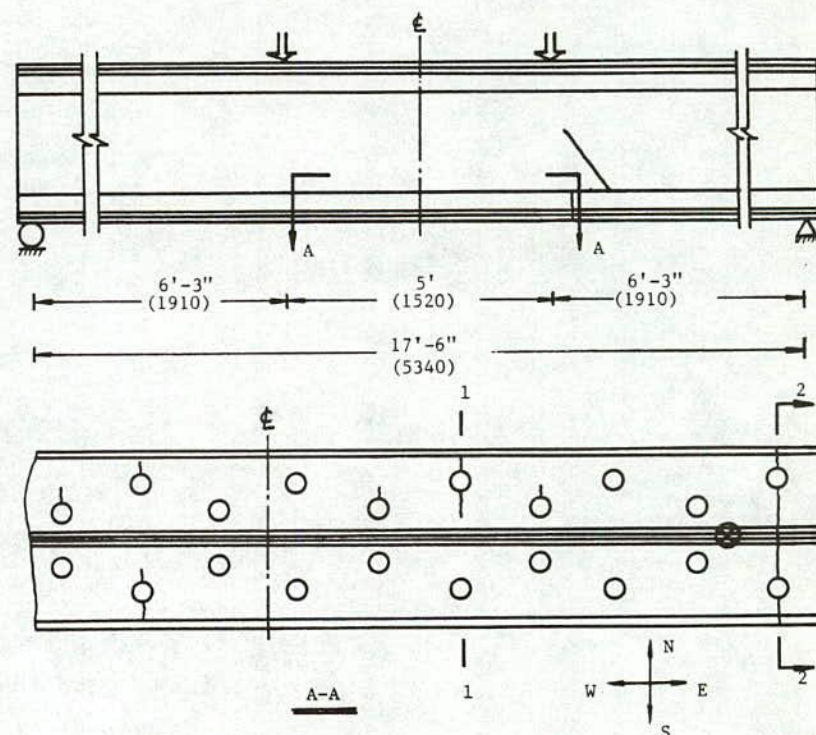
Fatigue crack initiation: within constant moment region, through riveted holes.

Load redistribution: Cracks were detected in seven cross-sections at 2.63 million cycles. Section 2-2 became critical while the others were arrested. As one component cracked, the others took up the load, and the girder moved sideways. Adding bottom flange lateral bracing contributed to fatigue life.

At failure: 100% net section area lost; all components failed; rapid deflection increment was observed; residual static capacity of the girder was 40% of maximum fatigue loading.

Girder No. 4

Section 2-2
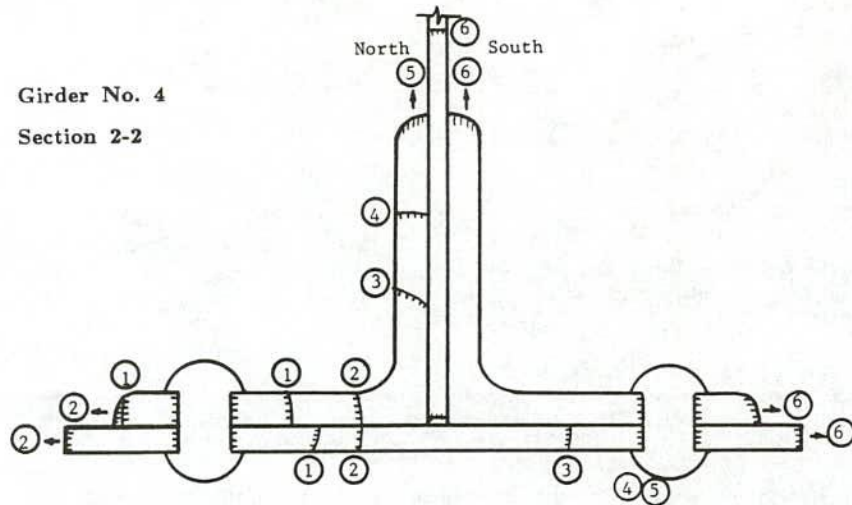
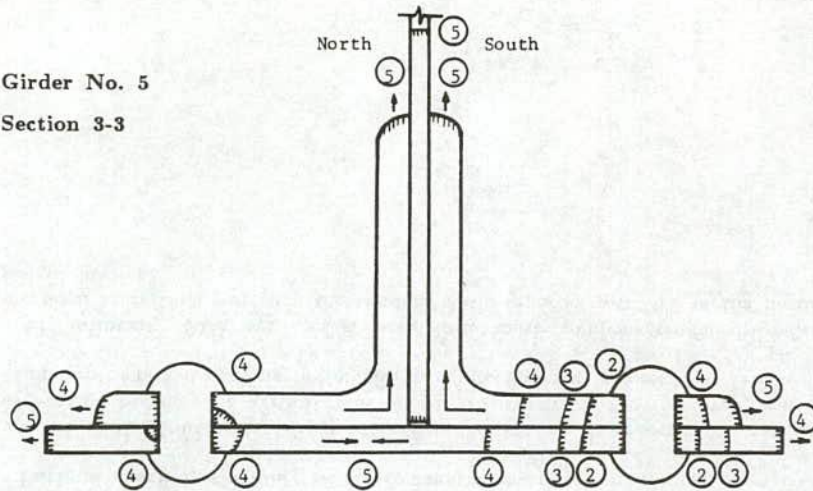| Stage	Cycles $\times 10^6$	A_c/A_n %	Temp. °F (°C)	P_{max} kip (KN)	$S_{max,net}$ ksi (MPa)	Note
1	2.630	10	Rm.T.	110 (489)	15.6 (108)	Cracks were found at seven net-sections in constant moment region
2	2.752	22	Rm.T.	110 (489)	17.9 (124)	Bottom flange lateral bracings were added.
3	2.783	40	-120 (-84)	110 (489)	23.5 (162)	Diagonal crack grew into web in shear span.
4	2.797	48	Rm.T.	110 (489)	27.1 (187)	Stable crack growth
5	2.816	54	Rm.T.	110 (489)	30.4 (210)	Stable crack growth
6	2.838	100	Rm.T.	110 (489)	>F_u	All components failed in a ductile behavior.
7	2.838	100	Rm.T.	44 (196, static)	>F_u	Residual static capacity

Figure B7. Girder 4 at 2,838,000 cycles (section 2-2, south side).
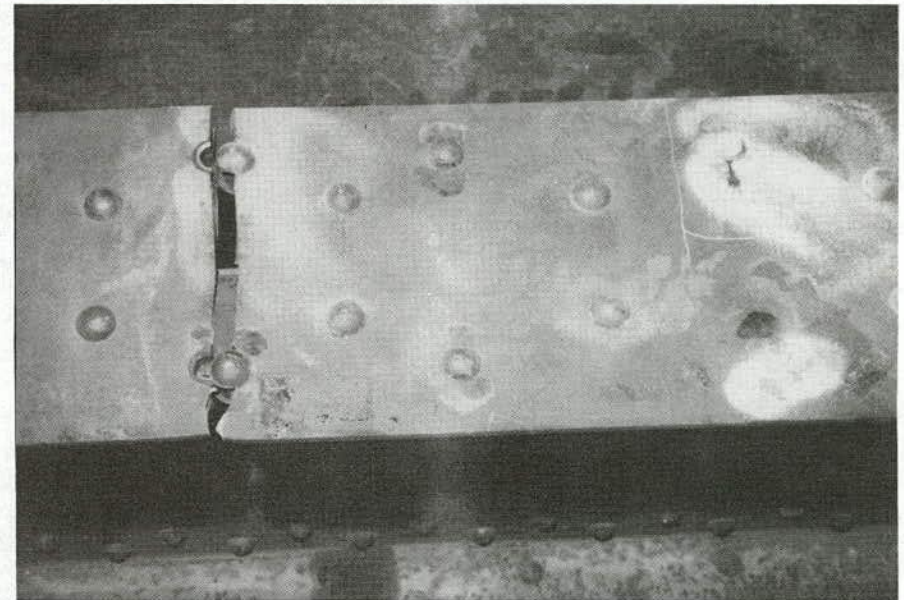
Figure B8. Girder 4 at 2,838,000 cycles (section 2-2, bottom view).

Girder No. 5: $S_r=12$ ksi (83 MPa), $S_{min}=8$ ksi (55 MPa)

10' (3050) — 5' (1520) — 10' (3050)

25' (7620)

A-A

Girder No. 5
Section 1-1

Girder No. 5
Section 2-2
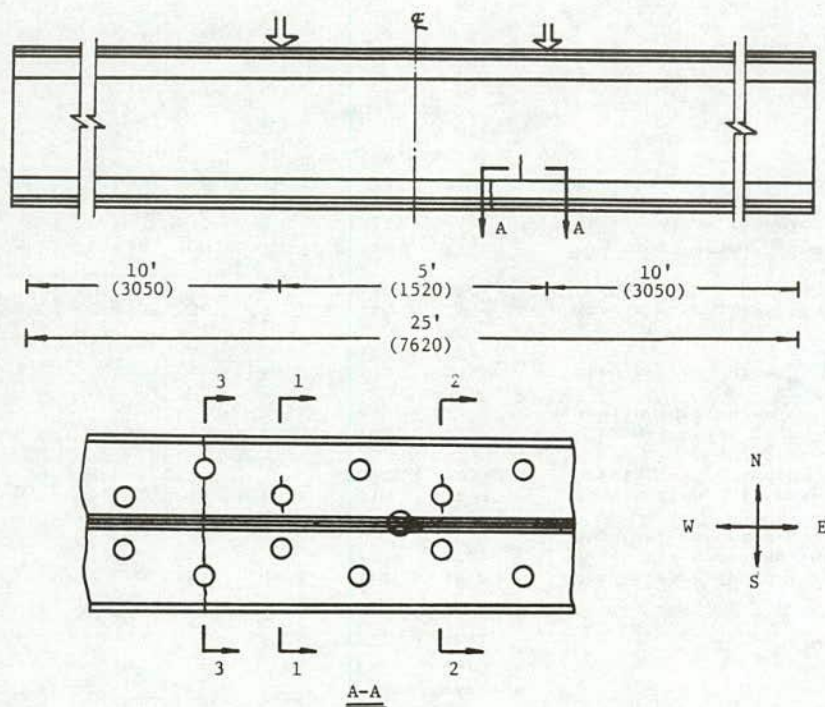
Fatigue crack initiation: within or near constant moment region, through rivet holes.

Load redistribution: Cracks were detected in three cross-sections at 2.344 million cycles. Section 3-3 later became critical while the others were arrested. Load redistribution was observed as one or more components cracked. Lateral bracing was added to the bottom flange.

At failure: 100% net section area lost; all components failed; rapid deflection increment was observed; residual static capacity of the girder was 30% of the maximum fatigue loading.

Girder No. 5

Section 3-3

| Stage	Cycles x10^6	A_c/A_n %	Temp. °F (°C)	P_{max} kip (KN)	$S_{max,net}$ ksi (MPa)	Note
1	2.344	4(1-1) 3(2-2)	Rm.T.	100 (445)	20.8 (144)	Crack initiation in constant moment region
2	2.370	6(1-1) 6(2-2) 5(3-3)	Rm.T.	100 (445)	21.1 (145)	Stable crack growth
3	2.727	9(1-1) 6(2-2) 9(3-3)	Rm.T.	100 (445)	21.9 (151)	Stable crack growth
4	2.727	12(1-1) 6(2-2) 26(3-3)	Rm.T.	100 (445)	27.1 (187)	Stable crack growth
5	2.728	100 (3-3)	-100 (-73)	100 (445)	$>F_u$	Brittle fracture under reduced temperature
6	2.728	100 (3-3)	Rm.T. Rm.T.	30 (133,static)	$>F_u$	Residual static capacity
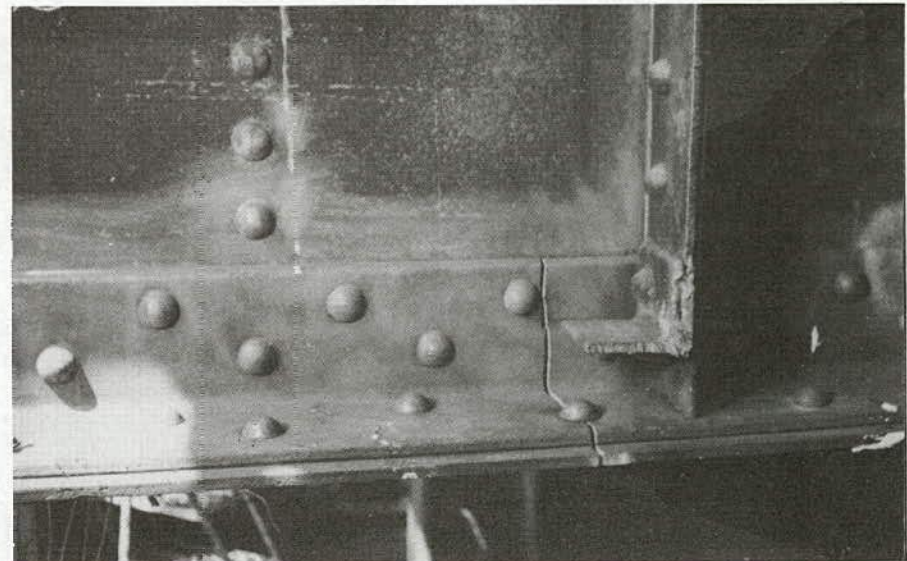
Figure B9. Girder 5 at 2,728,000 cycles (section 3-3, south side).
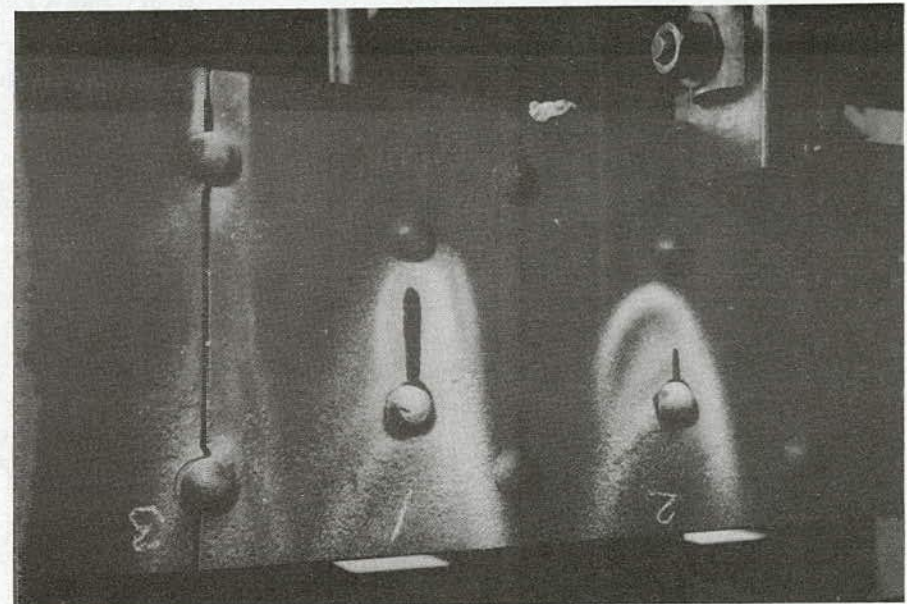
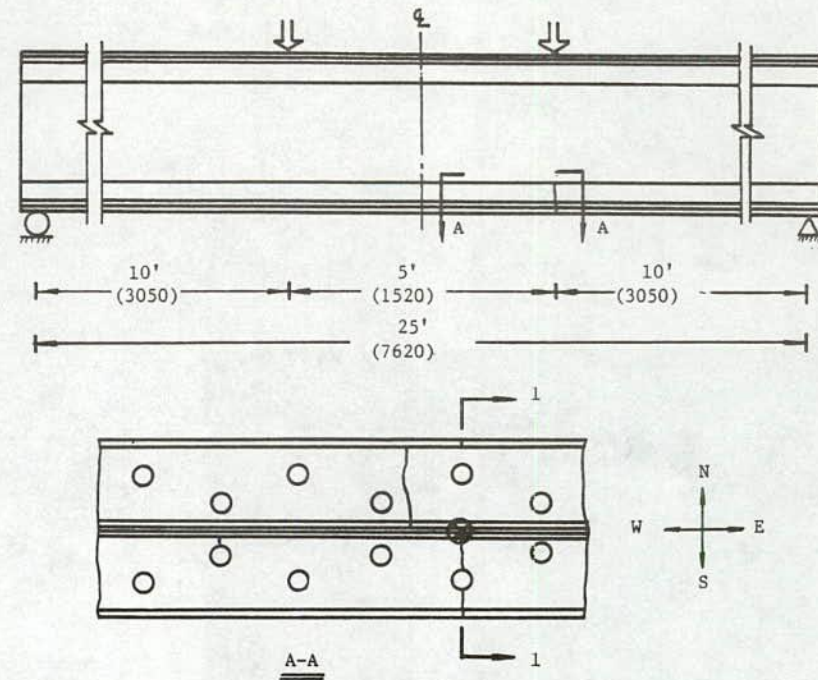*Figure B10. Girder 5 at 2,728,000 cycles (section 3-3, bottom view).*

Girder No. 6: S_r=12 ksi (83 MPa), S_{min}=8 ksi (55 MPa)
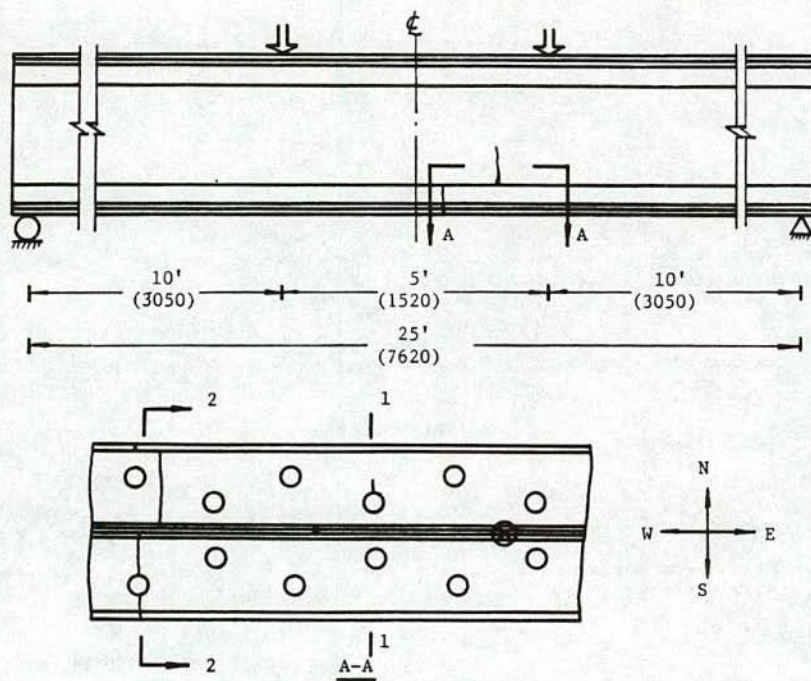
Girder No. 6

Section 2-2

A-A

Fatigue crack initiation: within constant moment region, through rivet holes.

Load redistribution: Cracks were detected in two cross-sections. Section 2-2 eventually became the critical one. Load redistribution was observed when the components cracked. Adding bottom flange lateral bracing increased the fatigue life.

At failure: 95% net section area lost; most components failed; deflection increased more than one inch; the residual static capacity was 50% of the maximum fatigue loading.

Girder No. 6
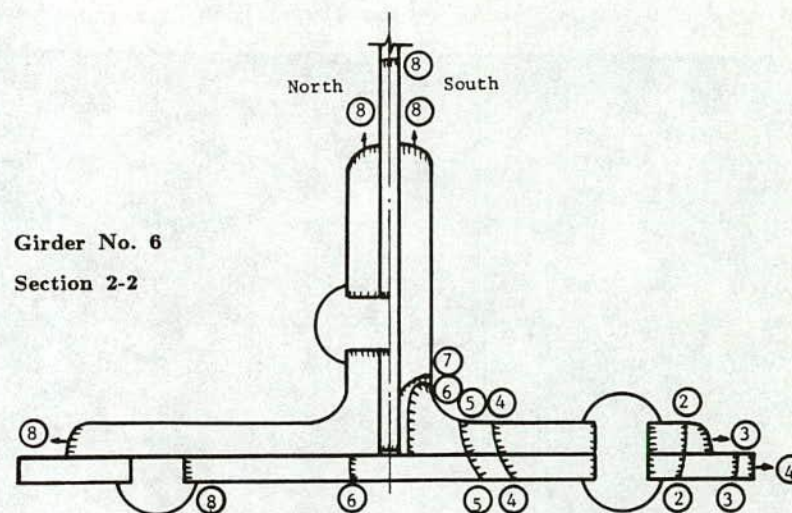
Stage	Cycles $\times 10^6$	A_c/A_n %	Temp. °F (°C)	P_{max} kip (KN)	$S_{max,net}$ ksi (MPa)	Note
1	2.575	–	Rm.T.	95 (423)	20.0 (138)	A crack was detected at section 1-1.
2	2.790	4	Rm.T.	95 (423)	20.8 (143)	Second crack was detected at section 2-2.
3	2.922	8	Rm.T.	95 (423)	21.6 (149)	Stable crack growth
4	2.963	18	Rm.T.	95 (423)	24.5 (169)	Stable crack growth
5	2.976	22	-60 (-51)	95 (423)	25.5 (176)	No fracture under reduced temperature
6	3.001	34	Rm.T.	95 (423)	30.3 (209)	Stable crack growth
7	3.004	36	-60 (-51)	95 (423)	31.3 (215)	No fracture under reduced temperature
8	3.005	95	-60 (-51)	95 (423)	>F_u	Brittle fracture under reduced temperature
9	3.005	95	Rm.T.	47 (209,static)	>F_u	Residual static capacity
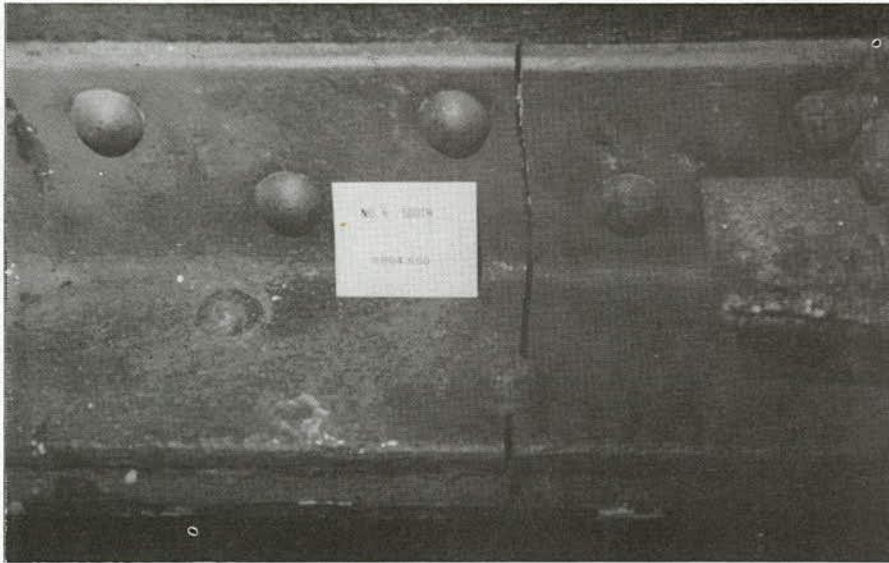
Figure B11. Girder 6 at 3,005,000 cycles (section 2-2, south side).

Figure B12. Girder 6 at 3,005,000 cycles (section 2-2, bottom view).
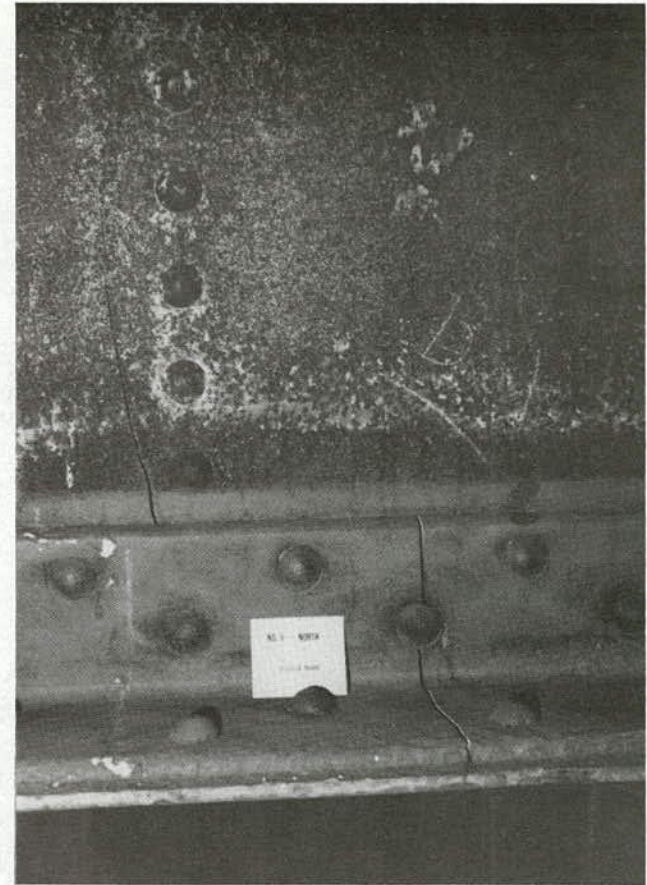
Figure B13. Girder 6 at 3,005,000 cycles (section 2-2, north side).
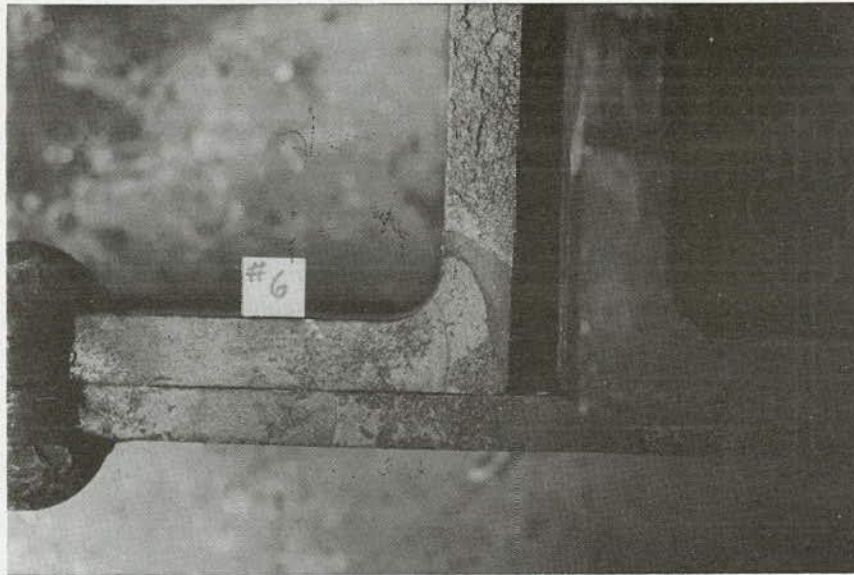
Figure B14. Cracked surface of section 2-2, girder 6.
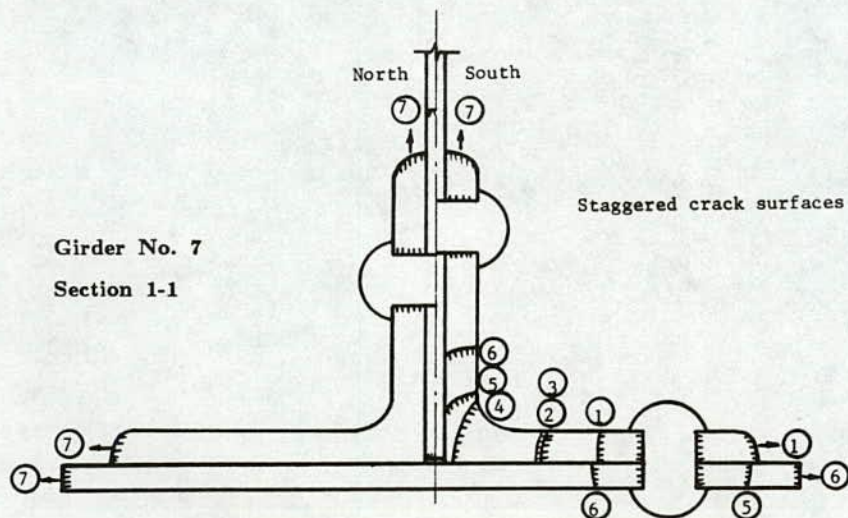
10' (3050) 5' (1520) 10' (3050)

25' (7620)

A-A

N
W — E
S

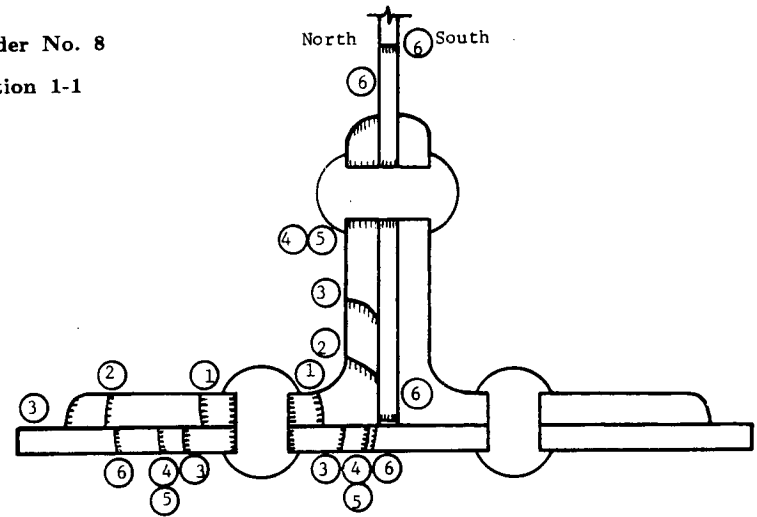Girder No. 7

Section 1-1

North South

Staggered crack surfaces

Fatigue crack initiation: within constant moment region, through rivet holes.

Load redistribution: Cracks were detected in two cross-sections at 0.601 million cycles. Section 1-1 became the critical section while the other one arrested. Load redistribution was observed as the components cracked. Bottom flange lateral bracing was added.

At failure: 100% net section area lost; all components failed; deflection increment of more than one inch was observed; the residual static capacity of the girder was 50% of the maximum fatigue loading.
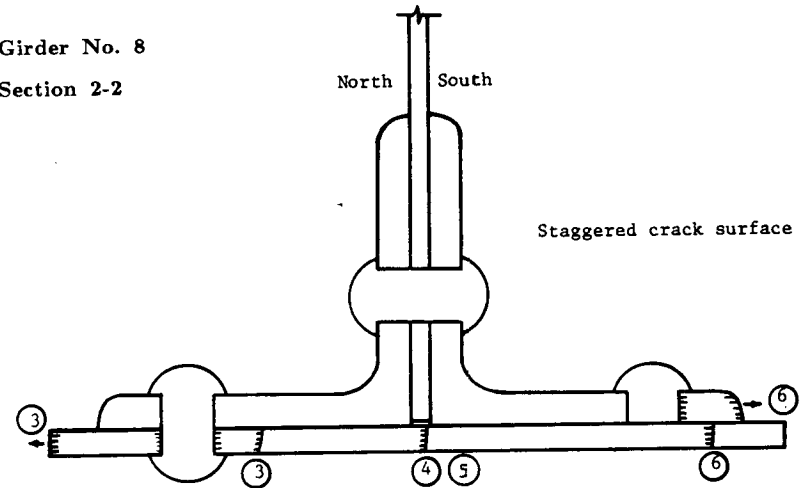
Girder No. 7

Stage	Cycles $\times 10^6$	A_c/A_n %	Temp. °F (°C)	P_{max} kip (KN)	$S_{max,net}$ ksi (MPa)	Note
1	0.601	6	Rm.T.	90 (400)	21.3 (147)	Crack initiated at two net-sections at constant moment region.
2	0.651	9	Rm.T.	90 (400)	22.0 (152)	Stable crack growth
3	0.673	10	-65 (-54)	90 (400)	22.1 (153)	No fracture under reduced temperature
4	0.739	15	Rm.T.	90 (400)	23.6 (163)	Stable crack growth
5	0.751	21	-40 (-40)	90 (400)	25.3 (175)	No fracture under reduced temperature
6	0.766	28	Rm.T.	90 (400)	27.8 (192)	Stable crack growth
7	0.773	100	-60 (-51)	90 (400)	$>F_u$	Brittle fracture under reduced temperature
8	0.773	100	Rm.T.	43 (191,static)	$>F_u$	Residual static capacity
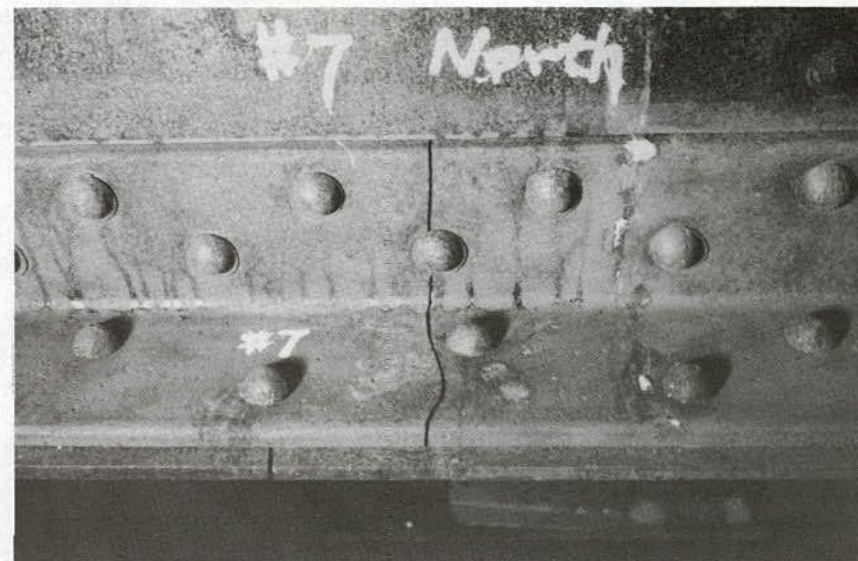
Figure B15. Girder 7 at 773,000 cycles (section 1-1, north side).
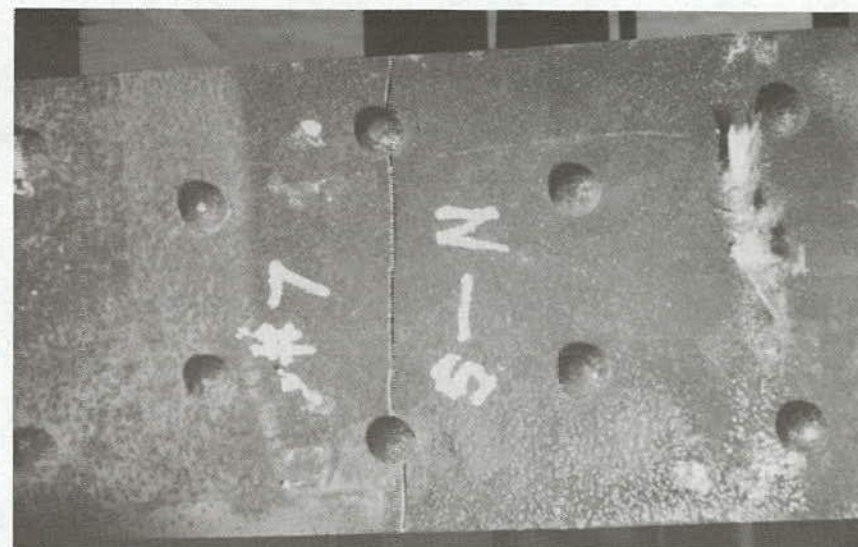
Figure B16. Girder 7 at 773,000 cycles (section 1-1, bottom view).

Girder No. 8: $S_r=15$ ksi (103 MPa), $S_{min}=8$ ksi (55 MPa)
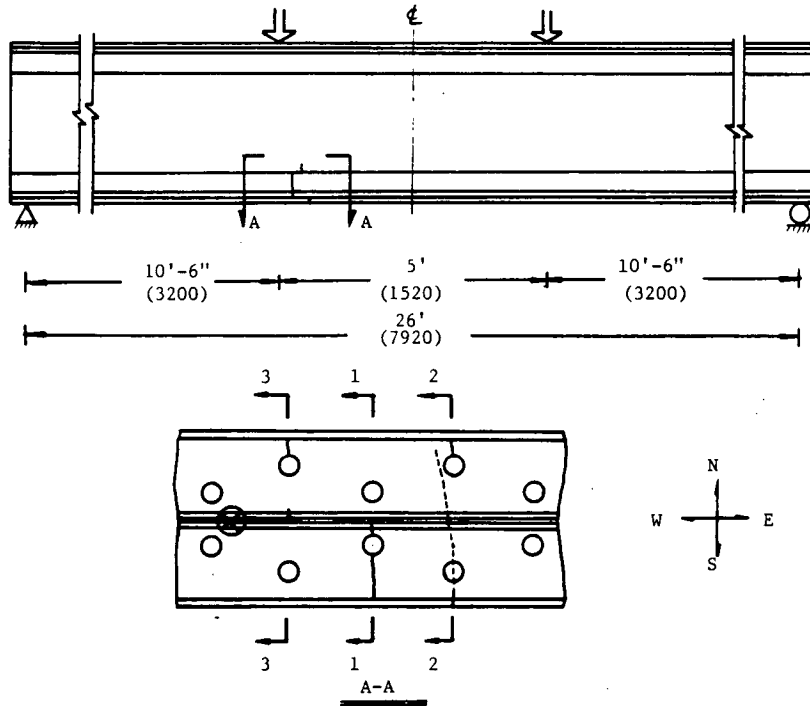
10'-6"
(3200)

5'
(1520)

10'-6"
(3200)

26'
(7920)

3   1   2

3   1   2

A-A

N
W — E
S

Girder No. 8

Section 1-1

North   South

Girder No. 8

Section 2-2

North   South

Staggered crack surface

Fatigue crack initiation: within constant moment region, through riveted holes.

Load redistribution: Cracks were detected in three cross-sections. None of them became the single major crack as the case of most test girders.

At failure: By adding lost areas of different sections together, at least 90% of the net section area lost; all components failed (in different sections); deflection increment of more than one inch was observed; the residual static capacity of the girder was 80% of the maximum fatigue loading.
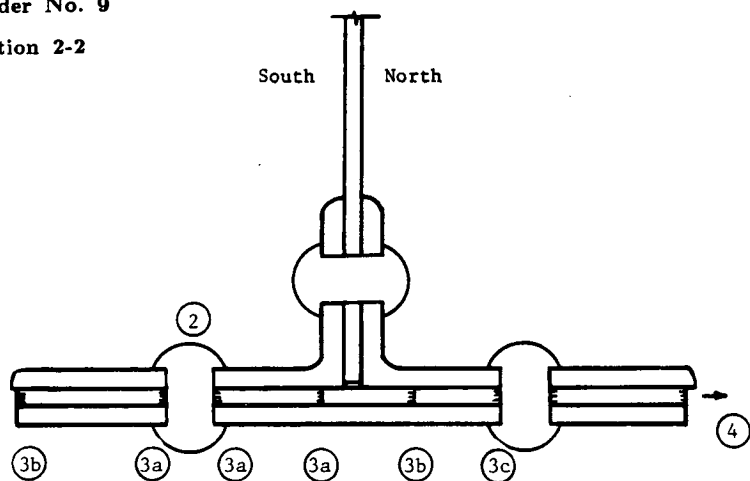
Girder No. 8
Section 3-3

Girder No. 8

Stage	Cycles x10^6	A_c/A_n %	Temp. °F (°C)	P_{max} kip (KN)	$S_{max,net}$ ksi (MPa)	Note
1	0.923	4(1-1)	Rm.T.	105 (467)	24.0 (166)	A crack was detected in section 1-1.
2	1.230	16(1-1)	Rm.T.	105 (467)	27.3 (188)	Stable crack growth
3	1.266	27(1-1) 8(2-2)	Rm.T.	105 (467)	>F_Y	Second crack was found in section 2-2
4	1.283	34(1-1) 15(2-2)	-65 (-54)	105 (467)	>F_Y	A clear noise was heard. No fracture under reduced temperature
5	1.293	34(1-1) 15(2-2)	Rm.T.	105 (467)	>F_Y	Static test -- not failed yet.
6	1.315	51(1-1) 33(2-2) 20(3-3)	-50 (-46)	105 (467)	>F_u	Fracture experienced under reduced temperature.
7	1.315	51(1-1) 33(2-2) 20(3-3)	Rm.T.	83 (369,static)	>F_u	Residual static capacity

Figure B17. Girder 8 at 1,315,000 cycles (section 1-1 and 2-2, north side).
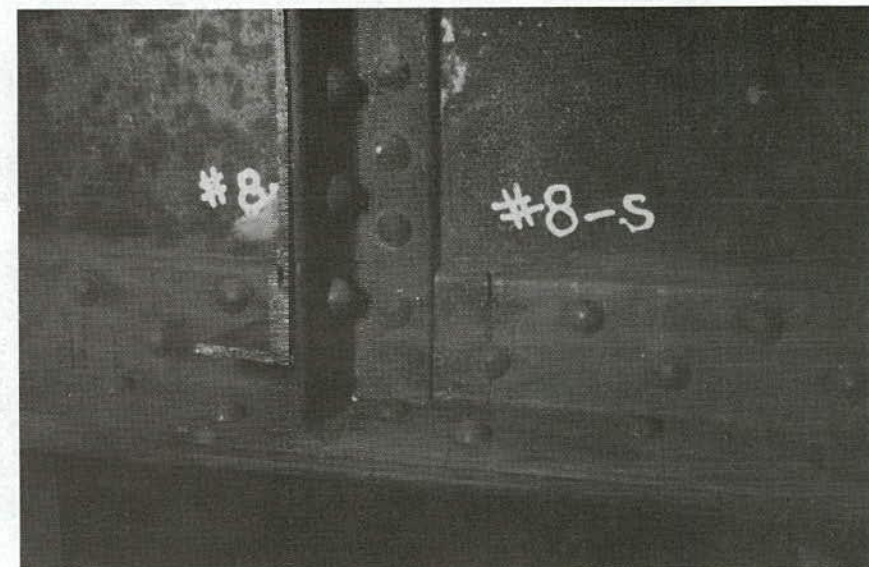
Figure B18. Girder 8 at 1,315,000 cycles (section 2-2 and 3-3, south side).
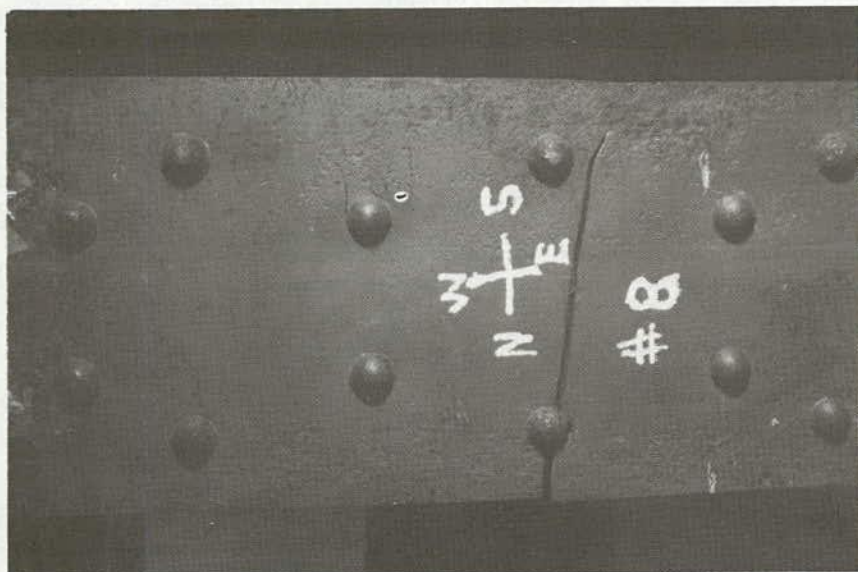
Figure B19. Girder 8 at 1,315,000 cycles (section 2-2, bottom view).
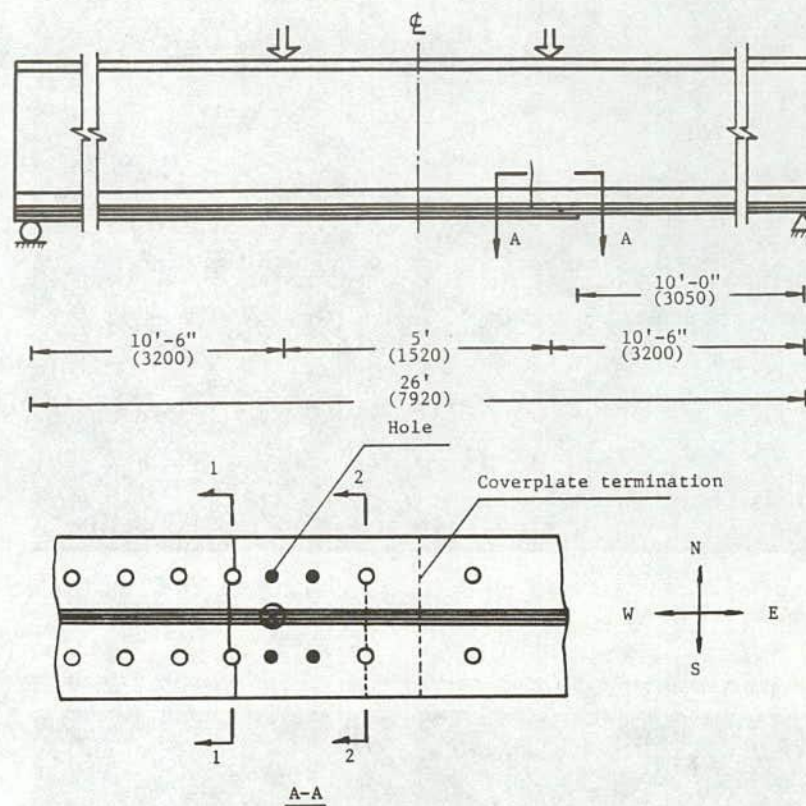
Angle fracture under static loading: due to the combination of overloading, stress concentration near external coverplate termination, and material property.

Fatigue crack initiation: at middle coverplate. adjacent to the external coverplate termination, through rivet holes.

Load redistribution: As both flange angles fractured, the other components still last 0.415 million fatigue cycles.

At failure: About 80% net section area lost; all components failed; deflection increment of more than one inch was observed; the residual static capacity of the girder was 64% of the maximum fatigue loading.

Girder No. 9

Section 1-1
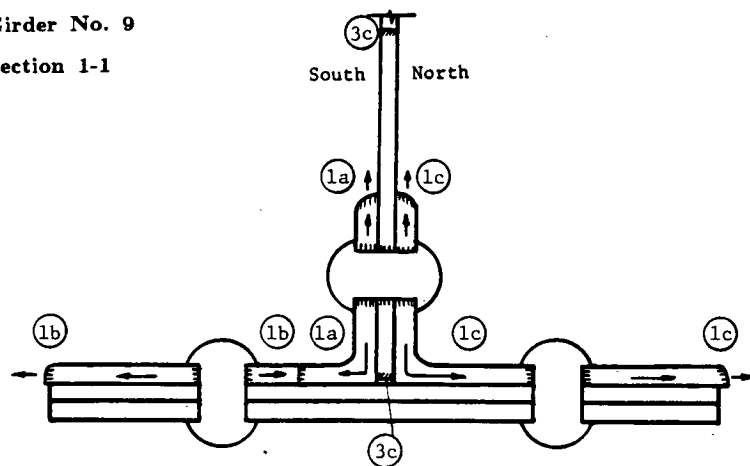
Girder No. 9

Section 2-2

Girder No. 9

Stage	Cycles $\times 10^6$	A_c/A_n %	Temp. °F (°C)	P_{max} kip (KN)	$S_{max,net}$ ksi (MPa)	Note
$1_{a,b,c}$	0	37(1-1) 11(2-2)	Rm.T.	90 (400)	$>F_Y$	Angles fractured under static proof test.
2	0.240	37(1-1) 11(1-1)	Rm.T.	42 (187)	26.9 (186)	Rust powder was seen around rivet in section 2-2.
3_a		37(1-1) 17(2-2)	Rm.T.	42 (187)	30.4 (210)	Stable crack growth
3_b		37(1-1) 24(2-2)	Rm.T.	42 (187)	35.9 (248)	Stable crack growth
3_c	0.415	37(1-1) 30(2-2)	Rm.T.	42 (187)	$>F_Y$	Most components failed. A crack grew into web. Coverplate end separated
4	0.415	45(1-1) 38(2-2)	Rm.T.	27 (120,static)	$>F_u$	Residual static capacity
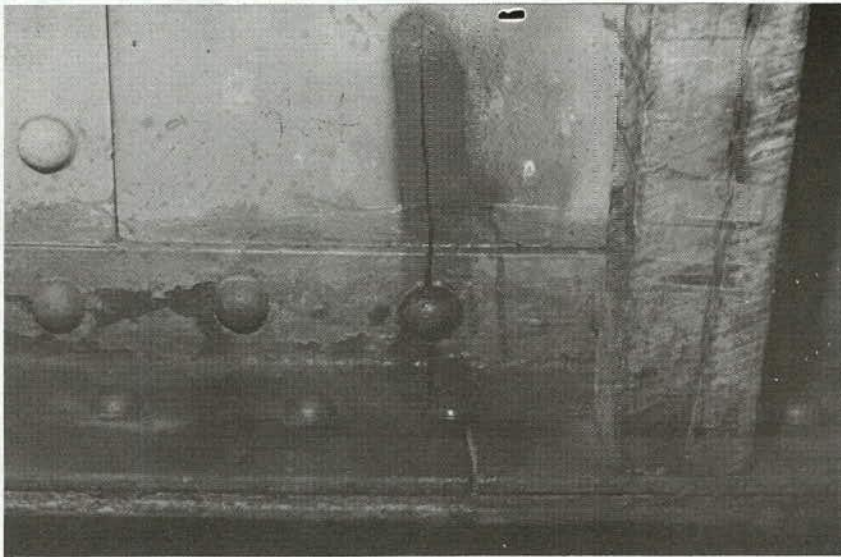
Figure B20. Fractured flange angles of girder 9 (section 1-1, south side).
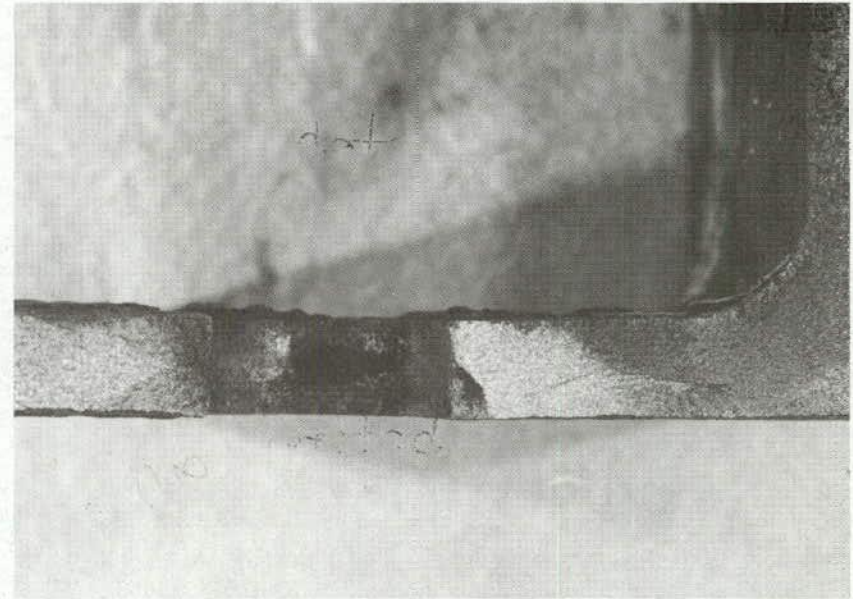
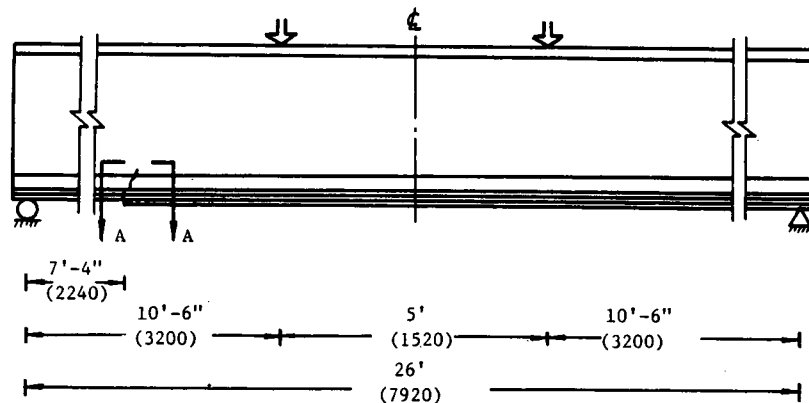Figure B22. Crack at rivet hole (girder 9, section 2-2).
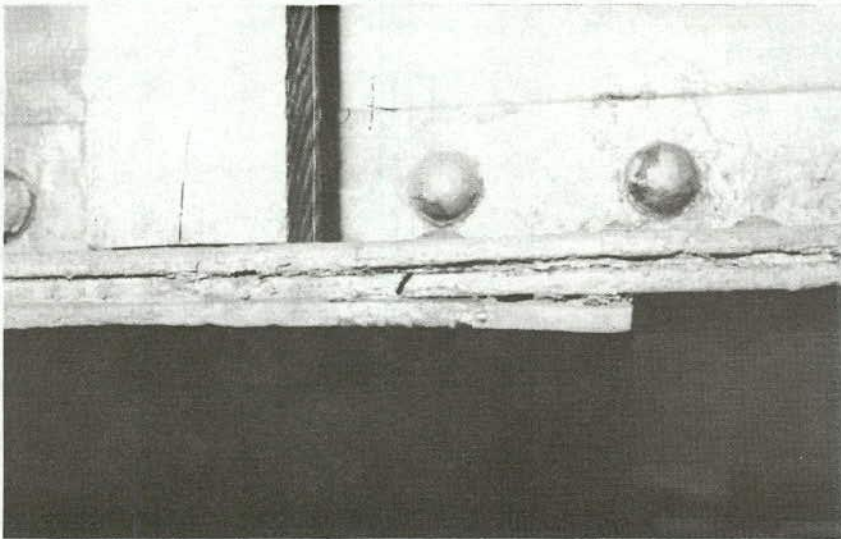
Figure B21. Girder 9 at 415,000 cycles (section 2-2, south side).

Girder No. 10: $S_r=15$ ksi (103 MPa), $S_{min}=8$ ksi (55 MPa)
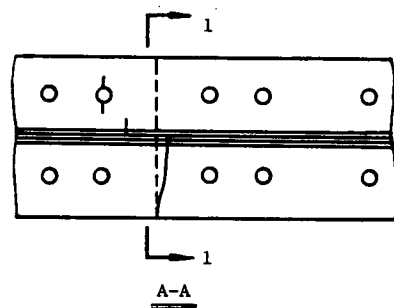
7'-4"
(2240)

10'-6"
(3200)

5'
(1520)

10'-6"
(3200)

26'
(7920)

1

A-A

N

W ← → E

S

Fatigue crack initiation: at coverplate termination, through corrosion reduced cross-section.

At failure: More than 85% net section area lost; all components failed; deflection increment of more than one inch was observed; the residual static capacity of the girder was 70% of the maximum fatigue loading.

Girder No. 10

Section 1-1

North   South

Staggered crack surface
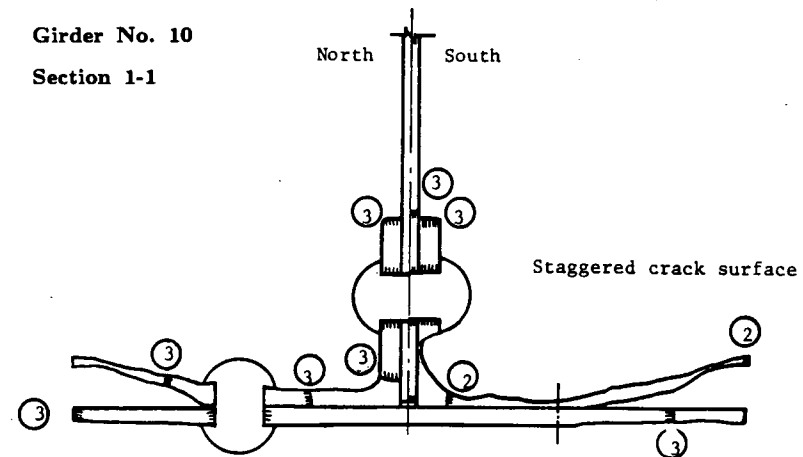
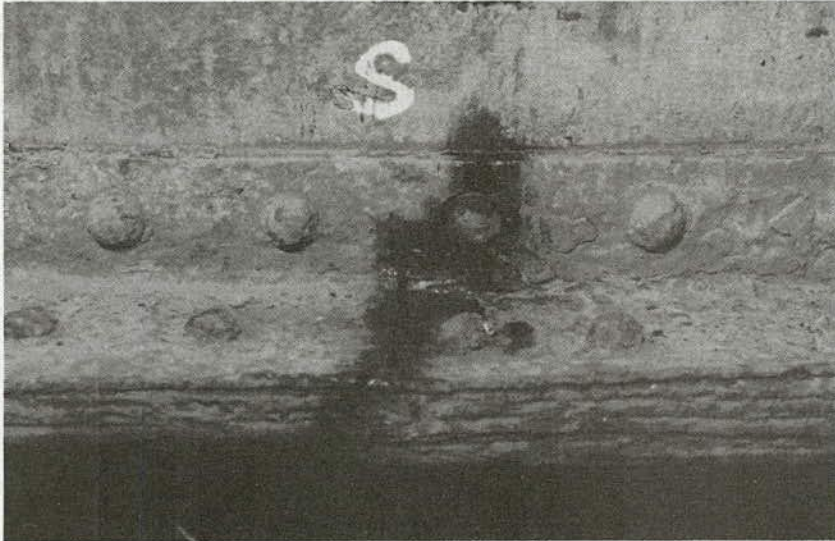| Stage	Cycles x10^6	A$_c$/A$_n$ %	Temp. °F (°C)	P$_{max}$ kip (KN)	S$_{max,net}$ ksi (MPa)	Note
1	–	25	–	–	–	Corrosion reduction of net area.
2	0.471	40	Rm.T.	90 (400)	38.3 (264)	Crack initiated at cover-plate termination, through corrosion reduced cross-section.
3	0.512	85	Rm.T.	90 (400)	>F$_u$	Most components failed. Machine stopped by deflection control device.
4	0.512	100	Rm.T.	64 (285,static)	>F$_u$	Residual static capacity

Figure B23. Girder 10 at 512,000 cycles (section 1-1, south side).
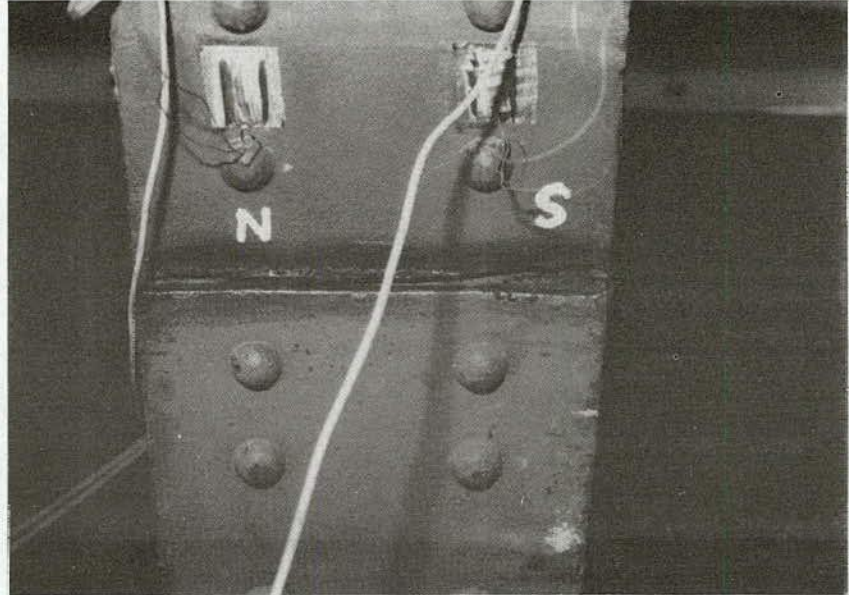

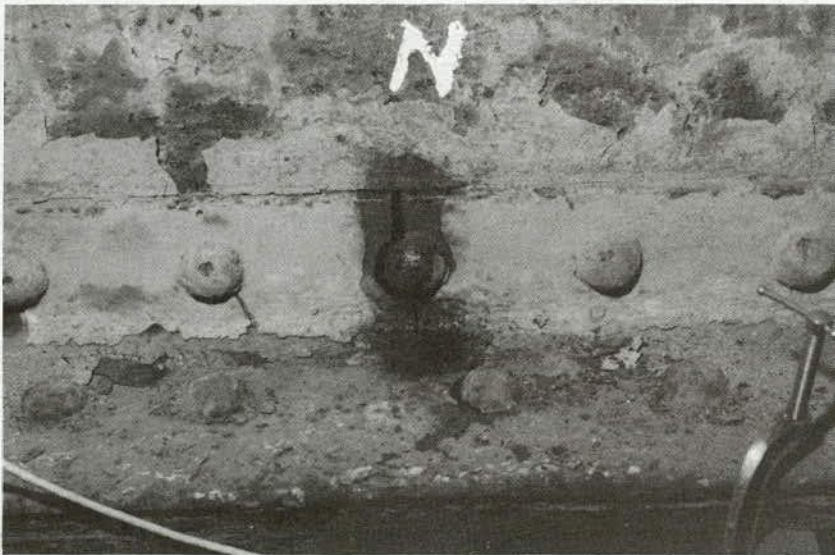Figure B25. Girder 10 at 512,000 cycles (section 1-1, bottom view).

Figure B24. Girder 10 at 512,000 cycles (section 1-1, north side).

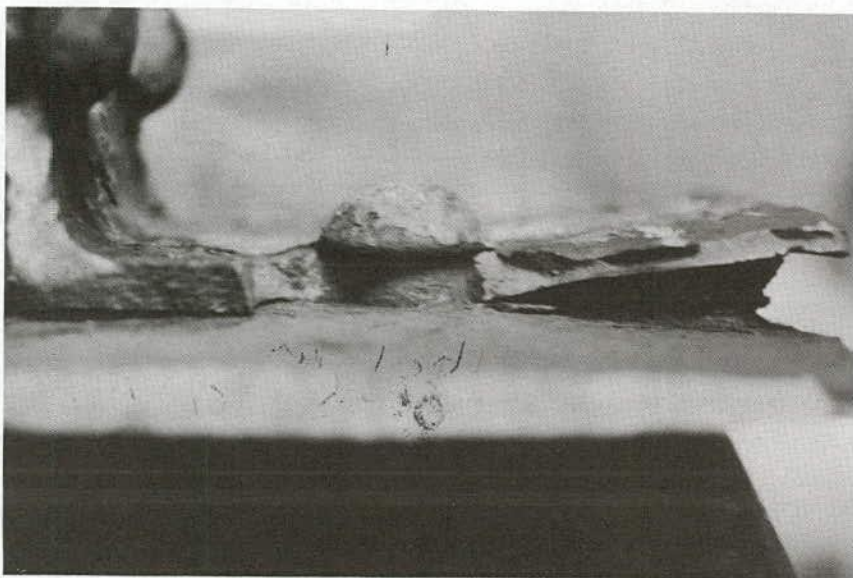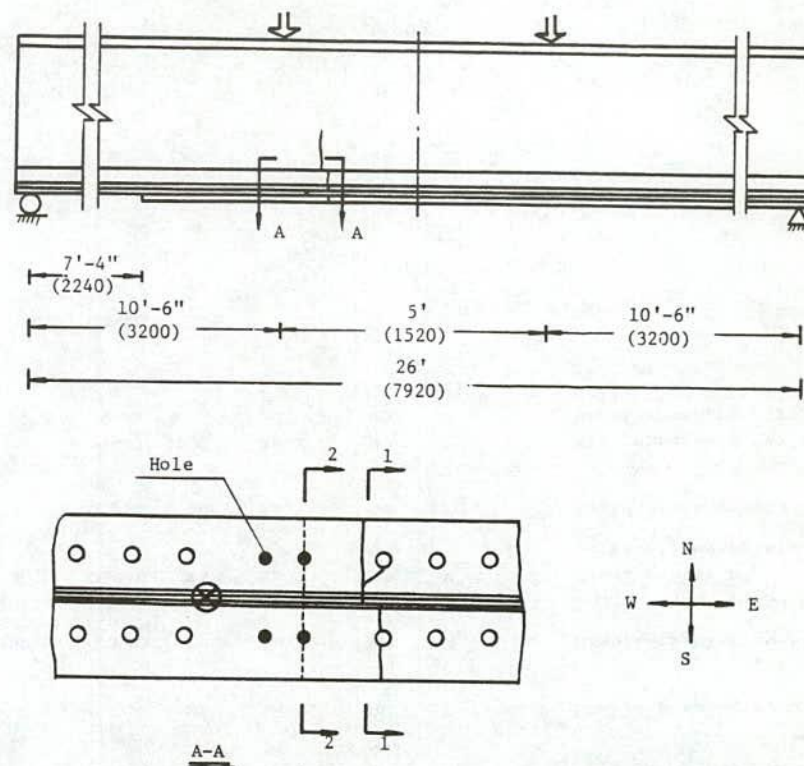Figure B26. Cracked section 1-1 of girder 10.

Figure B27. Cracked section 1-1 of girder 10 (close-up view).

Girder No. 11: S_r=12 ksi (83 MPa), S_{min}=14 ksi (97 MPa)

Fatigue crack initiation: within constant moment region, through corrosion reduced cross-section.

Load redistribution: Fatigue cracks in two cross-sections caused the failure. The sequence indicated the redistribution. Bottom flange lateral bracing was added.

At failure: 100% net section area lost (in different cracked sections); all components failed; deflection increment of more than one inch was observed; residual static capacity test was not carried out because of excessive deflection.

73

Girder No. 11

Section 1-1

Staggered crack surface
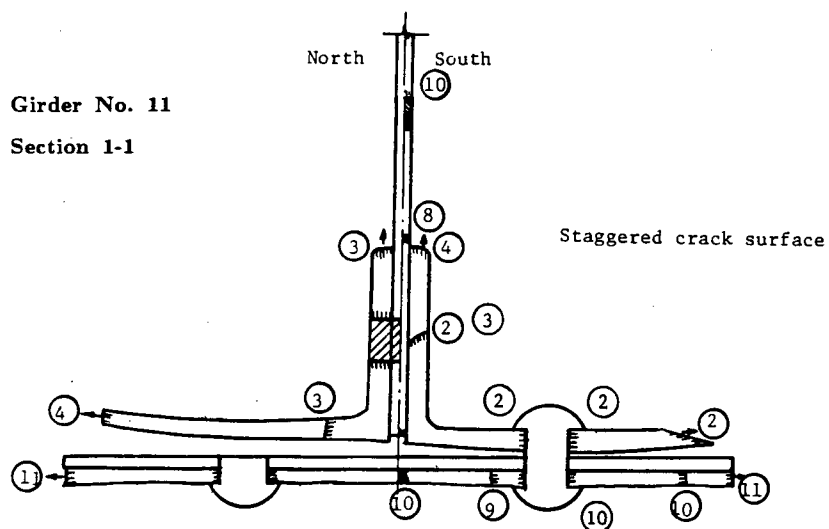
Girder No. 11
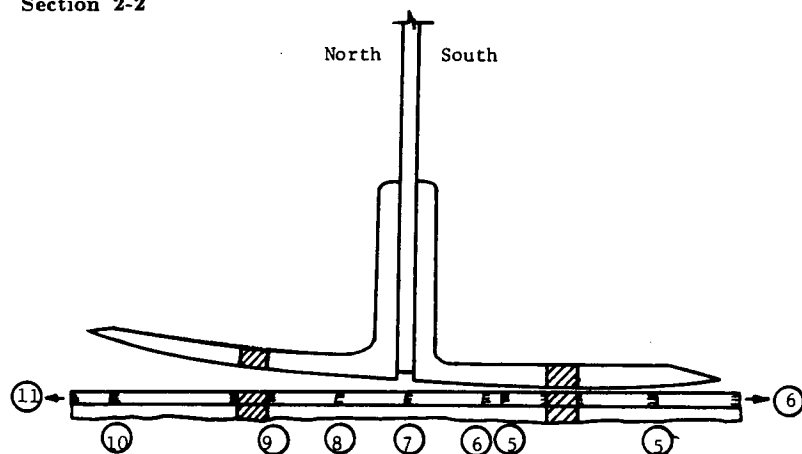
Section 2-2

Girder No. 11

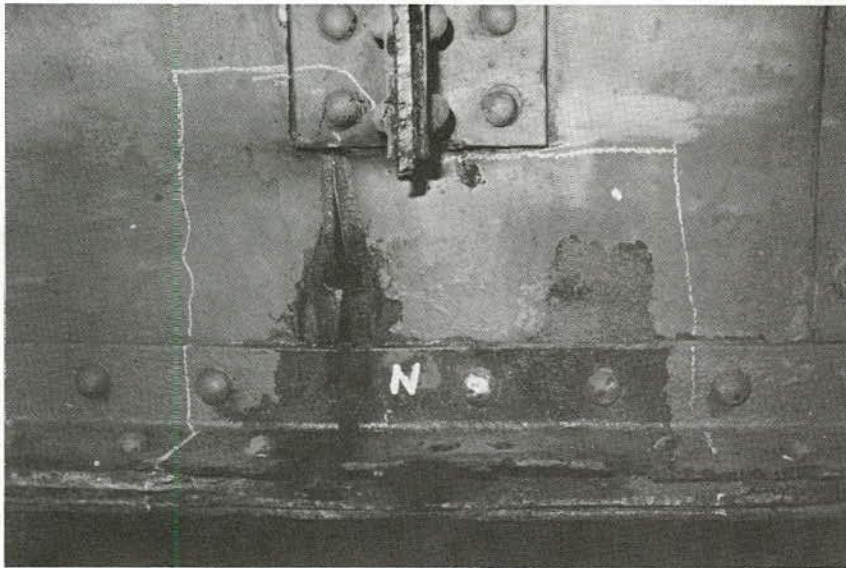| Stage	Cycles $\times 10^6$	A_c/A_n %	Temp. °F (°C)	P_{max} kip (KN)	$S_{max,net}$ ksi (MPa)	Note
1	–	20	Rm.T.	–	–	Corrosion reduction of net-section area
2	0.522	35	Rm.T.	90 (400)	32.0 (221)	Cracks initiated at corrosion-notched cross-section.
3	0.542	43	Rm.T.	90 (400)	36.0 (252)	Crack reinitiated at north angle.
4	0.549	55	Rm.T.	90 (400)	$>F_Y$	Crack extension to angle tips.
5	0.611	60	Rm.T.	90 (400)	$>F_u$	Crack growth at mid-coverplate.
6	0.618	63	Rm.T.	90 (400)	$>F_u$	Stable crack growth
7	0.631	65	Rm.T.	90 (400)	$>F_u$	Stable crack growth
8	0.640	70	Rm.T.	90 (400)	$>F_u$	Stable crack growth
9	0.649	75	Rm.T.	90 (400)	$>F_u$	Crack growth at external coverplate.
10	0.656	90	Rm.T.	90 (400)	$>F_u$	Rapid crack growth
11	0.657	100	Rm.T.	90 (400)	$>F_u$	All components failed. Machine stopped by deflection control device.

Figure B28. Girder 11 at 657,000 cycles (section 1-1, north side).
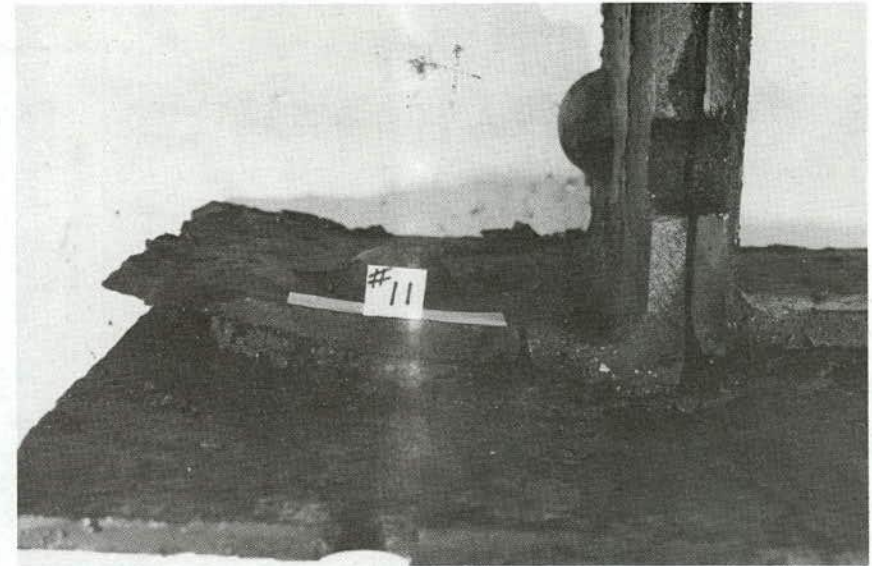

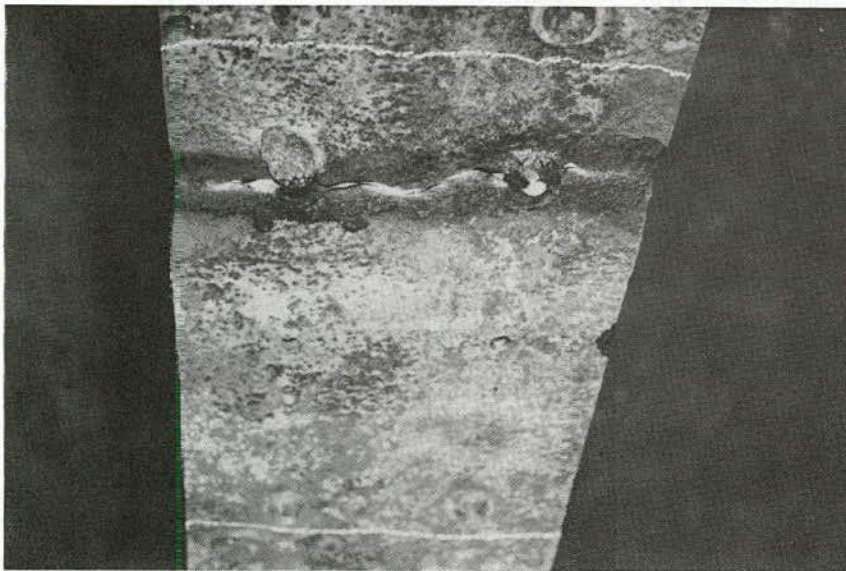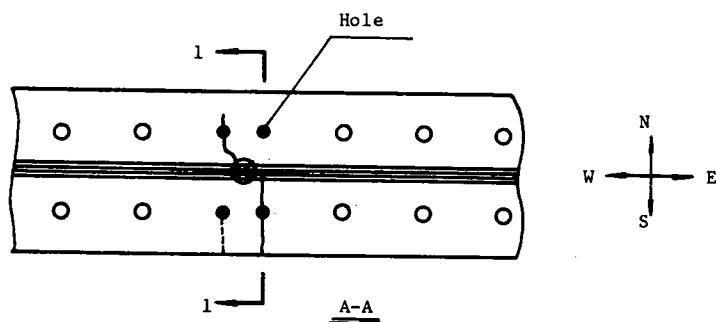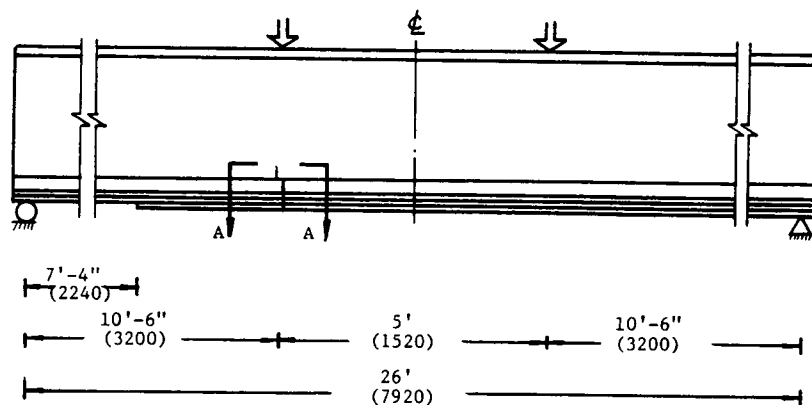Figure B30. Corrosion-reduced cross section of girder 11.

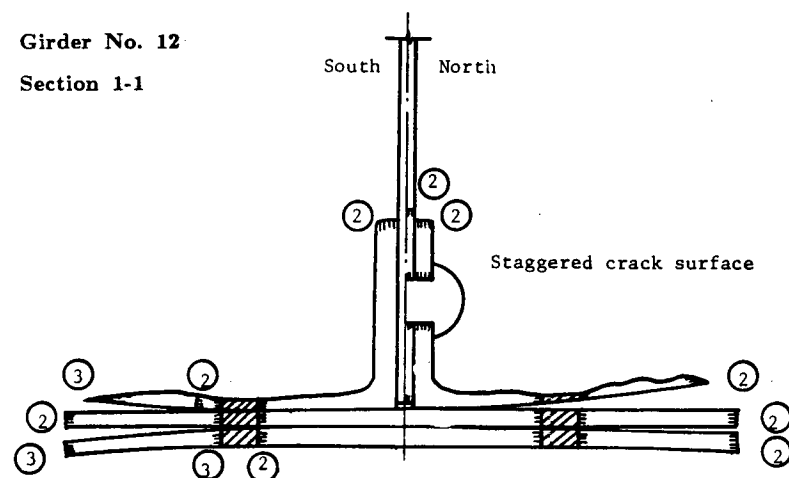Figure B29. Girder 11 at 657,000 cycles (section 1-1, bottom view).

Girder No. 12: S_r=18 ksi (124 MPa), S_{min}=2 ksi (14 MPa)

Girder No. 12

Section 1-1

Staggered crack surface

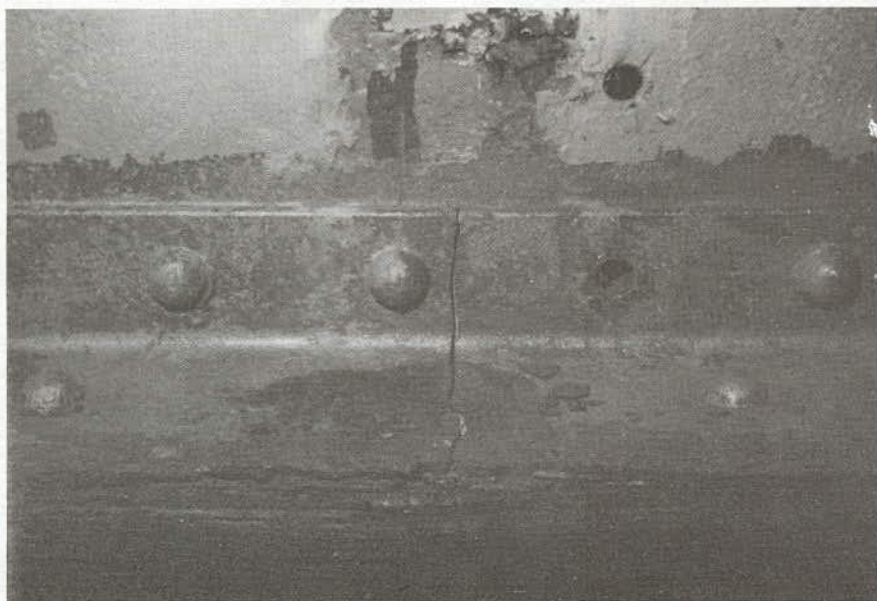| Stage	Cycles x10^6	A_c/A_n %	Temp. °F (°C)	P_{max} kip (KN)	$S_{max,net}$ ksi (MPa)	Note
1	–	40	Rm.T.	–	–	Corrosion reduction of net area
2	0.827	90	Rm.T.	57 (254)	>F_u	Sound of fracture was heard. Failure occurred at corrosion reduced area.
3	0.827	100	Rm.T.	48 (214,static)	>F_u	Residual static capacity

Hole

N
W   E
S

A-A

Fatigue crack initiation: at constant moment region, through corrosion reduced area.

At failure: 100% net section area lost; all components failed; the residual static capacity of the girder was 84% of the maximum fatigue loading.
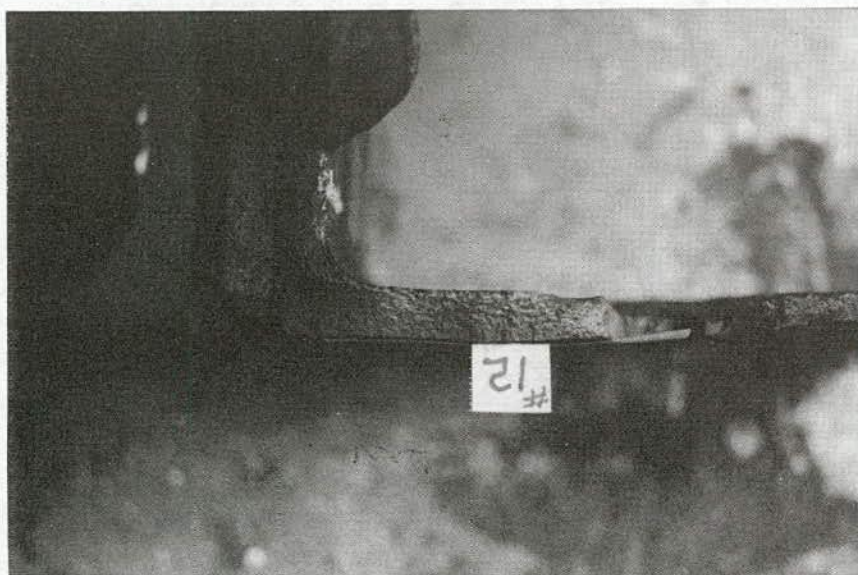
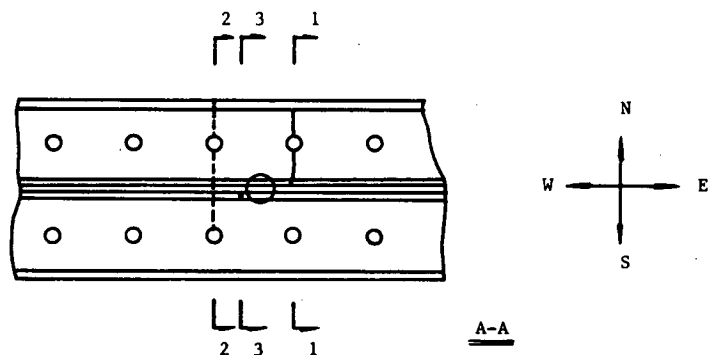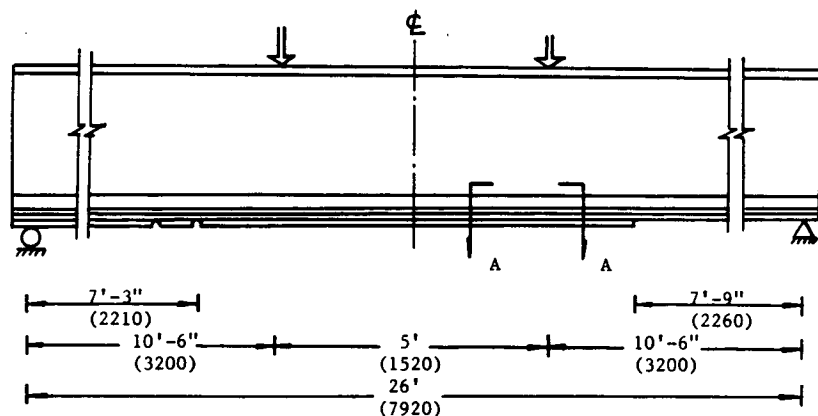Figure B31. Girder 12 at 827,000 cycles (section 1-1, south side).

Figure B33. Corrosion-reduced area of girder 12.

Figure B32. Girder 12 at 827,000 cycles (section 1-1, bottom view).

Girder No. 13: $S_r=12$ ksi (83 MPa), $S_{min}=8$ ksi (55 MPa)

Girder No. 13

Section 1-1

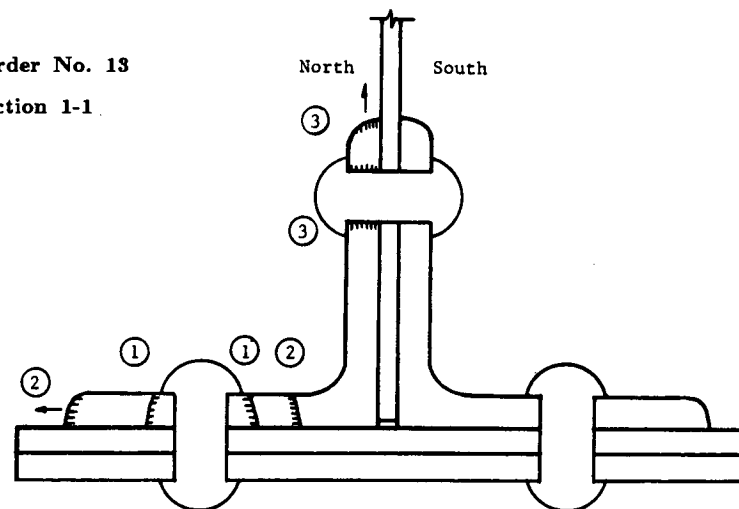**Girder No. 13**

Section 2-2

Fatigue crack initiation: within constant moment region, through rivet holes.

Load redistribution: As one component cracked, the others took up the load and the girder moved sideways. Bottom flange lateral bracing was added.

At failure: More than 70% net section area lost; most components failed; deflection increment of more than one inch was observed; girder failed in a ductile way with crack opening of more than half an inch; residual static capacity of the girder was more than 100% of the maximum fatigue loading.
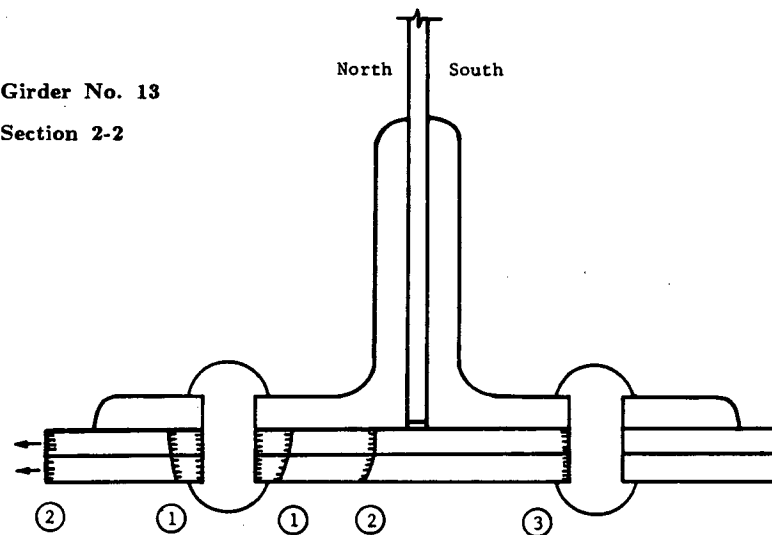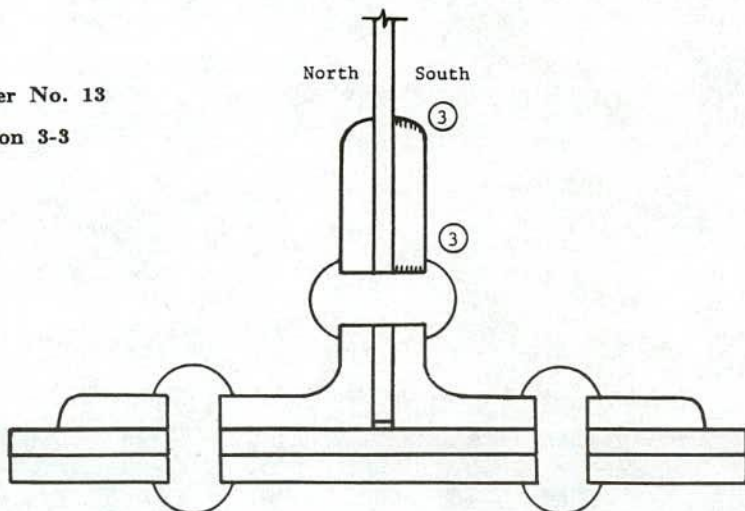
Girder No. 13

Section 3-3

North | South

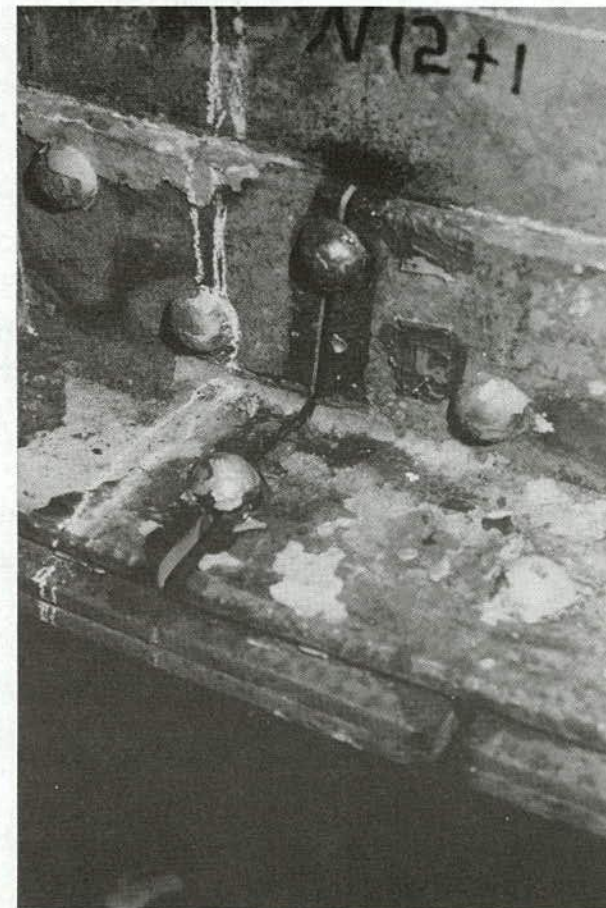| Stage	Cycles $\times 10^6$	A_c/A_n %	Temp. °F (°C)	P_{max} kip (KN)	$S_{max,net}$ ksi (MPa)	Note
1	3.040	5(1-1) 5(2-2)	Rm.T.	104 (463)	22.2 (153)	Cracks initiated at sections 1-1 and 2-2.
2	3.568	9(1-1) 21(2-2)	Rm.T.	104 (463)	28.7 (198)	Stable crack growth
3	3.613	25(1-1) 36(2-2) 8(3-3)	-40	104 (463)	>F_u	Brittle fracture under reduced temperature
4	3.613	25(1-1) 36(2-2) 8(3-3)	Rm.T.	110 (489,static)	>F_u	Residual static capacity

Figure B34. Girder 13 at 3,613,000 cycles (section 1-1 and 2-2, north side).
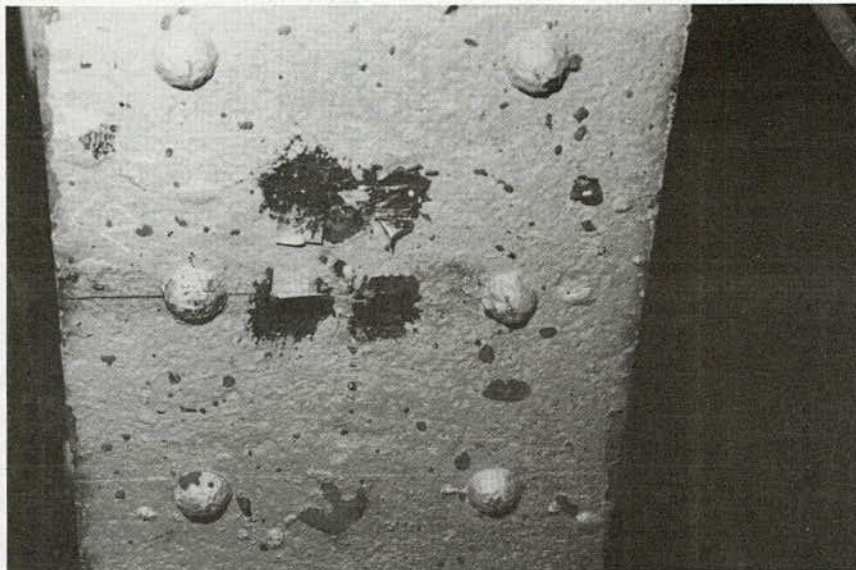
Figure B35. Girder 13 at 3,613,000 cycles (section 2-2, bottom view).
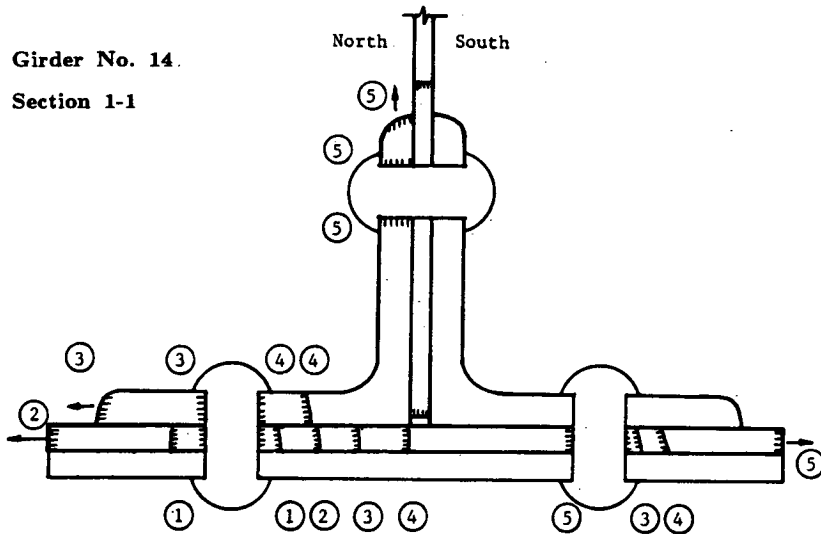
Coverplate Termination

A-A
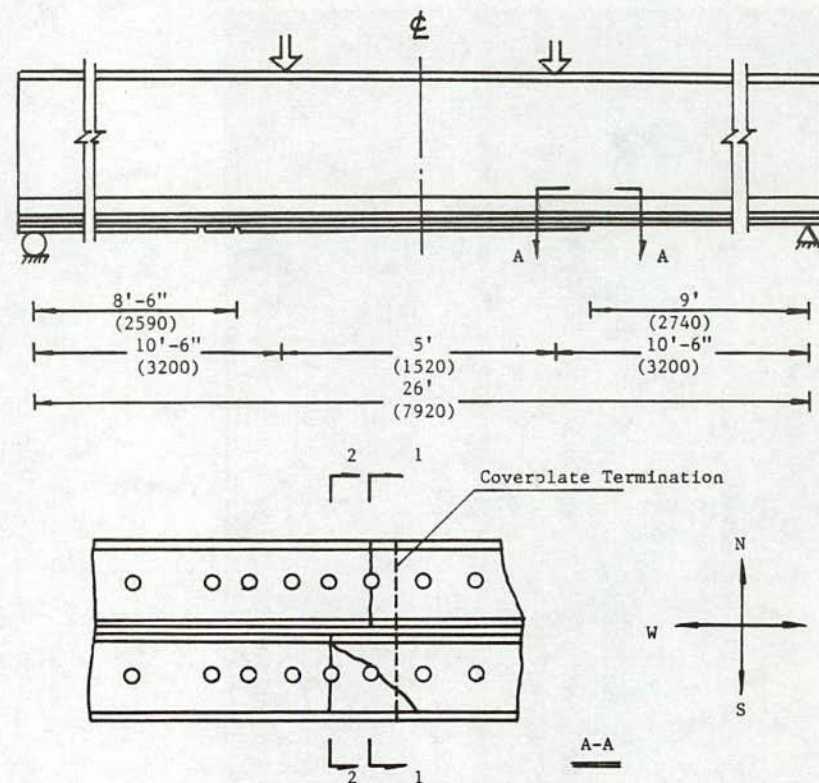
Fatigue crack initiation: near coverplate termination, through rivet holes.

At failure: More than 85% net section area lost; most components failed; deflection increment of more than one inch was observed; the residual static capacity was 57% of the maximum fatigue loading.

Girder No. 14

Section 1-1

North   South
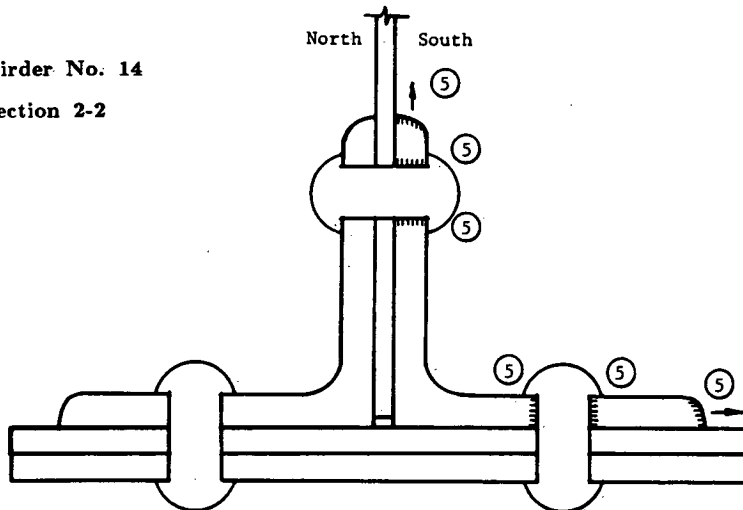
Girder No. 14

Stage	Cycles $\times 10^6$	A_c/A_n %	Temp. °F (°C)	P_{max} kip (KN)	$S_{max,net}$ ksi (MPa)	Note
1	<1.446	2	Rm.T.	93 (414)	23.5 (162)	A crack initiated from mid-coverplate, section 1-1.
2	1.446	9	Rm.T.	93 (414)	25.3 (174)	Stable crack growth
3	1.544	16	Rm.T.	93 (414)	27.5 (190)	Stable crack growth
4	1.547	22	Rm.T.	93 (414)	29.5 (203)	Stable crack growth
5	1.563	85	-60 (-51)	93 (414)	>F_u	Brittle fracture under reduced temperature
6	1.563	85	Rm.T.	53 (236,static)	>F_u	Residual static capacity

Girder No. 14

Section 2-2

North   South

Figure B36. Girder 14 at 1,563,000 cycles (section 1-1, north side).

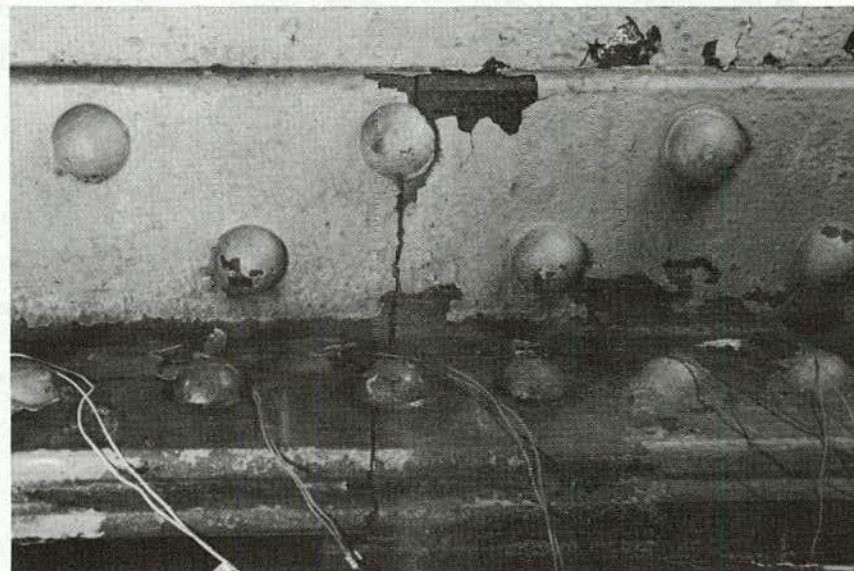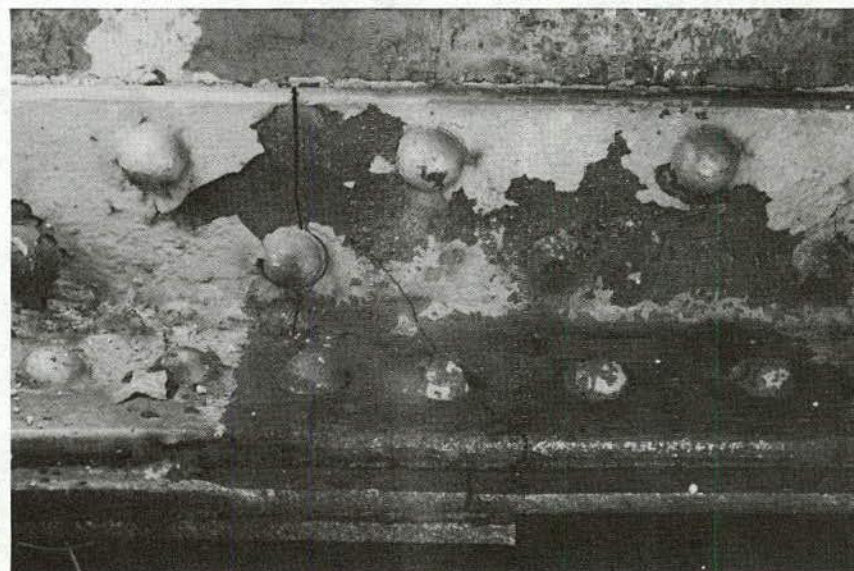Figure B37. Girder 14 at 1,563,000 cycles (section 2-2, south side).

APPENDIX C

EXAMPLES OF RIVETED BRIDGE FATIGUE EVALUATION

(Unless noted otherwise, article references in this appendix refer to the AASHTO **Standard Specifications for Highway Bridges.**)

EXAMPLE I—FATIGUE EVALUATION OF A RIVETED PLATE GIRDER

1. Description of the Structure

The structure is an existing twin bridge of continuous riveted plate girder with five spans, three built-up girders, and a 7-in. thick concrete deck. Under four-lane, two-way highway traffic, the bridges have been in service for 33 years. The structure is shown schematically in Figure C1.

2. Evaluation Based on Section 5.2.4 *(Ch. Five of Main Report)*

The riveted built-up plate girders have three or more tensile-resistant components. The rating procedure consists of the following:

- *Truck Load:* A single HS-20 truck is applied.
- *Impact Factor (AASHTO 3.8.2):*
  $I = 50/(L + 125) = 50/(80 + 125) = 0.244$ for span 1
  $I = 50/(L + 125) = 50/(105 + 125) = 0.217$ for span 2
- *Lateral Distribution of Wheel Loads (AASHTO 3.23.2 Footnote f):* For single lane loading of $S > 10$ ft, simple beam analogy is used:

$$DF_{wheel} = 1 + (S - 6)/S = 1 + (11 - 6)/S = 1.455$$

- *Section Modulus:* Net section modulus S_{net} is used in fatigue evaluation.
- *Nominal Stress Range:* S_r is calculated for three critical cross sections, using moment range, M_r (sum of positive and negative M_{L+I}), and net section modulus, S_{net}.

Section	M_r (k-ft)	S_{met} (in.³)	S_r (ksi)	Note
1	1111	1576	8.46	> 7.0 ksi
2	1097	1933	6.81	
3	1035	1221	10.17	> 7.0 ksi

S_r is higher than 7.0 ksi; therefore, further check is required.

3. Evaluation Based on NCHRP Report 299, Appendix A

As suggested in Section 5.2 (Ch. Five of main report), "If the stress range determined from Article 5.2.4.1 exceeds 7 ksi, the evaluation procedure provided in *NCHRP Report 299* should
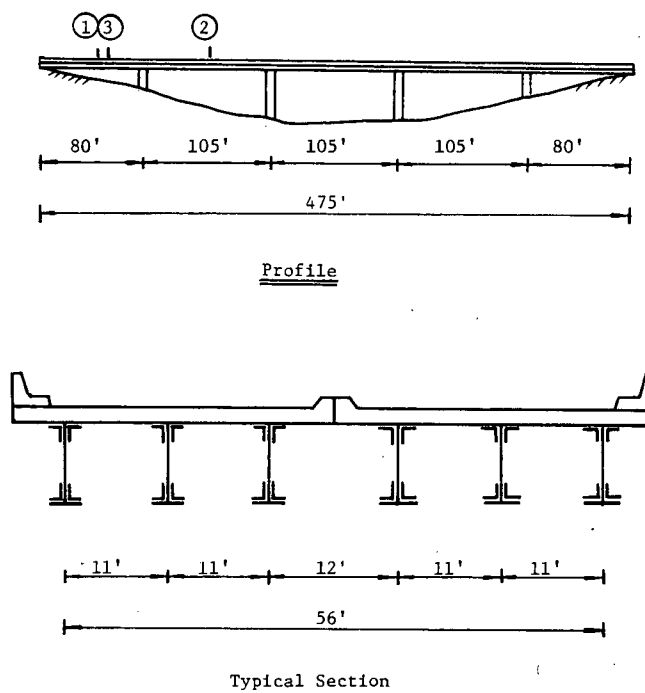

Figure C1. Riveted plate girder bridge.

be followed as amended in Article 5.2.5." Basic reliability factor $R_{so} = 1.35$ is used. Detail constant K = 12, corresponding to Detail Category C, is used in the calculation of remaining life. The rating procedure consists of the following:

- *Truck Load (Fig. 6.2.2A):* Fatigue truck (equivalent to HS-15 truck with fixed 30-ft main axle spacing) is used.
- *Impact (Article 6.2.4):* $I = 0.10$ for smooth road surfaces.
- *Lateral Distribution of Truck Load (Article 6.2.6):*
  $DF_{truck} = S/D = 11/21.3 = 0.516$
  $< (S - 3)/S = (11 - 3)/11 = 0.73$
- *Truck Superposition (Article 6.2.3):* This is ignored because none of the special conditions is present.
- *Section Modulus (Article 6.2.7.1):* There are no shear connections between slab and girder. Also no visual separation of deck and girder is observed. Use steel section alone increased by 30 percent.
- *Nominal Stress Range:* S_r is calculated for three critical cross sections, using moment range M_r (sum of positive and negative M_{L+I}) and increased steel section modulus S.

Section	M_r (k-ft)	S (in.^{3})	S_r (ksi)
1	425	2049	2.49
2	454	2513	2.17
3	416	1587	3.15

- *Reliability Factor R_s (Article 6.2.8):*
  R_{so} = 1.35
  F_{s1} = 1.0 (no measurements)
  F_{s2} = 1.0 (standard fatigue truck)
  F_{s3} = 1.0 (basic procedure for estimating girder distribution)
  For remaining safe life: $R_s = R_{so}(F_{s1})(F_{s2})(F_{s3})$ = 1.35.
  For remaining mean life: R_s = 1.0.
- *Check for Infinite Life (Article 6.3.1):*
  S_{FL} = 3.7 ksi [Category C]
  Factored stress = 1.35 × 3.15 = 4.25 > 3.7 ksi
  Therefore the section has finite life.
- *Truck Traffic (Article 6.3.5):* Present average daily truck volume in the outer lane, T:
  ADT = 32,500 veh/day
  F_T = 0.12 [Recorded truck ratio]
  F_L = 0.85 [2 lanes, 1-way traffic]
  T = (ADT) $F_T F_L$ = 3,315 trucks/day

  Life time average daily truck volume, T_a:
  Present age of bridge, a = 33 years
  Assume growth rate = 4%
  Using Figure 6.3.5.2a, T_a/T = 1.15
  T_a = 1.15(3315) = 3,800 trucks/day
- *Cycles Per Truck Passage C (Article 6.3.4):* C = 1.0 for continuous span, above 40 ft.
- *Remaining Safe Fatigue Life (Article 6.3.2):*
  Detail Constant, K = 12
  Present Age, a = 33 years
  $Y_f = [fK \times 10^6]/[T_a C(R_s S_r)^3] - a$ = [1.0 × 12 × 10^6]/[3800 × 1.0 (1.35 × 3.15)^3] − 33
  = 8 years
- *Remaining Mean Fatigue Life (Article 6.3.2):*
  f = 2.0
  R_s = 1.0
  $Y_m = [fK \times 10^6]/[T_a C(R_s S_r)^3] - a$ = [2.0 × 12 × 10^6]/[3800 × 1.0 (1.0 × 3.15)^3] − 33
  = 169 years

EXAMPLE II—FATIGUE EVALUATION OF A RIVETED HANGER

1. Description of the Structure

An existing riveted steel truss bridge, under two-lane two-way highway traffic, has been in service for 30 years. The structure is shown schematically in Figure C2.

2. Evaluation Based on Section 5.2.4 *(Ch. Five of Main Report)*

The number of tensile-resistant components of the riveted built-up hanger is more than three. The rating procedure consists of the following:

- *Truck Load:* A single HS-20 truck is applied.
- *Impact Factor (AASHTO 3.8.2):*
  $50/(L + 125) = 50/(36.5 + 125) = 0.31 > 0.30$
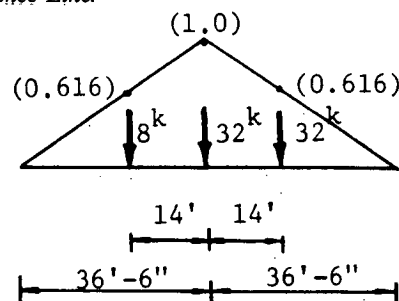 Use I = 0.30
- *Section Area:* Net section area A_{net} is used in fatigue evaluation.
- *Lateral Distribution of Wheel Load:* The deck is assumed as a simple beam for lateral load distribution. Therefore the truss takes $(39 - 8)/39 + (39 - 14)/39 = 1.44$ wheel loads.
- *Nominal Stress Range S_I:*
  Influence Line:

$P = 4(0.616 + 16(1.0) + 16(0.616) = 28.3$ kip
$S_r = [(1.44)(1.30)28.3]/7.47 = 7.1$ ksi > 7.0 ksi
Further check is required.

3. Evaluation Based on NCHRP Report 299, Appendix A

As suggested in Section 5.2 of Ch. Five of the main report, "If the stress range determined from Article 5.2.4.1 exceeds 7 ksi, the evaluation procedure provided in *NCHRP Report 299* should be followed as amended in Article 5.2.5." Basic reliability factor R_{so} = 1.35 is used. Detail constant K = 12, corresponding to Detail Category C, is used in calculation of remaining life. The rating procedure consists of the following:

- *Truck Load (Fig. 6.2.2A):* Fatigue truck (equivalent to HS-15 truck with fixed 30-ft main axle spacing) is used.
- *Impact (Article 6.2.4):* I = 0.10 for smooth road surfaces.
- *Truck Superposition (Article 6.2.3):* A red light is near the bridge and the gross weight of the fatigue truck is increased by 15 percent.
- *Lateral Distribution of Truck Load (Article 6.2.6):* The deck is assumed as a simple beam for lateral load distribution. Therefore the truss takes $(39 - 11)/39 = 72$ percent of the truck load.
- *Section Area (Article 6.2.7.2):* Net section area A_{net} is used in fatigue evaluation.
- *Nominal Stress Range S_r:*
  Influence Line:
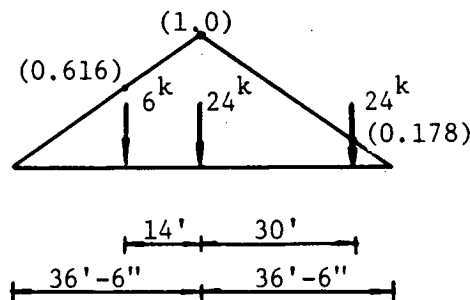
$P = 6(0.616) + 24(1.0) + 24(0.178) = 32.0$ kip

$S_r = (0.72)(1.10)(1.15)32.0/7.47 = 3.90$ ksi

- *Reliability Factor R_s (Article 6.2.8):*

  $R_{so} = 1.35$

  $F_{s1} = 1.0$ (no measurements)

  $F_{s2} = 1.0$ (standard fatigue truck)

  $F_{s3} = 1.0$ (basic procedure)

  For remaining safe fatigue life: $R_s = R_{so}(F_{s1})(F_{s2})(F_{s3}) = 1.35$

  For remaining mean fatigue life: $R_s = 1.0$.

- *Check for Infinite Fatigue Life (Article 6.3.1):*

  $S_{FL} = 3.7$ ksi [Category C]

  Factored stress $= 1.35 \times 3.90 = 5.27 > 3.7$ ksi

  Therefore the hanger has finite fatigue life.

- *Truck Traffic (Article 6.3.5): Present average daily truck volume in the outer lane, T:*

  ADT $= 12,000$ vehicles/day

  $F_T = 0.10$ [Truck ratio for urban highways]

  $F_L = 0.60$ [2 lanes, 2-way traffic]

  $T = 12,000(0.10)(0.60) = 720$ trucks/day

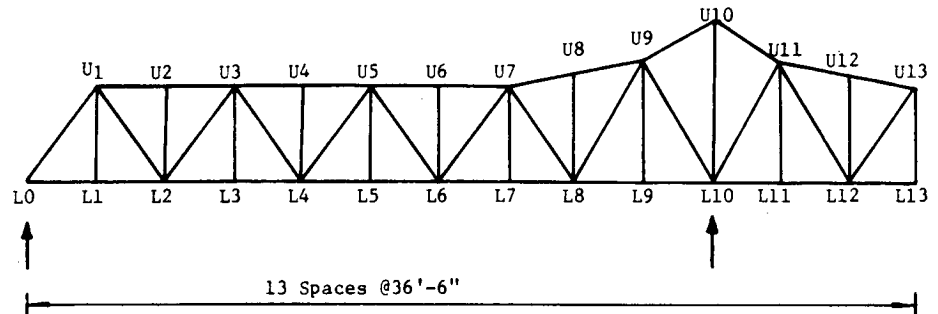 Life Time Average Daily Truck Volume, T_a:

  Present age of bridge, $a = 30$ years
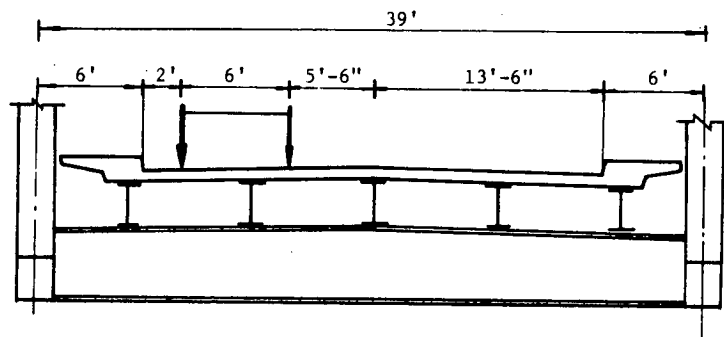
  Assume growth rate $= 4\%$

  Using Figure 6.3.5.2a

  $T_a = 1.22T = 1.22 \times 720 = 880$ trucks/day

- *Cycles Per Truck Passage C (Article 6.3.4): C $= 1.0$ for trusses.*

- *Remaining Safe Fatigue Life (Article 6.3.2):*

Profile

Typical Section
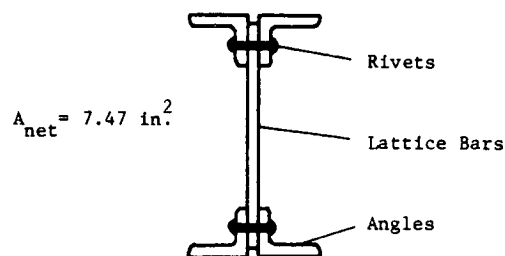
Hanger U1-L1 Section

Figure C2. Riveted truss bridge.

Detail constant, K = 12

Present age, a = 30 years

$Y_f = [fK \times 10^6]/[T_a C(R_s S_r)^3] - a = [1.0 \times 12 \\ \times 10^6]/[880 \times 1.0(1.35 \times 3.90)^3] - 30 \\ = 63$ years

- *Remaining Mean Fatigue Life (Article 6.3.2):*

  $f = 2.0$

  $R_s = 1.0$

  $Y_m = [fK \times 10^6]/[T_a C(R_s S_r)^3] - a = [2.0 \times 12 \\ \times 10^6]/[880 \times 1.0(1.0 \times 3.90)^3] - 30 \\ = 430$ years

THE TRANSPORTATION RESEARCH BOARD is a unit of the National Research Council, which serves the National Academy of Sciences and the National Academy of Engineering. It evolved in 1974 from the Highway Research Board, which was established in 1920. The TRB incorporates all former HRB activities and also performs additional functions under a broader scope involving all modes of transportation and the interactions of transportation with society. The Board's purpose is to stimulate research concerning the nature and performance of transportation systems, to disseminate information that the research produces, and to encourage the application of appropriate research findings. The Board's program is carried out by more than 270 committees, task forces, and panels composed of more than 3,300 administrators, engineers, social scientists, attorneys, educators, and others concerned with transportation; they serve without compensation. The program is supported by state transportation and highway departments, the modal administrations of the U.S. Department of Transportation, the Association of American Railroads, the National Highway Traffic Safety Administration, and other organizations and individuals interested in the development of transportation.

The National Academy of Sciences is a private, nonprofit, self-perpetuating society of distinguished scholars engaged in scientific and engineering research, dedicated to the furtherance of science and technology and to their use for the general welfare. Upon the authority of the charter granted to it by the Congress in 1863, the Academy has a mandate that requires it to advise the federal government on scientific and technical matters. Dr. Frank Press is president of the National Academy of Sciences.

The National Academy of Engineering was established in 1964, under the charter of the National Academy of Sciences, as a parallel organization of outstanding engineers. It is autonomous in its administration and in the selection of its members, sharing with the National Academy of Sciences the responsibility for advising the federal government. The National Academy of Engineering also sponsors engineering programs aimed at meeting national needs, encourages education and research, and recognizes the superior achievements of engineers. Dr. Robert M. White is president of the National Academy of Engineering.

The Institute of Medicine was established in 1970 by the National Academy of Sciences to secure the services of eminent members of appropriate professions in the examination of policy matters pertaining to the health of the public. The Institute acts under the responsibility given to the National Academy of Sciences by its congressional charter to be an adviser to the federal government and, upon its own initiative, to identify issues of medical care, research, and education. Dr. Samuel O. Thier is president of the Institute of Medicine.

The National Research Council was organized by the National Academy of Sciences in 1916 to associate the broad community of science and technology with the Academy's purposes of furthering knowledge and advising the federal government. Functioning in accordance with general policies determined by the Academy, the Council has become the principal operating agency of both the National Academy of Sciences and the National Academy of Engineering in providing services to the government, the public, and the scientific and engineering communities. The Council is administered jointly by both Academies and the Institute of Medicine. Dr. Frank Press and Dr. Robert M. White are chairman and vice chairman, respectively, of the National Research Council.

TRANSPORTATION RESEARCH BOARD

National Research Council

2101 Constitution Avenue, N.W.

Washington, D.C. 20418

ADDRESS CORRECTION REQUESTED

00001SM003
MATERIALS ENGR
IDAHO TRANS DEPT DIV OF HWYS
P O BOX 7129
BOISF   ID 83707